Pure

Bangor University

DOCTOR OF PHILOSOPHY

Natural regeneration models for Sitka spruce and other conifers in continuous cover forestry

Bianchi, Simone

Award date:
2018

Awarding institution:
Bangor University

Link to publication

Bangor University

College of Natural Sciences

School of Environment, Natural Resources and Geography

Natural regeneration models for Sitka spruce and other conifers in continuous cover forestry

By

Simone Bianchi

Thesis for the degree of Doctor of Philosophy

2018

Declaration and Consent

Details of the Work

I hereby agree to deposit the following item in the digital repository maintained by Bangor University and/or in any other repository authorized for use by Bangor University.

Author Name: ………Simone Bianchi………………………………………….

Title: Natural regeneration models for Sitka spruce and other conifers in continuous cover forestry

Supervisor/Department: ....Dr. James Gibbons, Dr. Christine Cahalan, SENRGy...

Funding body (if any): ....Forestry Commission/Scottish Forestry Trust.................

Qualification/Degree obtained: ………Ph.D. in Forestry………………………………….

This item is a product of my own research endeavours and is covered by the agreement below in which the item is referred to as "the Work". It is identical in content to that deposited in the Library, subject to point 4 below.

Non-exclusive Rights

Rights granted to the digital repository through this agreement are entirely non-exclusive. I am free to publish the Work in its present version or future versions elsewhere.

I agree that Bangor University may electronically store, copy or translate the Work to any approved medium or format for the purpose of future preservation and accessibility. Bangor University is not under any obligation to reproduce or display the Work in the same formats or resolutions in which it was originally deposited.

Bangor University Digital Repository

I understand that work deposited in the digital repository will be accessible to a wide variety of people and institutions, including automated agents and search engines via the World Wide Web.

I understand that once the Work is deposited, the item and its metadata may be incorporated into public access catalogues or services, national databases of electronic theses and dissertations such as the British Library's EThOS or any service provided by the National Library of Wales.

I understand that the Work may be made available via the National Library of Wales Online Electronic Theses Service under the declared terms and conditions of use (http://www.llgc.org.uk/index.php?id=4676). I agree that as part of this service the National Library of Wales may electronically store, copy or convert the Work to any approved medium or format for the purpose of future preservation and accessibility. The National Library of Wales is not under any obligation to reproduce or display the Work in the same formats or resolutions in which it was originally deposited.

Statement 1:

This work has not previously been accepted in substance for any degree and is not being concurrently submitted in candidature for any degree unless as agreed by the University for approved dual awards.

Signed …………………………………….. (candidate)

Date …………27-Feb-2018………………………………..

Statement 2:

This thesis is the result of my own investigations, except where otherwise stated. Where correction services have been used, the extent and nature of the correction is clearly marked in a footnote(s).

All other sources are acknowledged by footnotes and/or a bibliography.

Signed …………………………………………… (candidate)

Date ……………27-Feb-2018…………………………………

Statement 3:

I hereby give consent for my thesis, if accepted, to be available for photocopying, for inter-library loan and for electronic storage (subject to any constraints as defined in statement 4), and for the title and summary to be made available to outside organisations.

Signed …………………………………………… (candidate)

Date ……………27-Feb-2018……………………………….

Statement 4:

Choose **one** of the following options

a)	I agree to deposit an electronic copy of my thesis (the Work) in the Bangor University (BU) Institutional Digital Repository, the British Library ETHOS system, and/or in any other repository authorized for use by Bangor University and where necessary have gained the required permissions for the use of third party material.	**X**
b)	I agree to deposit an electronic copy of my thesis (the Work) in the Bangor University (BU) Institutional Digital Repository, the British Library ETHOS system, and/or in any other repository authorized for use by Bangor University when the approved **bar on access** has been lifted.	
c)	I agree to submit my thesis (the Work) electronically via Bangor University's e-submission system, however I **opt-out** of the electronic deposit to the Bangor University (BU) Institutional Digital Repository, the British Library ETHOS system, and/or in any other repository authorized for use by Bangor University, due to lack of permissions for use of third party material.	

Options B should only be used if a bar on access has been approved by the University.

In addition to the above I also agree to the following:

1. That I am the author or have the authority of the author(s) to make this agreement and do hereby give Bangor University the right to make available the Work in the way described above.

2. That the electronic copy of the Work deposited in the digital repository and covered by this agreement, is identical in content to the paper copy of the Work deposited in the Bangor University Library, subject to point 4 below.

3. That I have exercised reasonable care to ensure that the Work is original and, to the best of my knowledge, does not breach any laws – including those relating to defamation, libel and copyright.

4. That I have, in instances where the intellectual property of other authors or copyright holders is included in the Work, and where appropriate, gained explicit permission for the inclusion of that material in the Work, and in the electronic form of the Work as accessed through the open access digital repository, *or* that I have identified and removed that material for which adequate and appropriate permission has not been obtained and which will be inaccessible via the digital repository.

5. That Bangor University does not hold any obligation to take legal action on behalf of the Depositor, or other rights holders, in the event of a breach of intellectual property rights, or any other right, in the material deposited.

6. That I will indemnify and keep indemnified Bangor University and the National Library of Wales from and against any loss, liability, claim or damage, including without limitation any related legal fees and court costs (on a full indemnity bases), related to any breach by myself of any term of this agreement.

Signature: ……… …… ……………………………. Date:……27-Feb-2018…….

A mia madre.

Acknowledgements

x

Executive Summary

This thesis aimed to develop models for the natural regeneration of Sitka spruce that could be applied to stands under continuous cover forestry in the UK. The models followed the development of Sitka spruce seedlings from the establishment phase until their recruitment to the overstorey.

First, I prepared models for estimating the presence and density of Sitka spruce seedlings under canopy cover. I simulated the likelihood of seedling presence according to a combination of stand and site characteristics, and stand management history. I estimated the seedling density by generating random numbers from a Weibull distribution. The calibration data came from an existing dataset extensively collected all around the UK, and I carried out an independent validation with newly collected data in two sites in Wales and England.

Then, I modelled the early height and diameter growth of Sitka spruce and western hemlock, and the early growth of Douglas fir, as a function of light availability. I compared light-growth models based on non-linear asymptotic functions, including tree size and intra-regeneration competition as predictors. Results showed that different non-linear structures best simulated the growth of different species. I carried out an analysis of the crown plasticity, observing that both the apical dominance and live crown ratios were negatively correlated with light availability for all species, although with some species-specific differences. Overall, I defined a shade-tolerant ranking as Douglas fir $\leq$ Sitka spruce < western hemlock. For this study I collected data across several forests in Wales, England and Scotland.

Given the importance of the below-canopy light regime analysis in this study, I investigated a possible technological improvement for its assessment. I demonstrated that hemispherical photography carried out with smartphone cameras equipped with fish-eye lenses can be an adequate alternative to traditional cameras, with cheaper equipment and faster methods. The data were collected during the above field campaign.

Finally, I tested the feasibility of using the models aforementioned for simulating Sitka spruce natural regeneration in a continuous cover forestry scenario in the UK. I integrated the Sitka spruce regeneration presence, density, and early growth models into MOSES_GB, a forest growth simulator under development by the Forestry Commission. I simulated the development over 15 years of a regeneration layer under an overstorey layer, the development of which was simulated by MOSES_GB. I simulated two different virtual stands, and followed the

establishment, growth, and recruitment of the regeneration into the overstorey, comparing two different spatial modelling approaches and two thinning regimes. A spatially-explicit approach, which considered the local variability in the light-availability, seemed to be more accurate. Some issues and potential problems in the simulations were identified, together with the future studies that can address them.

Table of contents

List of figures

List of tables

List of abbreviations

ADR	Apical dominance ratio
AIC	Akaike Information Criteria
BA	Basal Area
CCF	Continuous Cover Forestry
CO	Canopy Openness
COMP	Competition
DBH	Diameter at Breast Height
DBHg	Diameter at Breast Height, growth
DBHp	Diameter at Breast Height, previous to the growth
DBHt	Diameter at Breast Height, total
DDS	Decision Support System
DF	Douglas fir
DRC	Diameter above Root Collar
DSF	Direct Site Factor
FOV	Field of View
GF	Gap fraction
GLMM	Generalized Linear Mixed Model
GSF	Global Site Factor
H	Height
Hg	Height, growth
Hp	Height, previous to the growth
Ht	Height, total
HP	Hemispherical Photography
ISF	Indirect Site Factor
LCR	Live crown ratio
MAE	Mean Absolute Error
MAPE	Mean Absolute Percentage Error
OV	Overstorey
QMD	Quadratic Mean Diameter
RMSE	Root-Mean-Square Error
SDI	Stand Density Index
SDIr	Stand Density Index regeneration
sm	Smartphone

SNR	Soil Nutrient Regime
SPH	Stems Per Hectare
SS	Sitka spruce
TC	Thinning Class
TG	Total Gap
WH	Western hemlock

1 Introduction

Forest modelling has always accompanied forest management (Robinson & Ek 2000). It is widely accepted that modern forestry sciences originated in 18th century Europe. Hartig (1764-1837) and Cotta (1763-1844) first proposed forest management approaches aimed at stabilising the annual yield by regulating either the harvestable volume or the felled area. Those objectives were more easily achieved with the establishment of even-aged, single species forests that soon became widespread. In the late 18th and early 19th centuries, forestry scientists in Central Europe prepared the first models to predict the development of those relatively simple ecosystems, structured as yield tables simulating growth regarding general stand-level parameters (Pretzsch *et al.* 2008). Forest managers could use yield tables as a support tool to plan activities, but the silvicultural options available were very limited (von Teuffel *et al.* 2006).

Since the 19th century, the development of British forestry has followed the same trends as Continental Europe. In 1827, David Douglas (1799-1834) introduced to the United Kingdom (UK) the first conifer species from Western North America, the aptly named Douglas fir (*Pseudotsuga menziesii* (Mirb.) Franco), then followed by Sitka spruce (*Picea sitchensis* (Bong.) Carr) and other conifers from the same region (James 1981). Those exotic species performed very well, and a century later, at the time of the first modern UK forest census in 1924 (Forestry Commission 1928), the area covered by conifers or mixed conifers/broadleaves was almost 70% of all productive high stands. British foresters started publishing yield tables for such stands at the beginning of the 20th century (Maw 1912). Presently, the main modelling reference in the UK is the yield tables produced by the Forestry Commission for pure, even-aged stands of the major native and exotic forest species (Edwards & Christie 1981). The only silvicultural variables that forest managers can consider are the density of planted seedlings, the intensity of thinning treatments, and the timing of the final clear-cut.

During the last century, concerns over worldwide environmental degradation and unsustainable use of natural resources led to the 1992 Earth Summit in Rio de Janeiro. The summit initiated a process that brought profound transformations to the forestry sector (Forestry Commission 2017). To face such concerns, forest ecosystems were now expected to fulfill simultaneously a wider array of functions to varying extents: not only wood production, but other ecosystem

services such as biodiversity conservation, hydrological and soil protection, carbon sequestration, and recreation, just to name a few (Führer 2000). Many studies have indicated that an increase in the diversity of the forest structure is one possible way to obtain multiple benefits from managed stands (Malcolm, Mason & Clarke 2001; Spiecker 2003; Gamfeldt *et al.* 2013; Macpherson *et al.* 2017). Thus, to increase such diversity, forestry research increasingly focused on what are now called close-to-nature or nature-oriented forestry approaches (Koch & Skovsgaard, 1999; Motta 2000; O'Hara, 2001; Mielikäinen & Hynynen, 2003). Those approaches propose a shift from the traditional methods of clear-felling and artificial regeneration to smaller interventions and natural restocking. These nature-oriented methods have the potential to lead to uneven-aged, multi-species stands without interrupting the forest cover of the area (Mason & Kerr 2004; Pukkala *et al.* 2011). Even if such approaches are the target of newly rediscovered interest, it is important to remember that they have old historical roots. The *method of control*, originally applied to the *futaie jardinées* to ensure a permanent forest cover, was introduced by Gurnaud in France already in 1878 (Pardé 1991), while Möller proposed the idea of *Dauerwald* (or permanent forest) in Germany at the beginning of the 20th century (Pignatti 2012).

Today, all the approaches based on the use of continuous natural regeneration can be classified as Continuous Cover Forestry (CCF) (von Gadow *et al.* 2002; Ní Dhubháin 2003; Pignatti 2012). Mason *et al.* (1999), reminding us that CCF "is more than a silvicultural system", indicates the following guiding principles: management of the forest ecosystems rather than just the trees; use of natural processes as the basis for stand management; adaptation to the site limitations; and the creation of a diverse stand structure with a range of species. It is important to remember that although CCF can be considered closer to nature than other approaches, it is still an anthropic management. Failing to understand that point may lead to many misconceptions (Davies *et al.* 2008). First of all, irregularity is not necessarily the norm in European forests, which most of the times tends, in the long-term, towards a homogenous state, particularly where a species is growing in its optimum site (Schütz 2002; Paci 2004). Moreover, CCF can be applied not only to stands of native species but also to exotic trees as long as they are site-adapted, as happens in the UK (Davies, Haufe & Pommerening 2008; Kerr *et al.* 2012), and some of the historical CCF methods, such as the already mentioned method of control and *Dauerwald* forest, are based on a strict anthropic control of the tree sizes distribution in the forest (Susmel 1980; Schütz 2006).

Under CCF management, forest development has no beginning nor end, and in uneven-aged forests, the traditional yield tables that estimated forest parameters based only on the age of pure stands cannot be used (von Gadow & Hui 1999). New forest growth simulators are required to satisfy the new user needs, and to move from estimating aggregated parameters for homogenous stands to studying the growth of individual trees in irregular situations (von Teuffel *et al.* 2006). At the same time, there is a need to link models simulating the establishment and early growth of regeneration with models simulating the growth of overstorey trees, so that the continuous stand development could be simulated (Miina & Saksa 2006). Various challenges are present for this latter objective. As it will become clear throughout this study, models predicting the regeneration processes are especially difficult to prepare since several factors involved: from seed production through seedling establishment, growth and survival until recruitment to the overstorey. Light is considered one of the main factors affecting regeneration under forest cover (Oliver & Larson 1996; Lieffers *et al.* 1999), so there will be a particular focus in this thesis on studying the specific light-growth responses of various tree species that are potential components of future mixed-species forests in the UK.

1.1 Continuous cover forestry in the United Kingdom

The road to CCF in the UK has been slow but steady. The UK Forestry Standard (Forestry Commission 2017) defines CCF as a "silvicultural system whereby the forest canopy is maintained at one or more levels without clearfelling", and suggests its implementation as an alternative to clearfelling (i.e. the "cutting down of an area of woodland … greater than 0.25 ha" regardless of whether a few scattered or clumped trees are retained), where "suitable sites and species combinations are allowed, and management objectives are compatible". This approach is explicitly promoted in the United Kingdom Woodland Assurance Scheme (UKWAS 2012): "lower impact silvicultural systems shall be increasingly favoured where they are suited to the site and species", and "where appropriate and possible use should be made of natural regeneration". Recently, Mason (2015) noted that while the area actively managed for CCF is just around 3% of the total forest area, there were aspirations to transform 20% of public forests to irregular structures in the future. He also observed that there were few examples of CCF being implemented in single-species conifer plantations, particularly in the extensive forests dominated by Sitka spruce. This species accounts in the UK for around half of the total standing coniferous volume (Forestry Commission 2011b) and for almost 23% of the total forest cover (Forestry Commission 2011a). Sitka spruce natural regeneration can establish abundantly and grow well under canopy cover, and its potential for CCF has already been

positively tested in various experiments (Malcolm *et al*. 2001; Mason 2015). Western hemlock (*Tsuga heterophylla* (Raf.) Sarg.) and Douglas fir, both associates of Sitka spruce in its natural range, are other successfully-introduced coniferous species in the UK that could be companions of Sitka spruce in mixed-species, uneven-aged forests (Cameron 2015).

As the basis of a national forest growth simulator to be used to support CCF management, the Forestry Commission is developing MOSES_GB (Forest Research 2010) from the original concept of MOSES (MOdeling Stand rESponse) (Hasenauer *et al*. 2006). Calibrated for the main forestry species in Austria, MOSES includes components to simulate i) overstorey trees growth and mortality; and ii) natural regeneration occurrence, growth, and mortality. The Forest Research agency is currently re-calibrating the components for the overstorey trees of Sitka spruce in the UK, although no work has been done on the regeneration components.

1.2 Aims and objectives

The overall aim of this thesis was **the development of models for Sitka spruce regeneration in continuous cover forestry scenarios in the UK**. After the literature review (Chapters 2 and 3) was carried out, I decided to model the stages of regeneration occurrence and regeneration early growth separately, and for the latter to focus especially on the relationship between light availability and growth. Thus, I posed the following main research questions.

1. *What are the best structures for Sitka spruce natural regeneration occurrence and density models?*

   What are the stand and site characteristics that significantly affect the occurrence and density of Sitka spruce seedlings under canopy cover? What are the best structures for empirical predictive models of those processes?

2. *Can the early growth of Sitka spruce, western hemlock, and Douglas fir be modelled as a function of the light environment under canopy cover?*

   Can light-growth models, both for height and diameter, be calibrated for those species? How do the regeneration size and the intra-regeneration competition affect the species-specific light-growth responses? Which are the best non-linear functions for modelling those processes?

Interspecific differences in shade tolerance significantly affect stand dynamics (Finzi & Canham 2000). Therefore, the third research question directly follows from the above question.

3. *Can the light-growth responses, regarding growth and canopy architecture, for Sitka spruce, western hemlock, and Douglas fir be used to define a shade tolerance ranking?*

Do light-growth responses inform us about the shade tolerance of these species? Do these species modify their canopy architecture under different light levels? Can we define a shade tolerance ranking using all this information?

Given the importance of the forest light environment analysis in this research, I also decided to explore a possible technological improvement for its assessment in the fourth research question.

4. *Can the light environment under canopy cover be adequately described using smartphone technology?*

Can hemispherical photography, a widely-used method for assessing light availability under canopy cover, be carried out in a faster and cheaper way with smartphone cameras? What are the differences between values obtained by traditional and smartphone cameras? What systems could be employed to reduce such possible differences?

Finally, I decided to test if the above models for regeneration occurrence and early growth can be integrated into MOSES_GB, leading to the last research question.

5. *Can the models for regeneration occurrence and early growth developed in this thesis be integrated into MOSES_GB?*

Can the models developed in this thesis be integrated as they are in the MOSES_GB framework? What is the best strategy for their integration? What are the steps required and what could be the main sources of problems?

1.3   Thesis structure

I have introduced the background, aim and research questions of the thesis in this chapter. In **Chapter 2** I present a literature review on forest regeneration modelling, and in **Chapter 3** on the ecology of Sitka spruce natural regeneration (both in its natural range and in the UK).

I present the experimental work in the following three chapters. In **Chapter 4** I describe a model simulating the regeneration presence and density of Sitka spruce in stands dominated by the same species (answering research question number 1). In **Chapter 5** I present height and radial growth models as functions of light availability, tree size and intra-regeneration competition for regenerating trees of Sitka spruce, western hemlock, and Douglas fir. I also

investigate the light response of crown architectural parameters and then use all the results to compare the shade tolerance of these species (answering research questions number 2 and 3). In **Chapter 6** I investigate the use of smartphone technology to estimate the forest canopy openness and the light regime under canopy cover (answering research question number 4).

In the following two chapters I describe attempts to integrate the models prepared here into MOSES_GB (answering research question number 5). In **Chapter 7** I compare various approaches that could be used in MOSES_GB to model the diameter growth of regenerating Sitka spruce trees until they move up into the overstorey class. In **Chapter 8** I describe simulations of a forest stand development produced by integrating into MOSES_GB the regeneration presence, density and early growth models described in the previous chapters.

Finally, in **Chapter 9**, I summarise the findings of this thesis, draw general conclusions and suggest future research objectives.

2 An overview of forest regeneration modelling

In this chapter, I introduce first some general principles about forest growth simulation, and then in more detail, I review how the natural regeneration modelling has been addressed.

2.1 Forest growth modelling approaches

From the first examples of the 18th-century yield tables, there is now in the literature a vast number of forest growth models prepared according to different approaches and objectives: Porté & Bartelink in 2002 reviewed almost 200 models. Many authors have prepared different classification systems, from the first attempt of Munro (1974), to Vanclay (1994), the already-mentioned Porté & Bartelink (2002), Monserud (2003), Pretzsch *et al.* (2006) and more recently Salas *et al.* (2016). As a general basis for this chapter, I will refer to the system suggested by Peng (2000), shown in Figure 2.1. As in all the systems, the classes are not totally distinct, and it is not always possible to draw clear borders between them. It is beyond the scope of this thesis to expand on the complex issue of classification: "labels are more often used by those who discuss models than those who construct them" (Robinson & Ek 2000). Still, a short description of the main classification criteria will help identify the best modelling methodologies to be applied in the context of the present thesis.
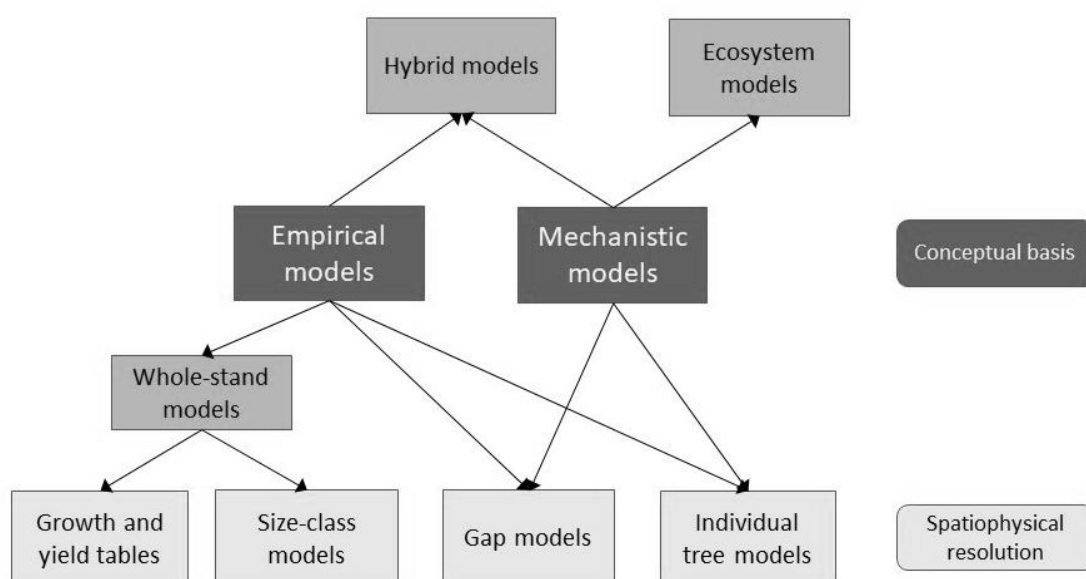
Figure 2.1. Classification method from Peng (2000) for forest growth models

The first discrimination level shown in Figure 2.1, between empirical and mechanistic models, depends on the conceptual basis of their preparation. Empirical models describe the observed phenomena as regression functions usually based on stand and site variables (Peng 2000), while mechanistic models consider their underlying physiological processes, such as photosynthesis, respiration and the allocation of photosynthates within the plant (Vanclay 1994). Robinson & Ek (2000) argued that even mechanistic models are based at a certain level on descriptive relationships between the environmental agents and the modelled process, and empirical model assumptions can be directly linked to the underlying physiological processes. The two model classes have clearer differences in their practical applications. Empirical models are focused more on description and management objectives; they are strongly dependent on the calibration data and so using them outside the original range may lead to extrapolation errors (Huang *et al*. 2003). Mechanistic models are focused more on explanatory and research objectives, have a wider applicability, and so they can be used for more research purposes, such as long-term successional studies or the potential effects of climate change on forest stands (Kellomäki *et al*. 1992; Peng 2000; Tchebakova & Parfenova 2003). At the same time, empirical models usually require as input more data than are usually available to forest managers and are considered not suitable for all end-users (Porté & Bartelink 2002). Still, some authors advocate a better integration of the two methods, especially through the incorporation of climatic variables in empirical models (Battaglia & Sands 1998; Price *et al*. 2001; Miina *et al*. 2006).

The second discrimination level shown in Figure 2.1 is based on the spatiophysical resolution, defined as "the dominant unit of interest or replication in the model" by Robinson & Ek (2000). From the lowest to the highest resolution we can broadly discriminate between: i) yield tables, which consider only aggregated stand-level statistics; ii) size-class models, which group together trees of similar diameter; iii) gap models, which consider the dynamics of a small collection of individual trees; and iv) individual tree models, which consider the growth of individual trees with respect to the competition with their neighbours (von Teuffel *et al.* 2006). MOSES, and in turn MOSES_GB, follows the individual tree approach, which has long been recognized as the best approach for simulating the growth of irregular stands (Curtis 1972). Already in the 1980s, there was an estimated number of several hundred individual tree digital computer models (Dale *et al*. 1985). The increasing availability of computers has been recognized as one of the driving factors of this fast development (Pretzsch 2009). Individual tree models can be defined as models that "describe and keep track of each individual in the stand", and are further classified as distance-dependent if each tree location is explicitly known,

or distance-independent where it is unspecified (Porté & Bartelink 2002). In the former, the availability of resources is computed for each tree according to the specific competition exerted by its neighbours, while in the latter all trees are subject to an average competition estimated at stand level. In this thesis, I will from now on refer to the distance-dependent attribute using the more compact and immediate *spatial* adjective, and *non-spatial* for the distance-independent, following the suggestion of Robinson & Ek (2000).

It must be noted that most of the forest growth models focus on the simulation of the growth of mature or overstorey trees. These trees are usually defined as being bigger than a specific artificial size threshold for each model, such as a height of 1.30 m or a particular minimum DBH, chosen with arbitrary and practical aspects like the design of inventory used for the calibration and the future application of the model (Vanclay 1994; Miina *et al*. 2006). Estimating if and how many new trees reach the overstorey class after the death or the cut of the overstorey is however crucial for CCF stands (Hasenauer 2006).

2.2   Simulating forest regeneration

Unfortunately, the simulation of natural regeneration has been found unsatisfactory in many forest growth models (Price *et al*. 2001; Porté & Bartelink 2002). There are many practical difficulties in the calibration of regeneration models due to the unpredictability and randomness of the several processes involved (from seed production, dispersal and germination, to seedling establishment, growth and survival), and the impossibility of measuring all the ecological factors affecting them (Curtis 1972; Vanclay 1994; Miina *et al*. 2006; Kerr & Mackintosh 2012). A classification of natural regeneration models can follow the definition of Vanclay (1994): regeneration models *sensu strictu*, which predict the development of trees from seed or seedlings, and recruitment models (sometimes called ingrowth by other authors, e.g. Miina *et al*. 2006), which simply predict the number of trees reaching the overstorey class in the time interval studied. Recruitment models are considered to lack details of regeneration dynamics that may be important for CCF (Ferguson 1996) and are therefore not of further interest in this thesis[1].

Regeneration models usually simulate separately the different stages of i) regeneration occurrence, and then ii) early growth and iii) mortality of the seedlings, until they reach the

---

[1] As will become clear in the next chapter, there was anyway a lack in the UK of the data necessary to calibrate recruitment models, and it was impossible to collect them in the timeframe of the thesis.

overstorey size threshold. Then, seedlings are moved to the overstorey class and become subject to its different modelling procedures. An exception is the model SORTIE (Pacala *et al.* 1996), which applies to the overstorey the same growth and mortality models prepared for the juvenile trees. The developers believed that the ability of juvenile trees to survive and grow is crucial for understanding forest successions, and so they focused on the regeneration components (Kobe *et al.* 1995). Most regeneration models easily allow enrichment planting: artificial seedlings can be added to the simulated forest stand and they will then follow the same rules for early growth and survival of natural seedlings (Kellomäki *et al*. 1992; Hasenauer *et al*. 2006). Throughout this thesis I will use "regeneration models" to refer to models that predict the development of trees from seed or seedlings until they reach the overstorey class, considering the different stages of regeneration occurrence, early growth and survival.

2.2.1 Regeneration occurrence

For the first step, regeneration occurrence, models generate new trees by predicting either the number of seed germinated or seedlings established, the latter being when the trees have passed the very first phase of growth and reached an arbitrary size threshold (e.g. 10 cm height, as in Schweiger & Sterba (1997)). Seed germination models are usually mechanistic, describing the phases of seed production, dispersal and germination, while seedling establishment models are generally empirical.

In the seedling establishment models, the process is often split into two stages: i) determining if regeneration is successfully occurring during the time interval studied, and if so ii) defining the species composition and density of the established seedlings (Miina *et al*. 2006). For the first stage, logistic equations with binomial distribution are often calibrated on various stand and site characteristics to estimate the probability of regeneration occurrence in a forest plot, considered to have a binary status of absence or presence, such as in PROGNOSIS (Ferguson & Carlson 1991), MOSES (Hasenauer & Kindermann 2006) and other models (Schweiger & Sterba 1997; Pausas, Ribeiro & Dias 2006). Stochastic approaches are common since forest regeneration, particularly in boreal and temperate regions, tends to be sporadic (Miina, Eerikäinen & Hasenauer 2006). Then, the species composition and density are defined using different statistical approaches, often based on the Weibull or Poisson distribution. The prediction of seedling density has been defined as "the most difficult part in assessing regeneration establishment" due to the many random factors involved (Ferguson 1996). A different approach is used in the model family originated by SORTIE (Pacala *et al.* 1996; then

LePage *et al.* 2000 for SORTIE-BC), which is based only on the seed production potential of mother trees. The model estimates in each simulation cycle the number of one-year old seedlings produced by mature trees as a direct function of their size, then distributes them stochastically around the source (Ribbens *et al*. 1994).

Imputation is another methodology sometimes used for empirically estimating the regeneration occurrence. Imputation involves replacing the missing (not sampled) regeneration measurements for any unit in the population with measurements from one or more units with similar characteristics (Ek *et al.* 1997; Hassani *et al.* 2004 for PROGNOSIS[BC]). This method has some advantages, such as not requiring any distributional assumption of the errors and being multivariate (that is, it may estimate several variables at the same time, such as regeneration presence, species, and density) (Miina *et al*. 2006).

2.2.2 Early growth

For the second step, early growth, specific growth models developed for juvenile trees are often used because models for mature trees may involve different processes and tend to have lower accuracy for smaller size classes (Boisvenue *et al*. 2004).

Some empirical models for juvenile trees follow the potential growth approach, such as FOREST (Monserud & Ek 1977) and MOSES (Hasenauer & Kindermann 2006). The assumption is that the potential growth of a tree of a certain dimension, defined as the growth that the same tree would have in the open, is reduced in the forest by the competition exerted by the neighbouring trees (Newnham 1964). In simple terms, this relationship is shown in Equation 2.1.

$$\text{Equation 2.1: } Observed\ growth\ = \frac{Potential\ growth}{Competition\ factor}$$

Widely used for overstorey trees, when this approach is applied to regenerating trees, the competition factor is generally an indication of the competition exerted by the overstorey crowns, calculated in different ways in the different studies. Other empirical early growth models not based on the potential growth approach fit the observed growth measurements directly to different combinations of stand characteristics (generally indications of the overstorey tree density), site characteristics (such as slope, aspect, site fertility, forest type) and silvicultural characteristics (such as thinning interventions) (Boisvenue *et al*. 2004; Eerikäinen *et al.* 2014).

As previously discussed, borders between models are blurred. Many empirical growth models use light availability, a basic ecological variable employed in mechanistic approaches (e.g. Kellomäki *et al.* 1992), as their main input (Pacala *et al.* 1994 for SORTIE; Wright *et al.* 1998; Finzi & Canham 2000; Wagner *et al.* 2009; Ligot *et al.* 2013). In those cases, non-linear asymptotic functions are often used to describe the light-growth responses. While for the practical application of this approach there is a need to use an additional model to estimate the light availability under canopy cover (such as the SORTIE-ND light model, described by Beaudet *et al.* (2011)), its applicability is less dependent on the overstorey characteristics used for calibration. The inclusion of other resources as additional growth predictors in the light-growth non-linear functions, such as soil moisture and nitrogen content, sometimes significantly improved the fit but not always with strong results (Finzi & Canham 2000; Wagner, Madsen & Ammer 2009).

2.2.3 Regeneration mortality

The third step, mortality, predicts how many regenerating trees will be removed by the simulation, although few examples are present in the literature. Empirical approaches usually consider density-induced mortality alone, i.e. establishing relationships between mortality and indices describing the competition from the overstorey (e.g. Eerikäinen *et al.* 2014), or together with random mortality as in MOSES (Hasenauer & Kindermann 2006). In many cases the forest simulators use the same mortality model for both the overstorey and regenerating trees (Ferguson & Crookston 1991 for PROGNOSIS; Hasenauer & Kindermann 2006 for MOSES; Dixon 2015 for FVS).

Other studies have built growth-mortality functions, using the recent growth history of regenerating trees to estimate their mortality probability (Kobe *et al.* 1995 for SORTIE; Kobe & Coates 1997; Wyckoff & Clark 2000; Kunstler *et al.* 2005). Growth-mortality functions can be defined as the "empirical summary of the complex relationship involving environmental stress, growth, and mortality risk" (Wyckoff & Clark 2000). Usually they are species-specific negative exponential relationships between the growth and the saplings' mortality probability, built thanks to the analysis of the growth of recently deceased seedlings and a count of live and dead seedlings in the area (Kobe *et al.* 1995). These functions can then be used together with existing light-growth functions to link directly light availability and mortality (Pacala *et al.* 1996).

In a forest growth simulator aimed at practical silvicultural applications, the harvesting damage on the existing regeneration should be considered. For example, in a model for regeneration development in uneven-aged, Norway spruce (*Picea abies* K.) dominated forests in Finland, a harvesting event reduced the probability of seedling survival (Eerikäinen, Miina & Valkonen 2007).

2.3   Conclusions

The main approaches for forest growth modelling, and for the integration of the simulation of natural regeneration in those models, were described in this chapter. The present thesis aims at producing tools for simulating regeneration that could be used for practical operative applications in continuous cover forestry situations. Thus, I selected as the approach for this research the regeneration model *sensu strictu*, with the aim of preparing different components for simulating regeneration occurrence, early growth and mortality. In the following chapter, I review the existing knowledge of Sitka spruce natural regeneration and the data available for the UK according to those three main modelling steps, to better identify the research framework and methods to be employed.

3 On the natural regeneration of Sitka spruce

In this chapter, I summarize all the published studies that I could retrieve on Sitka spruce natural regeneration both in the UK and in North America, grouped according to the main modelling steps indicated in Chapter 2 (regeneration occurrence and density, early growth, and mortality).

3.1 Introduction

Sitka spruce is a prolific seed producer with abundant natural regeneration after clear-cutting both in its natural range (Peterson *et al.* 1997) and in the UK, where it is the commercial conifer with the highest potential for natural regeneration: up to 400,000 seedlings per ha on favourable sites after clearcutting or wind-throw, although with high variation between and within sites (Nixon & Worrell 1999). Various reviews of the factors influencing the natural regeneration of Sitka spruce in the British Isles have been carried out, focusing on obtaining natural regeneration as a substitute for artificial planting in clear-felled areas (Clarke 1992; von Ow *et al*. 1996; Nixon & Worrell 1999). Sitka spruce also proved to have the potential for regeneration under canopy cover in the UK, and more recent studies researched how to obtain and use natural regeneration to transform even-aged, mono-specific conifer forests into irregular stands (Malcolm *et al*. 2001; Mason & Kerr 2004). Mason (2015) recently carried out an exhaustive review of the factors influencing Sitka spruce natural regeneration under canopy cover in the UK, summarized in Table 3.1. However, the UK has been defined "data-poor" regarding natural regeneration by Kerr *et al.* (2011), and even if the qualitative information is extensive, there are no existing models to quantitatively predict the regeneration occurrence of Sitka spruce.

The studies reviewed here carried out in forests managed using either with the shelterwood systems or the group selection system, both identified as possible CCF management methods for Sitka spruce forests (Malcolm *et al*. 2001). In the shelterwood systems mature trees are removed in a series of cuts to achieve regeneration under the protection of remaining trees, while the group selection system removes all the trees in a defined patch thus creating stand openings (generally with a width less than two times the height of adjacent mature trees) for

the establishment of the seedlings. The research frameworks therefore reflected the differences between these silvicultural practices and the results were not easily comparable. In addition, I present some studies carried out in nurseries or glasshouses.

Table 3.1. Some of the crucial factors influencing Sitka spruce natural regeneration, the general conclusions drawn in the literature about them, and the evidence quality of such conclusions. Adapted from Mason (2015).

Factor	Conclusions	Evidence Quality
Seed availability	Mast years very important, in British Sitka spruce stands happening every 4-5 years	Good-Moderate
Germination conditions	Favourable seedbed conditions: moist soils with needle litter or light moss cover	Moderate-Poor
Vegetation competition	Avoid fertile sites or competition from ericaceous vegetation	Moderate
Understorey microclimate	Retain some canopy cover to limit frost damage but provide adequate light	Moderate
Light requirements for growth	At least 20% of full light, plus an overstorey with basal area of 30 m^2/ha and reduced tree density	Good
Browsing pressure	Keep deer population below 5 animals per 100 ha	Moderate

3.2   Regeneration occurrence

For the occurrence of regeneration, seed availability is undoubtedly crucial. Sitka spruce seeds, like those of most temperate forest tree species, have a low survival rate in the forest soil and do not produce a viable seed bank. Sitka spruce in the UK starts to have a good seed crop at 25-35 years, after which the seed production increases with age and can reach high levels already at 35-40 years, depending also on the stand density (Nixon & Worrell 1999). Years of heavy cone production tend to be synchronised amongst trees and to happen at periodic intervals called mast years, that in the UK can happen every 3-6 years (Clarke 1992; Mason 2015).

Seed germination is then highly dependent on the seedbed characteristics. Nixon & Worrell (1999) indicated as the most favourable seedbed soils with low fertility (because they have less competing vegetation), with the presence of adequate moisture (neither too dry nor too wet), and without too much brash or needle litter (considered unfavourable due to low water retention). However, von Ow *et al*. (1996) found litter favourable to germination in Ireland, maybe because the very wet conditions addressed in their study improved the water retention. Low-growing mosses are generally considered favourable for regeneration (Mason 2015) due to good water retention, while taller mosses seemed to have a negative effect likely because they prevent the seedlings' root from reaching the mineral soil (von Ow *et al*. 1996). In the

coastal forests of North America, decayed logs are considered the most favourable seedbed for Sitka spruce seedlings (Harmon & Franklin 1989; Taylor 1990).

Stand structure can affect regeneration through different mechanisms. A certain level of overstorey cover was found to be beneficial for Sitka spruce regeneration both in its natural range (Greene *et al.* 1999; Burton 2016) and in the UK (Mason, Edwards & Hale 2004). The positive effect is likely to be due to the control of the growth of competing ground vegetation (Nixon & Worrell 1999), and the influence on the microsite temperature and moisture (Fairbairn & Neustein 1970). However, Mason (2015) found only one work (by Sellars 2005) studying how the understorey temperature and wind speed change under different Sitka spruce stand densities. On the other hand, the presence of overstorey trees reduces the light availability for seedlings.

Thinning interventions in shelterwood systems have been shown to have a positive effect by creating a favourable light environment. Studies carried out both in the UK and in North America generally compared a few stands with different stand densities. They generally found more Sitka spruce seedlings in the stands with lower densities, which were either more recently or more heavily thinned (Deal & Farr 1994; Page *et al.* 2001; Herd 2003; Glendinning 2014), but differences were not always observed between silvicultural treatments (Bertin *et al.* 2011). Nixon & Worrell (1999) observed that even if well-thinned according to the standard practices indicated in the UK yield tables (Edwards & Christie, 1982), Sitka spruce even-aged stands reaching maturity may have light levels under canopy cover not favourable for regeneration. Most of the studies in the UK considered stands originated from artificial planting. Regeneration density in such pure Sitka spruce stands after thinning varied from 4,500 to 70,000 seedlings per ha, but when small germinants under 20 cm height were considered the density could go up 270,000 seedlings per ha (Page *et al*. 2001; Herd 2003; Bertin *et al.* 2011; Glendinning 2014). In contrast, studies in North America focused on natural mixtures of Sitka spruce and western hemlock, and Sitka spruce regeneration occurred with lower densities (1,900-22,000 seedlings per ha) (Deal & Farr 1994). Mason *et al*. (2011) found even fewer Sitka spruce seedlings regenerating under Scottish larch stands (280-560 seedlings per ha), likely due to the lower seed availability and different ground vegetation conditions. When comparing local overstorey variables to seedling density, contrasting results were found: either no relationship was observed (Glendinning 2014), or only a weak positive correlation with basal area (Page *et al*. 2001), or a weak negative correlation with stems per ha (Deal & Farr 1994).

After a group felling, natural regeneration in gaps was observed with higher densities than in the shelterwood systems, with values more similar to those found after clearfelling (20,000-350,000 seedlings/ha) (McNeill & Thompson 1982; Page & Cameron 2006). Generally, the seedling density was higher in the northern side of the gap likely due to the higher light availability. Malcolm *et al.* (2001) suggested keeping the ratio of gap diameter to height of surrounding trees between 1 and 2 to obtain successful natural regeneration in Sitka spruce stands, but without establishing any quantitative relationship.

Comeau *et al.* (2010) investigated the relationship between understorey light and regeneration presence in many Sitka spruce plantations across different stands and treatments in the UK, assessing both areas where regeneration was present and where it was absent. The authors suggested a minimum threshold of 30% canopy gap fraction (the proportion of the overtopping hemisphere that is sky, calculated in a 90˚ overhead cone) necessary for Sitka spruce regeneration to establish and survive.

In order to overcome the problem of the paucity of regeneration data, Kerr *et al.* (2011a) constructed a Decision Support System (DSS) based on a combination of published literature and their own silvicultural experience: REGGIE, or REGeneration GuIdancE. The DDS estimates the "probability that successful natural regeneration will be achieved during a five year period" (considered as a density of 2,500 seedlings per hectare taller than 50 cm). A further analysis of the silvicultural experts' opinions led to the preparation of an improved DSS, described in Kerr *et al.* (2011b), that is based on (with decreasing order of importance): (i) density of existing regeneration; (ii) percentage of ground that is bare or covered by mosses; (iii) level of coning; (iv) time since last thinning. REGGIE has a strong biological validity and an ease of application that makes it very useful for real practice by any end user. On the other hand, it has never been validated and because of the importance given to advance regeneration, it relies on a field survey to estimate those variables; in addition, it does not give indications of how to obtain the initial stage of regeneration.

3.3 Early growth

Consistently with general plant biology, in most of the studies carried out in stands managed using shelterwood systems, height growth was reduced in denser stands, which were the ones with lower light availability on the forest floor (Page *et al.* 2001; Mason *et al.* 2011; Black 2013). However, only weak negative relationships were found between height growth and simple stand parameters such as stand basal area, and few situations were considered. Stronger relationships were found by Herd (2003) and Bertin *et al.* (2011) using light availability as

predictor for height growth, but again they considered only a few isolated cases or a few seedling size classes. When both the height and radial growth were analysed, sometimes contrasting results were found. In different controlled experiment (Brix 1972; Mason *et al*. 2004; Bertin 2009), light availability significantly increased diameter and/or biomass growth, but not height growth, while in another (Fairbairn & Neustein 1970) both diameter and height growth increased with higher light availability. Hale *et al*. (2004) ran a seedling biomass growth model to simulate Sitka spruce seedlings growing under different levels of below-canopy radiation. They found out that seedlings under a 20% relative light intensity (compared to full light) experienced a growth about half of that under full sunlight, and thus defined this light level as the minimum for good growth. Studies of regeneration in gaps have focused on the relationship between the gap size and seedling growth, comparing also the different areas within the gap. Both McNeill & Thompson (1982) and Page & Cameron (2006), found that seedlings of Sitka spruce grew taller in the central areas of the gap than in the shaded edge areas. In North America, Taylor (1990) observed that the radial growth rate of Sitka spruce increased with larger gaps, suggesting a minimum gap-size of 0.1 ha for good growth.

Mason (2015) in his review concluded that there is good evidence that Sitka spruce regeneration under canopy cover requires at least 20-25% of full light for adequate growth, and that such a light regime can be obtained with a basal area less than 30 m^2 ha^{-1} and stem density less than 460 trees ha^{-1} (according to Hale *et al.* 2009). As a comparison in Canada, Carter & Klinka (1992) found that Douglas fir reached a growth of about half that under full sunlight at values of 20-40% of full light, and western hemlock reached this level at 10-20% of full light (variable with soil moisture). Findings were similar for both height and diameter growth. Still in Canada, Wright *et al.* (1998), found that western hemlock reached about half of its growth under full sunlight at around 20% of full light for diameter growth and already at 5% of full light for height growth. Sitka spruce was considered by Minore (1979) to be more shade-tolerant than Douglas fir in its native habitat, while in the UK the reverse is reported by Malcolm *et al*. (2001) and Mason *et al*. (2004) consider them to have almost similar light requirements. Western hemlock was considered undoubtedly the most shade-tolerant species by all those authors.

3.4   Regeneration mortality

Few studies have attempted to measure the seedling survival rate, particularly past the establishment phase. As previously mentioned, in shelterwood systems a certain level of cover may be beneficial, and mortality was sometimes found to be higher in both very dense and

open conditions than in medium conditions of cover (Fairbairn & Neustein 1970; Mason *et al*. 2004). In contrast, Herd (2003) found that mortality increased significantly with stand density. Regarding studies of regeneration after group felling, McNeill & Thompson (1982) found uneven mortality across different positions in the gaps, and that the survival rate was not related to the growth rate (gap areas where the seedlings grew more were not the same as those where they survived best). Competing ground vegetation and drought were the major causes of death, both varying according to the position in the gap due to different light and solar energy levels. Mortality by browsing has been studied only a few times, with low observed levels in the field (McNeill & Thompson 1982; Page & Cameron 2006; Mason *et al*. 2011). Nixon & Worrell (1999) state that Sitka spruce is a relatively unpalatable species for deer, but it can be still damaged heavily. Butler (2016) carried out a growth-mortality study for Sitka spruce seedlings in one stand. He measured for both alive and recently deceased seedlings their relative height and diameter growth (respectively to their total height and diameter), averaged over their last three vegetative seasons. He found that the recently deceased seedlings had relative height growth of 15% and a relative diameter growth of 12%, significantly lower than for the alive seedlings. However, the study was carried out in only one study site and limited regarding the seedling size range and replicates.

Stokes, Kerr & Ireland (2009) studied harvesting damage on Sitka spruce regeneration, after thinning of mature crop trees in two Sitka spruce dominated stands. They found 49%-65% of regenerating trees taller than 200 cm with signs of heavy damage, while 45%-65% of the smaller trees were lost. Both the harvesting methods used (motor-manual felling and harvester felling) resulted in heavy losses and heavy damage, which happened mostly in the extraction racks. However, they found that despite the high losses, seedling density was likely to be sufficient to restock all sites.

3.5 Conclusions

In the UK, continuous cover forestry is still not widely developed and most of the examples available for Sitka spruce are from traditional artificially-planted stands at different stages of transformation towards more complex structures. Most of the studies carried out focused on comparing a few stands managed with different silvicultural treatments to provide broad guidance for forest managers. The situations covered were limited and may be different from the future and possibly more irregular forest structures. For these reasons, and considering also the literature review carried in the previous Chapter, I defined the following framework for the experimental work of this Thesis.

For regeneration occurrence, I selected the two-stage approach as described for the original MOSES. I decided to employ empirical methods to establish meaningful quantitative relationships between Sitka spruce regeneration occurrence and density and the wide range of stand and site characteristics found to be affecting those processes. Existing examples of predictive models in the UK, based on only few stand or management characteristics, have had little success in describing the complex regeneration processes. It is thus important to include the various key factors identified in this review (such as a combination of variables addressing seed availability, germination conditions, micro-climate and competition from the overstorey). For the regeneration occurrence, plots or stands where regeneration was not present were either not selected or not highlighted in most of the reviewed studies. The only example was from Comeau (2010), who defined a threshold in the overstorey gap fraction necessary for regeneration by comparing areas with presence and absence of regeneration. A regeneration occurrence model must include in its calibration situations with the absence of seedlings, otherwise it will be critically flawed (Miina *et al.* 2006).

Better results are found in literature for regeneration early growth modelling when a basic ecological variable such as light availability was considered as the main predictor, instead of simple stand or management characteristics. Thus, I decided to adopt a more mechanistic approach by investigating light-growth functions. I can calibrate such functions by sampling regeneration present in the few existing forest structures, and they will still have a wider range of application in the potentially-different future structures. For the time being, the existing model of light availability prepared for Sitka spruce stands in the UK by Hale *et al.* (2009) can be used as input, but for the future a light model with a wider range of use will also be required. The contrasting results sometimes found between height and diameter or biomass growth suggest the need to further study more growth parameters at the same time.

Regarding mortality, due to the lack of existing data, only the growth-mortality approach would have been possible, expanding for example on the work from Butler (2016). However, there was not enough time or resources to carry out this on the present study.

4 Predicting Sitka spruce natural regeneration presence and density

In this chapter, I investigate a model for estimating the likelihood of Sitka spruce regeneration presence, and one for simulating the seedling density in the plots with regeneration. I used for calibration a dataset from an existing survey. I tested the models' performances first by a cross-validation process, and then by an independent validation with newly collected plots.

4.1 Introduction

The aim of the work described in this chapter was to prepare predictive empirical models for the presence and density of Sitka spruce regeneration under canopy cover, by investigating as main predictors the factors previously identified (Chapter 3) as affecting such processes.

In the absence of studies following the development of such regeneration over time, the dataset generated by Kerr *et al.* (2011) is the most comprehensive regeneration survey of coniferous forests available in the UK to date, covering a wide range of forest structures and geographical areas. They recorded a wide range of variables known to be associated with Sitka spruce regeneration occurrence, from stand characteristics to site characteristics and management information. I thus decided to use this dataset for calibration. However, there were some limitations. The dataset was produced by a one-off sampling, including neither detailed information on the timing of the regeneration establishment nor on its size. A model calibrated on such data could not have a clear temporal horizon for past regeneration events whereas, for example, the MOSES regeneration tool was calibrated with seedlings that were no more than five years old (Hasenauer & Kindermann 2006). The age of the regenerating trees could have been highly variable, and so could the biological processes they had been through. For example, if seedlings had just recently germinated, they had undergone only the germination and establishment phases, but for older seedlings the long-term survival processes could have been important as well.

The only possible approach using such a dataset was to model the regeneration "presence", and not the regeneration "occurrence", the latter defined as the seedling establishment within a time interval. I calibrated models that could generate a regeneration tally like one produced from a field survey, for stands which do not have this information. I applied a two-stage approach like the one described in Chapters 2 and 3. First, I modelled the likelihood of Sitka spruce seedling

presence, then its density. For each stage I identified the significant variables within the wide range of those included in the original survey. I could not prepare models predicting the size of the established regeneration, as described for example by Ferguson *et al.* (1986), due to the lack of this information in the dataset. I considered plots as modelling units to allow the predictions to be sensitive to within-stand variations, as recommended by Miina *et al.* (2006). The models prepared were then validated with an independent dataset.

4.2 Methodology

4.2.1 Calibration dataset

Kerr *et al.* (2011) carried out multi-level sampling during 2008/09 in 129 stands of coniferous species located in 38 forests across most of Great Britain. From this, I extracted information on 34 artificially–planted, Sitka-spruce-dominated stands, located in 13 forests evenly distributed across most areas of Great Britain where Sitka spruce is present (see Figure 4.1). In the original survey, ten 0.01 ha circular plots (radius 5.6 m) were laid out in each stand, recording diameter at breast height (DBH, measured at 1.30 m above ground) and species for all trees more than 7 cm DBH. In a 2 m x 2 m square located at the centre of the circular plot, the number and species of all trees less than 7 cm DBH were recorded, differentiating between seedlings (height less than 1.30 m) and saplings (height more than 1.30 m). From the 340 plots retrieved, 138 showed at least one Sitka spruce seedling or sapling (40% of the total). I considered those plots to have presence of regeneration. Since saplings occurred in only four plots, in which seedlings were also present, I decided not to differentiate between them. From now on in this chapter, I will refer to all regenerating trees as seedlings. The main characteristics of the calibration dataset are indicated in Table 4.1.
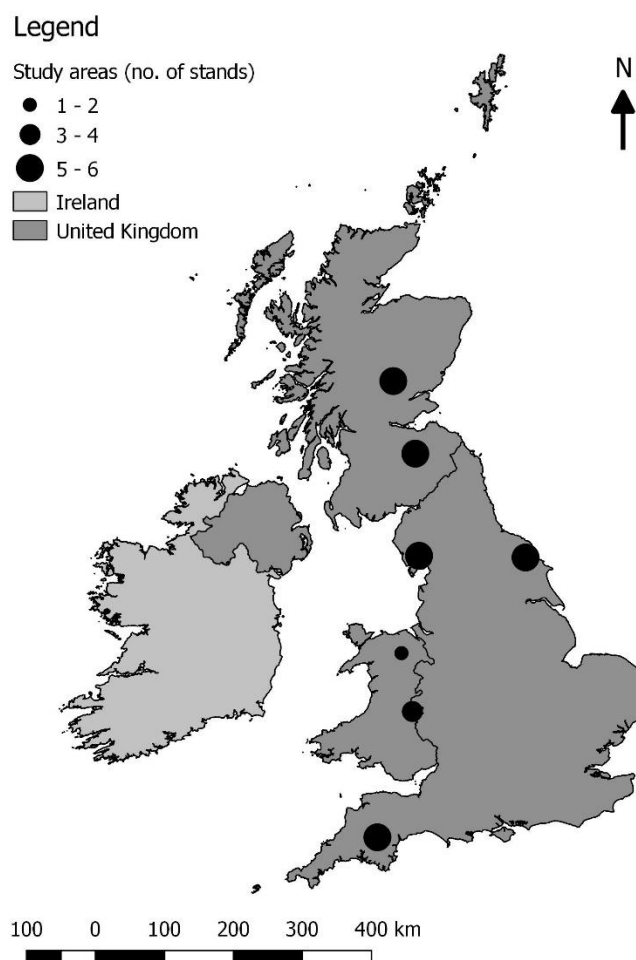
Figure 4.1. Location of study areas and number of stands sampled in each

Table 4.1. Details of calibration dataset. Values at stand (Age, Quadratic Mean Diameter, Soil nutrient regime, Time after last thinning and Deer Impact Index) and plot level (the remaining parameters).

Variable	Min.	1st Qu.	Mean	3rd Qu.	Max.
Age (years)	32	39	54.5	64	85
Basal area (m^2 ha^{-1})	1.6	43.6	58.0	70.0	196.0
Stems per hectare (n ha^{-1})	0	400	700	900	2,200
Quadratic mean diameter (cm)	17.3	21.1	27.9	31.9	51.9
Maximum diameter breast height (cm)	0	36.0	45.3	52.0	90.0
Gap fraction (%)	1.1	11.6	19.2	24.5	79.5
Global Site Factor	0.02	0.16	0.21	0.26	0.55
Bare ground (%)	0	0	1.2	0	85.0
Mosses (%)	0	5.0	41.6	80.0	95.0
Seedling density (ha^{-1})	0	0	20,780	10,000	450,000
Soil Nutrient Regime	**Very Rich**	**Rich**	**Medium**	**Poor**	**Very poor**
Plots (n)	10	10	130	180	10
Time after last thinning	**Class 1 (1-5 years)**		**Class 2 (6-10 years)**		**Class 3 (10+ years)**
Plots (n)	170		90		80
Deer Impact Index	**Low**		**Moderate**		**High**
Plots (n)	10		290		40

23

Age of the plantation in years (from now on simply Age), Soil Nutrient Regime (SNR), time after last thinning, and Deer Impact Index (DII) were recorded at stand level. I calculated from the original inventory the plot level values for basal area (BA), stems per ha (SPH), and the maximum DBH (maxDBH). Then, from those values I calculated the quadratic mean diameter (QMD, the diameter of a tree considered as having the average basal area) at stand level; the canopy gap fraction (GF) at plot level, using the relationship established from Comeau, Kerr & Hale (2010); and the Global Site Factor (GSF) at plot level, an indication of the canopy light transmittance, using the relationship established from (Hale *et al.* 2009).

As an indication of seed availability, I investigated the use of Age and two possible alternatives. Hasenauer & Kindermann (2006) for MOSES used maxDBH (at plot level) to represent a mother-tree effect, while Schweiger and Sterba (1997) used QMD (at stand level) as a substitute for age; both were positively correlated with regeneration occurrence in mixed-species, uneven-aged forests. However, in this dataset both maxDBH and QMD were negatively correlated with regeneration presence (preliminary results not shown). For this reason, maxDBH was considered as a possible indicator of local overstorey competition (see later) while QMD was discarded.

The SNR was estimated by the original field surveyor from analysis of the ground vegetation following the Ecological Site Classification criteria (Pyatt, Ray & Fletcher 2001). Most of the stands were located on sites with either medium or poor SNR (respectively 38% and 53% of the total plots). Those two classes did not show a significant difference from each other in terms of regeneration presence frequency (Fisher's exact test, two-sided: p=0.556, n=310), and only 9% of the plots were in other SNR classes, so I excluded this factor from further analysis. The SNR class indirectly influences regeneration due to its effect on ground vegetation, as described previously. Since the dataset included for the 2 m x 2 m plots the percentage of ground covered by different classes of vegetation, I decided to use as candidate variables the favourable ground cover classes of Mosses and Bare Ground, instead of SNR, consistent with the model prepared by Kerr *et al*. (2012).

I considered the plot-level stand density measures of BA, SPH and maxDBH as a negative proxy for the light regime under the forest cover (higher stand density, lower light level) and so expected to be negatively correlated with regeneration presence. On the other hand, both GF and GSF are a more direct indication the light regime under the forest cover, so I expected them to be positively correlated with regeneration presence. The time since the last thinning was estimated for each stand using both historical records and evidence on the ground; the expected

effect was a negative correlation between the time since the intervention and the likelihood of regeneration. I divided the stands in the present study into three different Thinning Classes (TC) as in Kerr *et al*. (2011): TC1, thinned in the last 1-5 years; TC2, thinned 6-10 years before; TC3, thinned more than 10 years before or never. I used discrete classes since there was often an uncertainty in the precise timing of the thinning. In some cases, it was observed that a thinning was carried out only in a fraction of the stand. Since I could not identify which specific plots were affected, I assigned an approximate thinning class to the whole stand with a subjective decision (for example, when only half of the stand was reported to be affected by a recent thinning as in TC1, and the rest by none, a TC2 was assigned to all the plots). I considered this variable as numeric.

The Deer Impact Index (DII) was visually estimated as low (no browsing observed), moderate (browsing damage on up to 25% of the regeneration) and high (browsing damage on more than 25% of the regeneration). Because of the unbalanced distribution (see Table 4.1) and the lack of significant differences in regeneration presence frequency between the moderate and high impact classes (Fisher's exact test, two-sided: $p=0.611$, $n=330$), this factor was discarded from further analysis.

Additionally, I retrieved stand-level geographical variables from topographic maps, namely northing, easting, elevation and aspect, and stand-level climatic variables from the Forestry Commission's decision support system ESC-DSS (Pyatt, Ray & Fletcher 2001), namely accumulated temperature above 5 ˚C, moisture deficit, Conrad continentality index and total summer and winter rainfall. Preliminary analysis (not shown) revealed that none of those variables was significant when included in a model and they were all discarded.

The density of Sitka spruce seedlings per plot was very different between the Thinning Classes, as shown in Figure 4.2, where only values from the plots with presence of regeneration are presented. Almost 97% of the seedlings in the study stands were Sitka spruce and different species were sporadic (present in only 2% of the plots); for simplicity the latter was ignored during the analysis. At stand level, considering all the plots with or without regeneration, there were on average of 20,740 seedlings per ha, with a minimum of 0 and a maximum of 250,000.
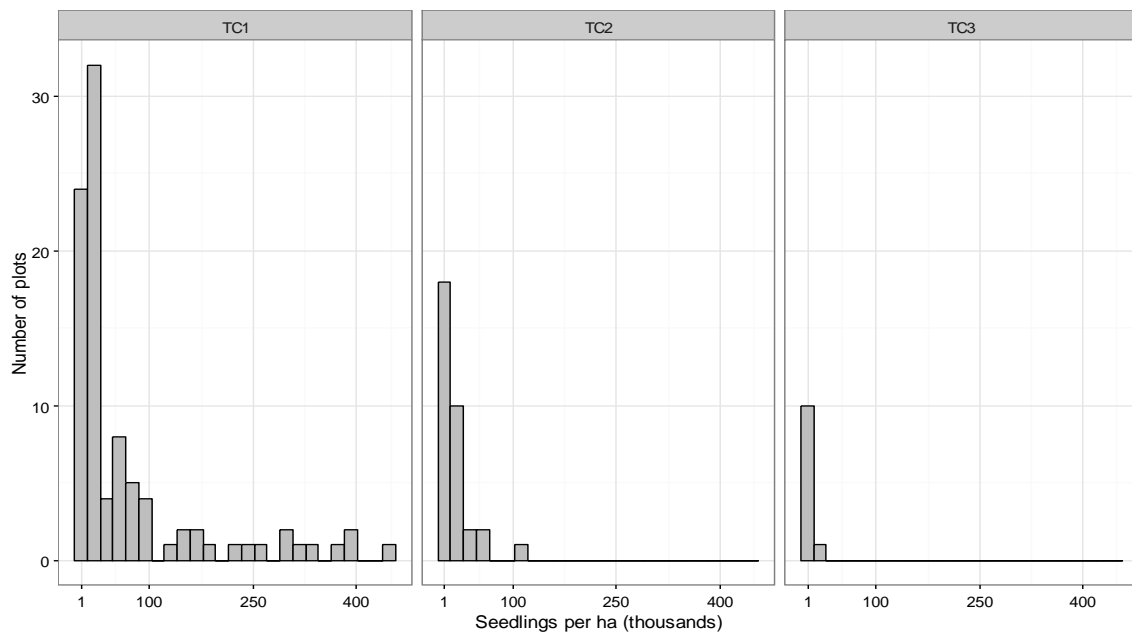
Figure 4.2. Frequency of seedlings per hectare in different Thinning Classes (TC1, TC2 and TC3), only plots with presence of regeneration, for the calibration dataset.

4.2.2 Independent validation dataset

For independent validation, I assessed in 2016 four Sitka spruce dominated stands in Clocaenog forest, Denbighshire, Wales (53° 04′ N, 3° 25′ W, 390-430 m altitude), and four in Kielder forest, Northumberland, England (55° 10′ N, 2° 29′ W, 200-250 m altitude). Both forests were originally artificial plantations, but have been managed in recent years according to different CCF principles, using silvicultural systems ranging from irregular shelterwood to group selection. All stands belonged to Thinning Class 2, but most of them were thinned more frequently or with higher intensity in the past than stands in the calibration dataset. The situation in all stands was generally a lower tree density than under the traditional management (as defined by Edwards & Christie 1981), leading to a larger amount of natural regeneration. In each stand, I laid out ten plots with a random-systematic approach. I drew random non-parallel transects on a desktop map and placed on them evenly spaced plots, later located in the field using a GPS receiver. The distance between plots varied with the size of the stand. I followed the same data collection protocol used for the calibration dataset and collected in this way 78 plots. The main characteristics of this dataset are shown in Table 4.2 for a comparison with the calibration dataset. SNR, DII and QMD were not considered, as in the calibration dataset. Again, I considered all seedlings and saplings as "seedlings", and a total of 62 plots (about 80% of the total) had at least one of these. At stand level, considering all the plots with or without

26

regeneration, there were on average 46,940 seedlings per ha, with a minimum of 4,500 and a maximum of 171,800.

Table 4.2. Details of validation dataset. Values at stand (Age and Time after last thinning) and plot level (the remaining parameters).

Variable	Min.	1st Qu.	Mean	3rd Qu.	Max.
Age (years)	60	65	69	77	80
Basal area (m² ha⁻¹)	7.6	28.8	41.4	53.8	107.2
Stems per hectare (n ha⁻¹)	50	200	284	400	1,100
Maximum diameter at breast height (cm)	35	44	50.6	55.8	85
Gap fraction	4.8	23.1	32.9	39.6	66.0
Global site factor	0.08	0.22	0.28	0.34	0.49
Bare ground (%)	0	0	0.1	0	4
Mosses (%)	0	70.6	82.3	99.7	100
Seedling density (ha⁻¹)	0	2,500	48,460	52,500	417,500
Time after last thinning	**Class 1** **(1-5 years)**		**Class 2** **(6-10 years)**		**Class 3** **(10+ years)**
Plots (n)	0		78		0
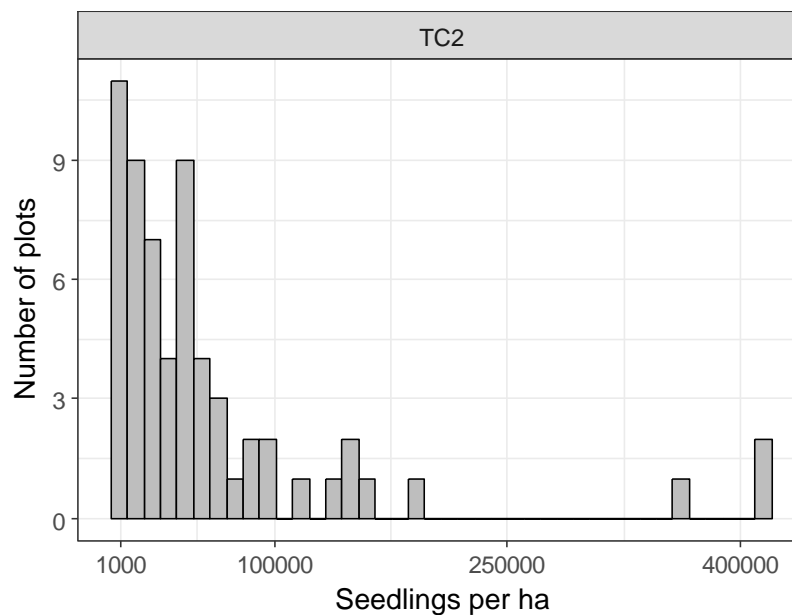
Figure 4.3. Frequency of seedlings per hectare, only plots with presence of regeneration, for the validation dataset.

4.2.3 Statistical analysis

4.2.3.1 Regeneration presence

I carried out all the analyses using the R Statistical Software (R Core Team 2017). To estimate the probability of regeneration presence, I used a Generalized Linear Mixed Model (GLMM) fit by maximum likelihood (Laplace Approximation) with Binomial function and Logit link, from the package *lme4* (Bates *et al.* 2014). Possible autocorrelation effects were considered

using the stand and forest levels as random "nesting" effects. The candidate fixed effects for the model were Age, BA, SPH, GF, GSF, maxDBH, Thinning Class, Mosses and Bare Ground. I included a quadratic term for BA, SPH, and maxDBH to check if the relationship between stand density and regeneration was non-linear, as a certain level of canopy cover can be beneficial to natural regeneration. Then I removed non-significant parameters using a step-wise approach aimed at reducing the Akaike Information Criterion (AIC) to select the final model (Yamashita, Yamashita & Kamimura 2007). I then re-calibrated the selected model structure on standardized variables. Standardization means rescaling the variables so that their new mean is equal to zero and the standard deviation to 1. This process transforms all the variables with different orders of magnitude to a similar scale, still maintaining their variability, and so also the magnitude of the model coefficients becomes directly comparable.

After I identified the best model, I assessed its accuracy with a cross-validation technique (Bennett *et al.* 2013). I re-calibrated the coefficients of the best model structure by removing all the plots belonging to one stand from the calibration dataset. Then I validated it on the plots belonging to the left-out stand and calculated their likelihood of regeneration presence. I repeated the process 34 times, once for each stand. After I estimated in such a way the likelihood of regeneration for each plot, to determine which ones the model would predict to have regeneration, I used two methods.

In the first method, I defined a cut-off likelihood value using the Receiver Operator Characteristics (ROC) curve method with the package *pROC* (Robin *et al.* 2011). I assigned the presence of regeneration to all plots with a likelihood above the cut-off, and otherwise the absence of regeneration. I estimated this cut-off as the likelihood value that would maximise the sum of sensitivity (the proportion of correctly identified positive plots, that is in this case with presence of regeneration) and specificity (the proportion of correctly identified negatives, that is with absence of regeneration). Once each plot was assigned its simulated status, I built a contingency table to compare the predictions with the observations. In the second method, I used a stochastic approach (e.g. as used in MOSES). I generated for each plot a pseudo-random number between 0 and 1. If that number was lower than the regeneration likelihood, the plot was considered to have regeneration; other plots were considered to be without regeneration. I ran the simulation 10,000 times, averaged the results, and built another contingency table. For both methods, I analysed the results also at stand level in the following way. For each stand, I calculated the difference between the total of all simulated regeneration plots minus the total observed ones. Then I checked the field notes to subjectively investigate why predictions were

in error for the stands with the worst results (as in Ferguson *et al*. 1986). For this analysis, I did not consider it important if individual plots were wrongly simulated if the overall predictions at stand level were accurate.

4.2.3.2 Regeneration density

I used two approaches. First, I investigated GLMMs using the same random and fixed effects as described above, using the sub-dataset for plots with presence of regeneration (n = 138). A Gamma distribution with log-link was the function best approximating the seedling distribution. Preliminary models based on all plots with presence of regeneration (n = 138) could not converge regardless of the combination of variables used (results not shown). The importance of the Thinning Class was evident from the sharp difference in seedling distribution amongst the classes, so I decided to calibrate separate models for TC1 and TC 2 & 3 (pooled together due to the lower number of observations). For those two subsets of data, I prepared GLMMs using the same random and fixed effects as described above (excluding obviously Thinning Class). Then I removed non-significant parameters using a step-wise approach aimed at reducing the AIC. I evaluated the accuracy of the resulting best GLMMs through comparing predicted and observed values at plot and stand level.

For the second approach, I simulated the seedling density simply by generating random numbers that approximated the observed density distribution for each Thinning Class. This method in its simpler form is as old as the model JABOWA (Botkin *et al*. 1972), and suggested with more refinement by PROGNOSIS (Ferguson & Carlson 1993; Schweiger & Sterba 1997) and MOSES (Hasenauer & Kindermann 2006). I fitted Weibull distribution functions to simulate the distribution pattern of the seedlings in each Thinning Class group using the package *MASS* (Venables & Ripley 2002). I used the values of seedlings per ha observed at plot level transformed to units of 1,000 for simplifying the calculations. For validation, in each plot observed with regeneration, I generated a random number 10,000 times from the resulting functions and averaged the results. I then compared the observations and simulations averaged at stand level. I did not compare results at plot level analysis since the random generation of numbers makes this analysis impossible.

4.2.3.3 Independent validation

With the resulting version of the model for regeneration presence as above, calibrated on the full dataset, I calculated the likelihood of regeneration presence in the independent validation plots. Then, I again used the same two methods as before to assign the presence of regeneration.

First, I considered the same cut-off likelihood value previously determined with the ROC method and I assigned the status of presence of regeneration to all plots above that threshold. Second, I used the stochastic method to randomly determine the presence or absence of regeneration. I built contingency tables for both methods for the results at plot level, and examined the performance at stand level by comparing the total numbers of simulated and observed plots with regeneration, with the same procedures described above for the cross-validation.

Then, I used both seedling density modelling methods prepared with the calibration dataset to simulate the density in the plots of the independent datasets with observed presence of regeneration. The simulated seedling density was compared with the observed values.

4.3 Results

4.3.1 Regeneration presence

The model structure after the step-wise AIC reduction process is shown in Model 4.1, with more details of the coefficients shown in Table 4.3.

$$\text{Model 4.1: } p_{\text{regen}} = \frac{1}{1 + e^{2.693 + 1.864 * TC - 0.087 * Age - 0.020 * Mosses + 1.569 * (BA/100)^2}}$$

The model did not converge when the forest-level random effect was included, so I maintained only the stand-level effect. The effect of bare ground was not significant, and it had a weak negative relationship with regeneration, contrary to the hypothesis. Only the quadratic term for BA remained in the best model structure amongst the stand density indicators. Note that values of BA were divided by 100 since they were on a different scale from the other variables.

Table 4.3. Details of coefficients of Model 4.1, estimating the likelihood of Sitka spruce regeneration presence at plot-level.

Fixed Effects	Value	St. Err	p-value
(Intercept)	-2.693	1.703	0.114
Thinning class	-1.864	0.556	0.001
Age	0.087	0.030	0.003
Mosses	0.020	0.007	0.005
(Basal area/100)^2	-1.569	0.886	0.076
Random Effects (intercept)	Variance		Standard Deviation
Stand	3.726		1.93

Figure 4.4 displays how the probability of regeneration changes according to variation in the model variables. Using Model (4.1), I calculated the likelihood of regeneration presence for

new virtual datasets. In Figure 4.3 a, I used a dataset where I allowed only TC to vary (from 1 to 3) while the other fixed effects were kept at the mean values of the calibration dataset (as seen in Table 4.1). In Figure 4.3 b, c and d, I allowed respectively Age, BA and Mosses to vary across the full range observed in the calibration dataset, while I kept the other fixed effects at their means except for TC. I repeated the analysis changing the Thinning Class, represented by the different lines (decreasing from 1 to 3 from top to bottom). Generally, from TC 1 to 2 there was a stronger decrease in regeneration likelihood than from TC 2 to 3. For TC 1, regeneration probability decreases more sharply for Age less than 60 years and BA more than 60 m^2 ha^{-1}. For TC 2, only in old stands (more than 70 years old) was the probability of regeneration above 0.5, while for TC 3 the likelihood was always low. The effect of mosses on regeneration likelihood was more linear.
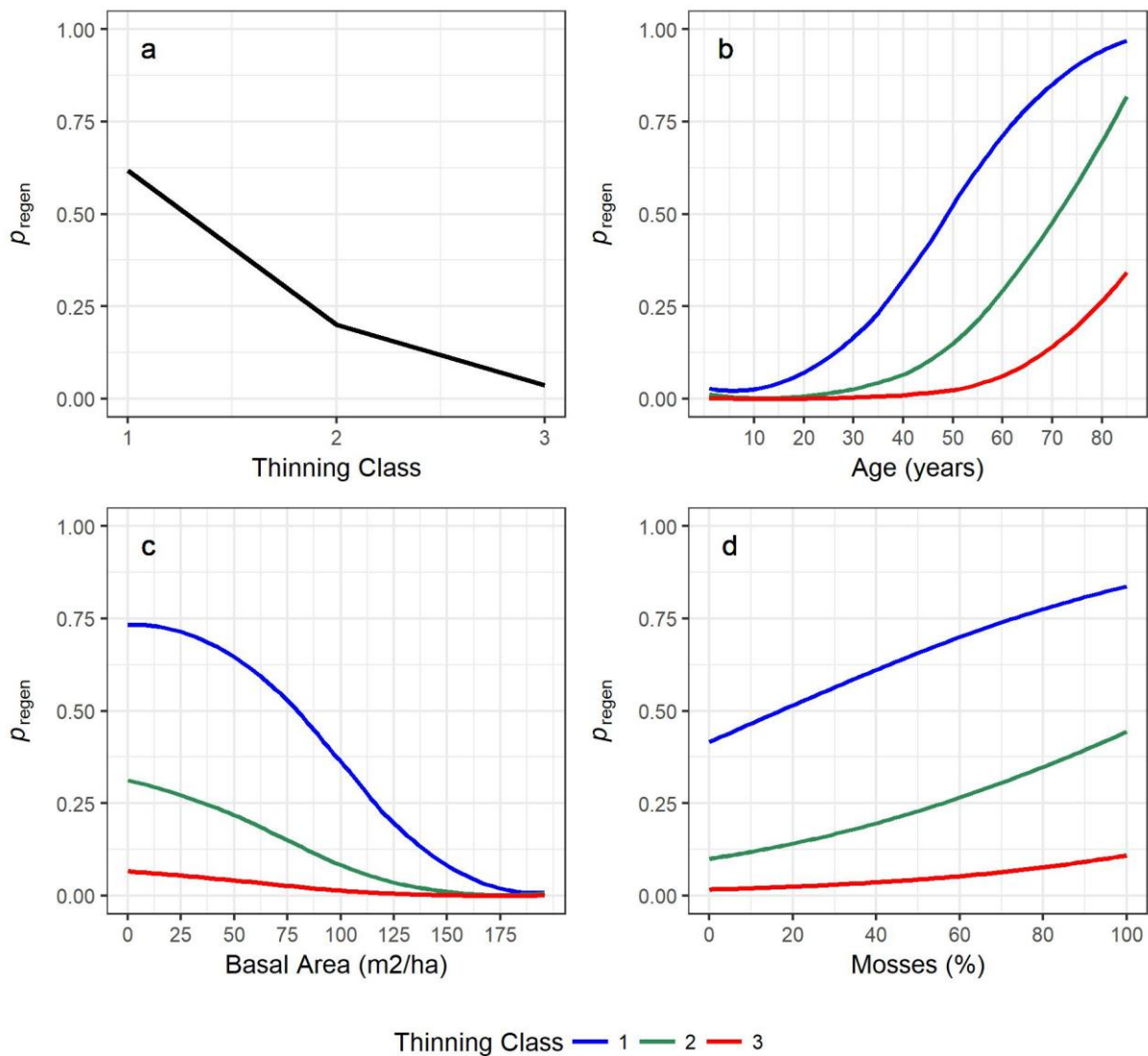
Figure 4.4. Regeneration presence likelihood (p_{regen}) as a function of the model variables. In each graph, the likelihood was estimated with only one variable varying across all its range (plotted on the x-axis), while the others were kept at the calibration population mean. Multiple lines indicate the analysis used different values of Thinning Class

Figure 4.5 shows the coefficient values for the model shown in Equation (4.1) when it was calibrated on the standardized variables. TC had the highest coefficient (i.e most influential) in absolute terms (1.522), followed by Age (1.255), Mosses (0.701) and BA (0.533).
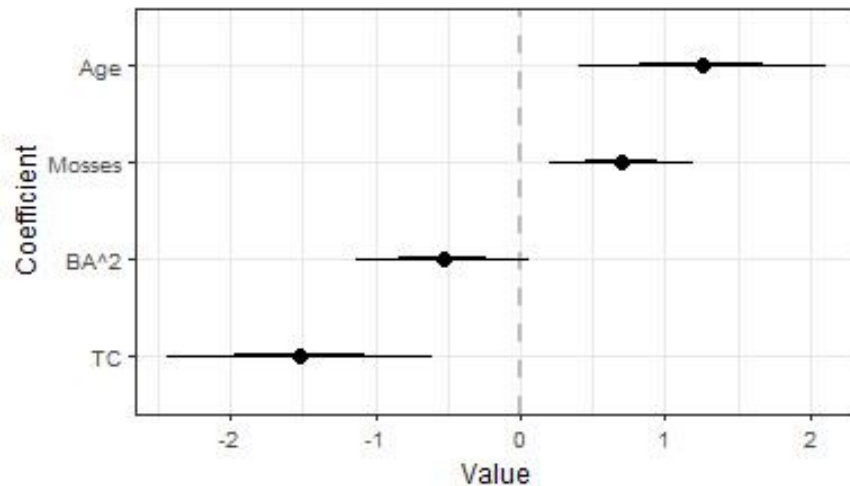
Figure 4.5. Coefficient values after standardization of the model variables (BA = Basal area, TC= Thinning class). The dot corresponds to the mean values, the wider blue line to the 90% confidence interval, the narrower blue line to the 95% confidence interval

After the cross-validation analysis, with the ROC method, the cut-off likelihood value for the regeneration presence probability was 0.3. Figure 4.6 shows the ROC curve, that is all the combinations of specificity and sensitivity values obtained by using all the possible cut-off values. The chosen cut-off was the one that maximised their sum and corresponded to the point on the curve closest to the upper left corner, which would be to the ideal case of both specificity and sensitivity equal to 1. For the ROC method, the plots that had an estimated likelihood above 0.3 were considered by the model to have presence of regeneration. For the stochastic method, the pseudo-random generated numbers were checked with the likelihood values for each plot. Table 4.4 shows the contingency table of using both methods. For the ROC method, the plots correctly predicted (true positives plus true negatives) amounted to 73% of the total. The model estimated with similar accuracy plots with or without presence of regeneration (respectively 76% and 71%). For the stochastic method, there was a markedly lower accuracy in sensitivity (55%) and only a slightly better specificity (74%), bringing the overall accuracy lower than in the ROC method (66%).
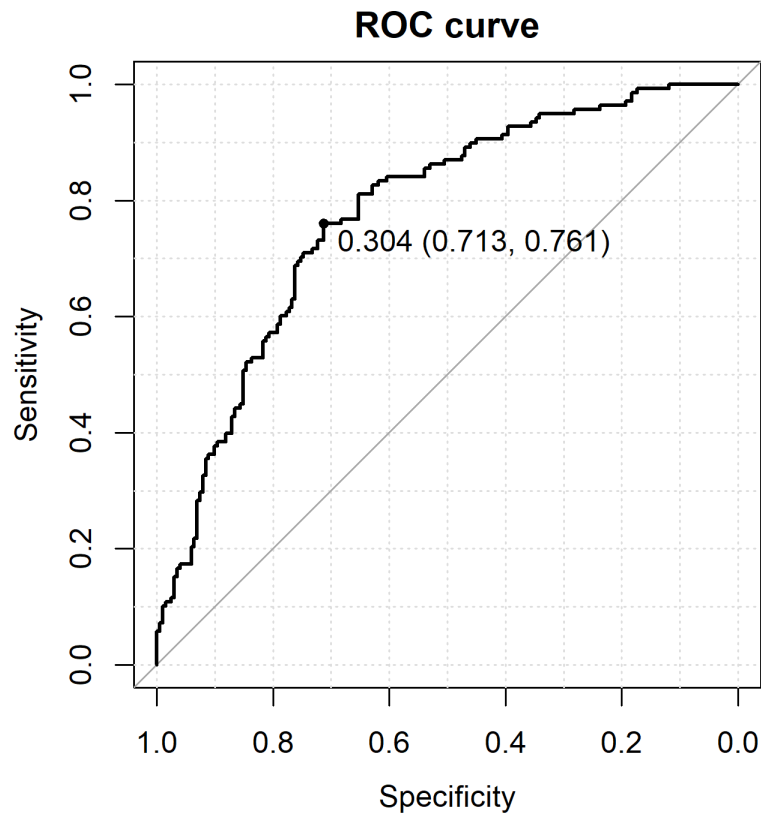
Figure 4.6. Receiver Operator Characteristics (ROC) curve for the cross-validation method. The dot represents the point with the highest sum of the specificity and sensitivity values (presented between parentheses) and shows the corresponding cut-off likelihood value.

Table 4.4. Contingency tables for the cross-validation results using the Response Operator Curve (ROC) method and stochastic method. YES indicates the presence of regeneration, NO the absence.

ROC method		Predictions			Partial Accuracy
		YES	NO	Total	
	YES	105	33	138	0.76
Observations	NO	58	144	202	0.71
	Total	162	178	340	
Overall accuracy					0.73

Stochastic method		Predictions			Partial accuracy
		YES	NO	Total	
	YES	76	62	138	0.55
Observations	NO	52	150	202	0.74
	Total	128	212	340	
Overall accuracy					0.66

The results aggregated at stand level for both methods are shown in Figure 4.7. Stands with negative values had fewer simulated regenerating plots than observed, and vice versa. For the ROC method, 21 stands out of 34 had a difference between total observed and predicted regeneration plots equal to or lower than 20% (11 with no difference), while five had a

difference equal to or larger than 50% (worse than chance). For the stochastic method, very similar results were obtained: 22 stands out of 34 had a difference between total observed and predicted regeneration plots equal to or lower than 20% (10 with no difference), while five had a difference equal to or larger than 50%.

The worst simulated stands were almost the same stands in both methods. The field notes provided additional insights about them, showing that they were generally the ones subjected to heterogeneous thinning interventions within the same stand, suggesting that the TC class was inaccurate. In stand with fewer simulated regenerating plots than observed, it was also observed that windblow events had opened gaps comparable to a thinning, or that there was precocious cone production in young stands. In stands with more simulated regenerating plots than observed, it was noted that in stands favourable for regeneration according to all the model variables, the limiting factors were likely to be: competing ground vegetation; presence of deer browsing; and lack of cone production. In the two worst over-simulated stands for both methods, the field notes declared that everything seemed suitable for regeneration and its total absence was inexplicable for the surveyor too.
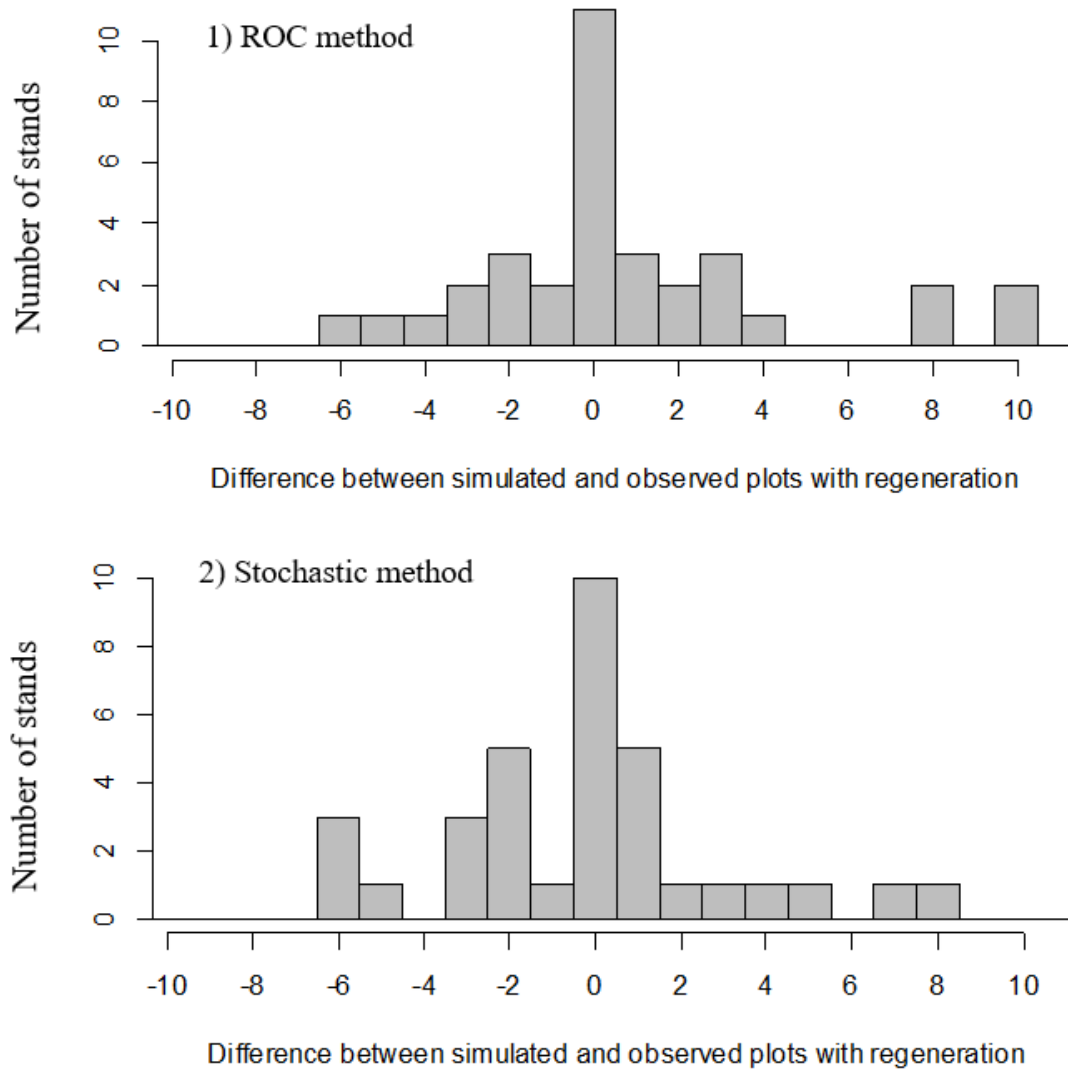
Figure 4.7. Differences between the total number of simulated and observed plots with regeneration presence at stand level for the Response Operator Curve (ROC) method (above) and for the stochastic method (below). Stands with negative differences had less simulated regenerating plots than observed, and vice versa.

4.3.2 Regeneration density

In the GLMMs calibrated for TC 1 and TC 2 & 3, only the effect of BA was significant, but with a positive relationship with seedling density in the former class (TC 1) and a negative relationship for the latter group (TC 2 & 3). However, both models showed a very poor fit between the simulated and observed density values and they were discarded (results not shown).

The Weibull distributions fitted to seedling density distribution in each TC are described by the parameters in Table 4.5. Figure 4.8 shows the comparison between the distribution of simulated values of seedlings per ha and the distribution of the observed values, considering all plots with regeneration. While the fit was adequate at whole-population level for each Thinning Class, at

stand level it did not provide good results: Figure 4.9 shows the comparison of the simulated values when aggregated at stand level. Generally, there was a poor correspondence between those values: only two stands had a simulated density ± 20% of the observed density. On average, the difference between simulated and observed values was 770 seedlings ha^{-1}, but with extremes of -177,500 and 59,000 seedlings ha^{-1}.

Table 4.5. Parameters for the Weibull distributions fitted to seedling density per ha (thousands)

	Shape	Rate
Thinning Class 1	0.696	52.555
Thinning Class 2	0.871	14.134
Thinning Class 3	1.834	4.651
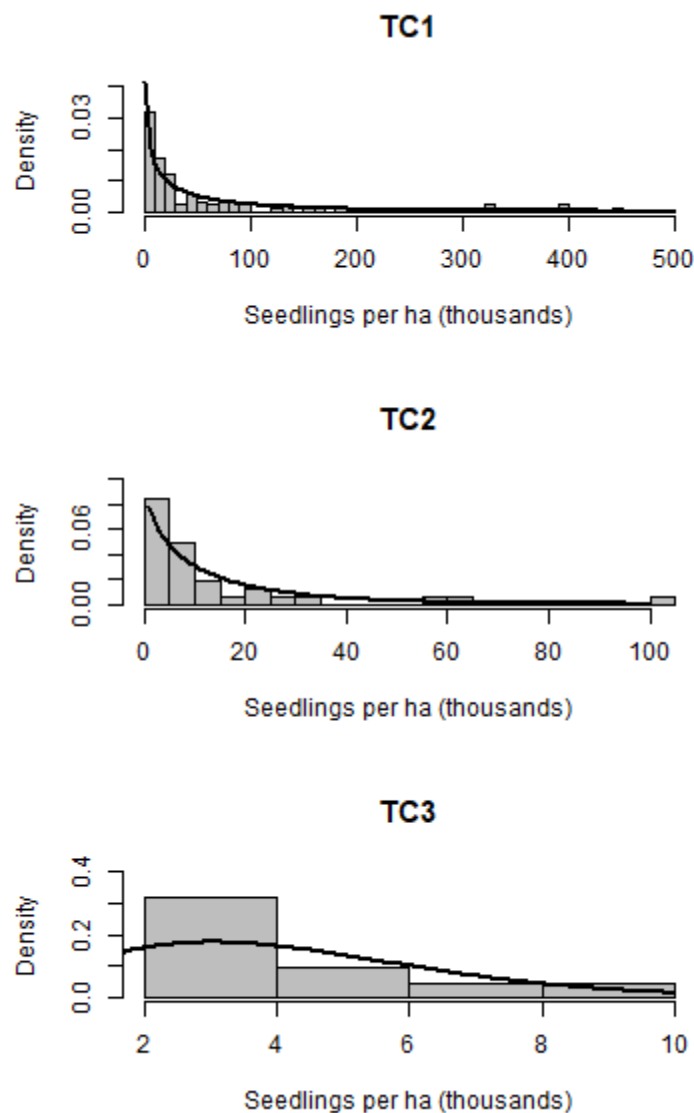
Figure 4.8. Weibull distributions (lines) vs observed number of seedlings per ha at plot level (bars), according to Thinning Class (TC).
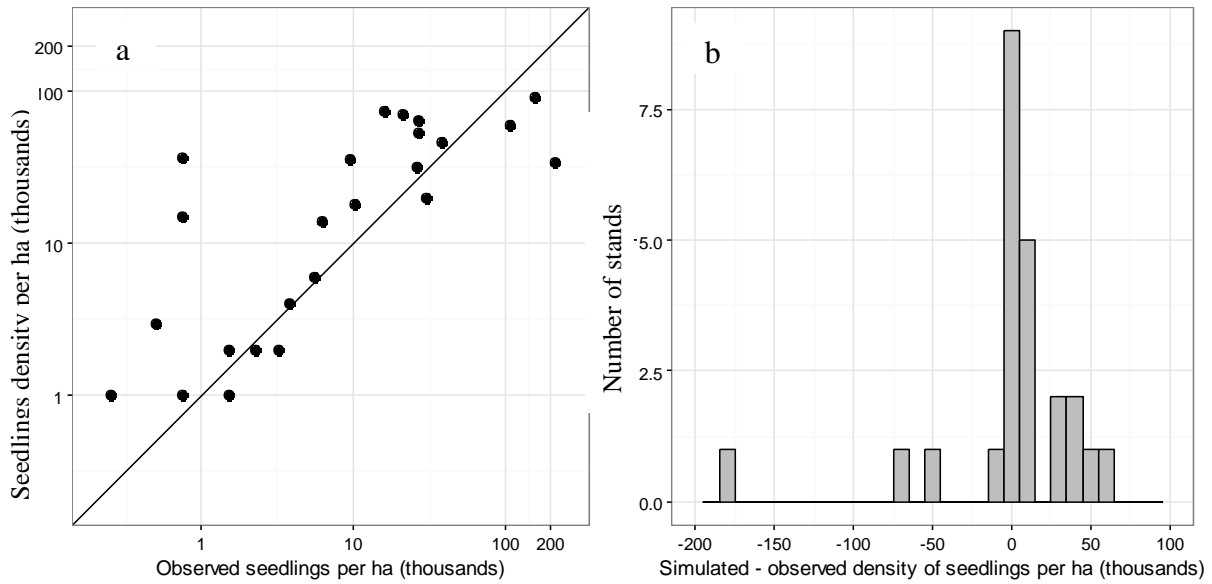
Figure 4.9. Left (a): scatterplot of Weibull simulated and observed seedlings per ha at stand level, plotted on logarithmic scales, using the calibration dataset. Right (b): distribution of differences between Weibull simulated and observed seedlings per ha at stand level, using the calibration dataset.

4.3.3 Independent validation

I used Model 4.1 to calculate the likelihood of regeneration presence in the independent dataset. Using the ROC method, I considered regeneration to be present only in the plots with a likelihood greater than the same cut-off likelihood value of the cross-validation process ($p = 0.3$). The resulting contingency matrix is shown in Table 4.6, together with the results of the stochastic method. For the ROC method, while the total accuracy was 82%, this was because almost all plots (76 out of 78) were predicted to have regeneration, giving a sensitivity of 100% and a specificity of only 12%. For the stochastic method, the overall accuracy was again lower than for the ROC method (64%), although there was a slightly more even balance between sensitivity and specificity. After aggregating the results at stand level, however, worse results were found for the ROC method than for the stochastic method: out of eight stands, respectively four for the ROC method and six for the stochastic method had a difference between total observed and predicted plot with regeneration equal to or lower than 20%. In both methods, two stands had no difference between total observed and predicted plots with regeneration, and none had a difference equal to or larger than 50%.

37

Table 4.6. Contingency tables for Independent validation results using the Response Operator Curve (ROC) method and the stochastic method. YES indicates the presence of regeneration, NO the absence.

ROC method		**Predicted**			**Partial accuracy**
		YES	NO	Total	
Observed	YES	62	0	62	1.00
	NO	14	2	16	0.12
	Total	76	2	78	
		Overall accuracy			0.82

Stochastic method		**Predicted**			**Partial accuracy**
		YES	NO	Total	
Observed	YES	44	18	62	0.71
	NO	10	6	16	0.39
	Total	54	24	78	
		Overall accuracy			0.64

Regeneration density was then estimated in the plots with observed regeneration presence (n=62). Only the Weibull distribution approach was used, with the function previously calibrated for Thinning Class 2. The GLMM approach was already deemed too inaccurate. After averaging the results, there was no good correspondence between the simulated and observed values, and no stands had a simulated density ± 20% of the observed value (see Figure 4.10). On average, the difference between simulated and observed values was -34,570 seedlings ha^{-1}, with extremes of -155,800 and 4,500 seedlings ha^{-1}.
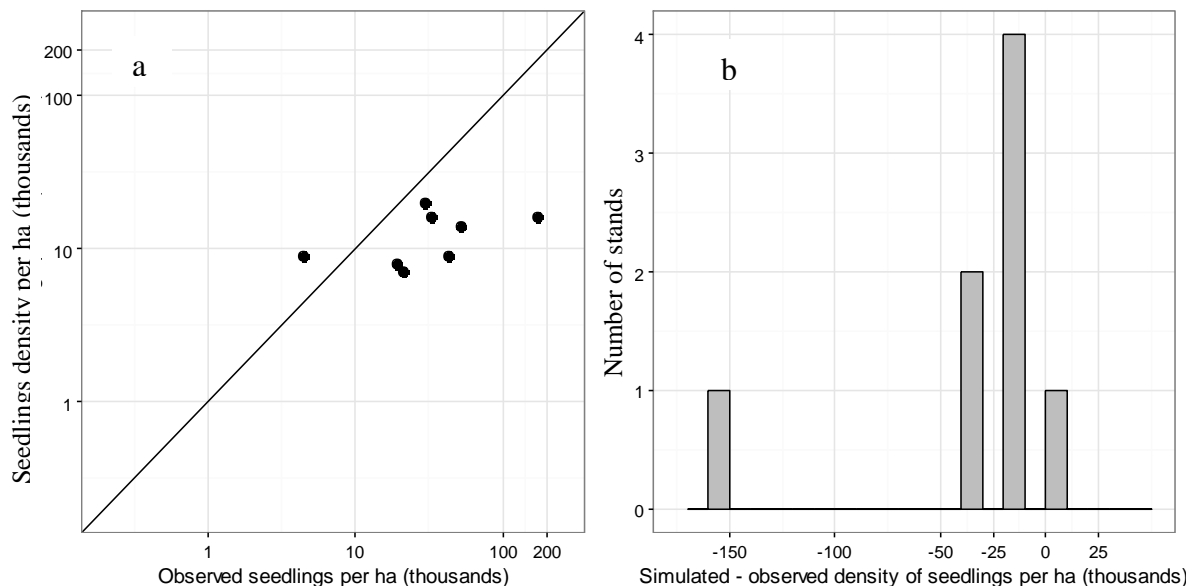
Figure 4.10. Left (a): scatterplot of Weibull simulated and observed seedlings per ha at stand level, plotted on logarithmic scales, using the validation dataset. Right (b): distribution of differences between Weibull simulated and observed seedlings per ha at stand level, using the validation dataset.

4.4 Discussion

A very important limitation of both models was the lack of data on the regeneration size or age. The latter could have been highly variable, and so too the biological processes they had been through. For example, if seedlings just recently germinated, they had undergone only the germination and establishment phases, but for older seedlings the long-term survival processes had been important as well. The stand characteristics at the moment of the regeneration event could have been very different from the survey data. Both the regeneration presence and density model did not consider the possibility of other tree species germinating and competing with Sitka spruce. This would likely be another crucial limitation of the use of these models in mixed forest stands resulting from continuous cover forestry practices. Presence of deer browsing, although not statistically significant in this analysis, was found in the field notes as a possible cause of limiting factor for regeneration in some sites where all the model variables were at a beneficial level for regeneration.

4.4.1 Regeneration presence

The model was based on the established knowledge of the biological and ecological characteristics of Sitka spruce described previously (Chapter 3). The effect of time since the last thinning showed the strongest significance in the model, and the largest coefficient after standardization. Consistently with Kerr *et al.* (2012), the model showed that probability of regeneration presence is high after an intervention, but it decreases rapidly and there is no positive effect after 10 years. If the operations are not repeated, the canopy can revert quickly to a closed status and small seedlings die off (Hale 2003). The field notes showed that inaccuracies in the thinning regime information, or the presence of windblown gaps not considered in the model, were likely causes of the errors in the worst-simulated stands. To improve the accuracy, it is necessary for the model to know which plots are affected by a tree removal, irrespective of whether it is due to natural mortality or timber extraction. In a continuous cover forestry scenario this is likely to be a priority.

The age of the plantation emerged as the second most important factor. Such a positive effect in the artificial plantations of the present study can be explained by the larger seed production of older trees, and possibly also by the higher number of gaps that can naturally occur in a mature canopy past the self-thinning stage. I tested the use of maximum DBH (at plot level) and quadratic mean diameter (at stand level) as possible alternatives to age, but in this research, they were both negatively correlated with regeneration presence. For maximum DBH, it is

likely that large trees present in the small study plots (5.6 m radius) were shading the ground and dispersing their seed outside the plots. Schweiger and Sterba (1997) considered quadratic mean diameter to be a compound measure of age, density and site quality, and here it seems the density effect was predominant. Sitka spruce is a prolific seeding species (up to 20 million seed per ha released under canopy) with an estimated dispersal distance of 60-80 m (von Ow *et al.* 1996; Nixon & Worrell 1999). In pure, even-aged stands seed availability is likely to be a factor not associated with the trees present at local level but with the general production at stand level, with little spatial variation (Malcolm *et al.* 2001). This may change in mixed-species, uneven-aged stands. In those situations, especially since age will not anymore be a suitable measure to describe the stand correctly, better studies on the role of mother trees and seed availability will be necessary. After checking the field notes, cone production that was exceptionally higher or lower than expected for that age of stand was a possible cause of error in the worst-simulated stands, suggesting that seed availability is not only controlled by age, even in single-species plantations.

Mosses showed a positive effect on regeneration, consistent with previous findings. A thin layer of moss cover is favourable for germination due to their water retention capacity, but heavy moss cover can prevent roots from reaching the mineral soil (von Ow *et al.* 1996). LePage *et al.* (2000) found that the same ground cover can have different effects on regeneration according to the overstorey characteristics: for example, the positive effects of moss cover decreased with an increase in canopy cover. These various aspects could be the cause of the relatively low effect of mosses in the model. The cover of mosses was also strongly and negatively correlated with the extent of what were considered negative ground cover classes, such as grasses, other herbs and ferns (results not shown). Still, in some stands the combined presence of competing ground vegetation and mosses seems to have affected the accuracy of the simulation. Further studies may be necessary, considering also the use of more specific classes (such as light and heavy mosses, deadwood in various stage of decomposition).

Increasing competition from the overstorey, expressed here as the quadratic term of basal area, influenced the regeneration negatively, although at low overstorey levels the effect was almost flat. This seemed to confirm the positive effect of a certain amount of shading. The same levels of basal area can be obtained with different numbers of trees, resulting in different canopy structures and thus light availability on the ground. When the number of trees is lower for a given basal area, there are likely to be more gaps between crowns and significantly more light at ground level (Hale *et al.* 2009). However, it is possible that the number of stems per ha was

not significant in the present study because both age and Thinning Class were already partially describing the reduced number of trees resulting from natural mortality and anthropic removals.

None of the topographic and climatic variables tested showed significance. The climatic data were interpolations for 10 km grid squares of average climatic data collected during 1960-90. They had already been found in another study to lack the precision needed for stand analysis (Moore *et al.* 2009). The under-canopy climate is also generally different from the climate of open sites, with a degree of variation according to the stand characteristics (Sellars 2005). Significant differences between forest districts were not identified in this study. Foresters have not observed regional differences in the occurrence of Sitka spruce natural regeneration across the UK (B. Mason, pers. comm.).

The cross-validation process with the use of the Response Operator Characteristics curve showed satisfactory statistical results at plot level: 73% of plots were correctly simulated, with similar values for specificity and sensitivity. The stochastic method, such as is employed by various models, showed worse results: 66% of total plots correctly simulated, with a larger difference between sensitivity and specificity. However, when aggregating the results at stand level and considering the difference between the total simulated and total observed plots with regeneration, the results were similar between methods: around two-thirds of the stands showed an acceptable error (simulated values within ± 20% of observed values). In a non-spatial forest growth simulator (*sensu* Robinson & Ek 2000) such as MOSES_GB, the accuracy at stand level may be more important than at plot level since the actual positions of the trees are not known.

The results of the independent validation with the Response Operator Characteristics curve method were not satisfactory since the model predicted regeneration in almost all plots, even if the total accuracy was 82%. Using the stochastic method, the total accuracy was worst (64%), although there was a slightly better balance between sensitivity and specificity. It is evident that the independent dataset is describing a situation largely different from the calibration dataset, noting the differences both in the stand variables (Tables 4.1 and 4.2) and the high frequency of plots with regeneration presence (about 80% in the independent dataset versus 40% of the calibration). The independent validation stands surveyed have been managed specifically to obtain natural regeneration. All the stands belonged to the Thinning Class 2, but, as already mentioned, most of them had been thinned more regularly and with higher intensity than those in the calibration dataset. When I aggregated the results at stand level and considered the difference between the total simulated and total observed plots with regeneration, the results were better for the stochastic method: two-thirds of the stands showed an acceptable error

(simulated values within ± 20% of observed values), against half for the Response Operator Characteristics curve method. It seems that the cut-off calculated for the cross-validation process cannot be applied to the independent dataset, and although the model still presents problems in its application to continuous cover forestry situations, the stochastic method gave better results in this case.

4.4.2 Regeneration density

Due to the many random factors involved, estimating the regeneration density is extremely difficult (Ferguson 1996). The models tested here did not give results of acceptable accuracy. Generating random numbers from Weibull distributions was, in the present study, the only option found and still produced inadequate results both during the auto-validation and independent validation.

Nonetheless, even if the models were deemed too inaccurate, it is interesting to note that the effect of basal area was significant and positive in the seedling density model based only on plots belonging to Thinning Class 1, suggesting a possible mother-tree positive effect. In the model for Thinning Class 2 & 3, basal area had a negative effect, maybe because the already-lower light availability is aggravated by bigger tree size and the overstorey competition effect becomes predominant. Similar results were observed by Page *et al*. (2001) in Sitka spruce forests in the UK.

5 Light-growth responses of Sitka spruce, Douglas fir and western hemlock regeneration

In this chapter, I prepare light-growth functions for various conifer species' regeneration, analyse their crown plasticity at variable light levels, and compare their differences in shade tolerance ranking.

5.1 Introduction

Continuous cover forestry (CCF), a range of different silvicultural approaches that involve uninterrupted maintenance of forest cover and avoidance of clearcutting (Pommerening & Murphy 2004), is becoming increasingly important worldwide (Schütz *et al.* 2011). Mason et al. (1999) indicated the following principles for CCF: management of the forest ecosystem rather than just the trees; use of natural processes as the basis for stand management; adaptation to site limitations; and creation of a diverse stand structure with a range of species. Amongst the consequences of those principles, there is an increasing focus on the use of natural regeneration to develop uneven-aged and mixed-species stands (Pommerening & Murphy 2004).

Light is considered one of the main factors affecting tree regeneration under forest cover (Oliver & Larson 1996; Lieffers *et al.* 1999). Measurements of the light regime under canopy have been widely used as main inputs for regeneration growth models, especially in uneven-aged and mixed-species stands (Pacala *et al.* 1996; Wright *et al.* 1998; Finzi & Canham 2000; Duchesneau *et al.* 2001; Grassi & Giannini 2005; Ligot *et al.* 2013). Canopy characteristics, and in turn light analysis based on those characteristics, are better predictors for regeneration growth models than traditional stand parameters, such as stem density or tree volumes, especially in those with uneven stands such as in CCF (Peng 2000; Chrimes & Nilson 2005).

There is a growing consensus that theoretically justified non-linear models are best suited to describe plant growth (Paine *et al.* 2012). Such models are based on specific hypotheses regarding the phenomenon to be described and use parameters that have a clear biological meaning (Fekedulegn, Siurtain & Colbert 1999). In the case of the light-growth response of regenerating trees, asymptotic non-linear functions have been commonly used, such as the Michaelis-Menten and the Logistic (Pacala *et al.* 1996; Paine *et al.* 2012; Ligot *et al.* 2013):

with increasing values of input (light), the response (growth) increases but eventually saturates and reaches a maximum value at a certain level of input. The two functions differ in the way the growth rate reaches the asymptote. The Michaelis-Menten always has a concave-down shape that passes through the origin (growth is zero at no light). The Logistic, in its "three-points" form, has a sigmoid shape that confers better flexibility, but while it has a lower asymptote set to zero, it is not constrained to pass through the origin (growth can be positive at zero light). Ecological theory suggests that trees under declining levels of light could reach a compensation point at which the photosynthesis equals the respiration costs, thus showing no growth at positive light levels (Givnish 1988). The asymptotic function with an offset (Pinheiro *et al.* 2016), from here on called Asymptotic-with-offset, can resolve this issue: it is an always concave-down function (in this regard similar to the Michaelis-Menten) but is not constrained to pass through the origin. See Figure 5.1 for examples of the three different equations.
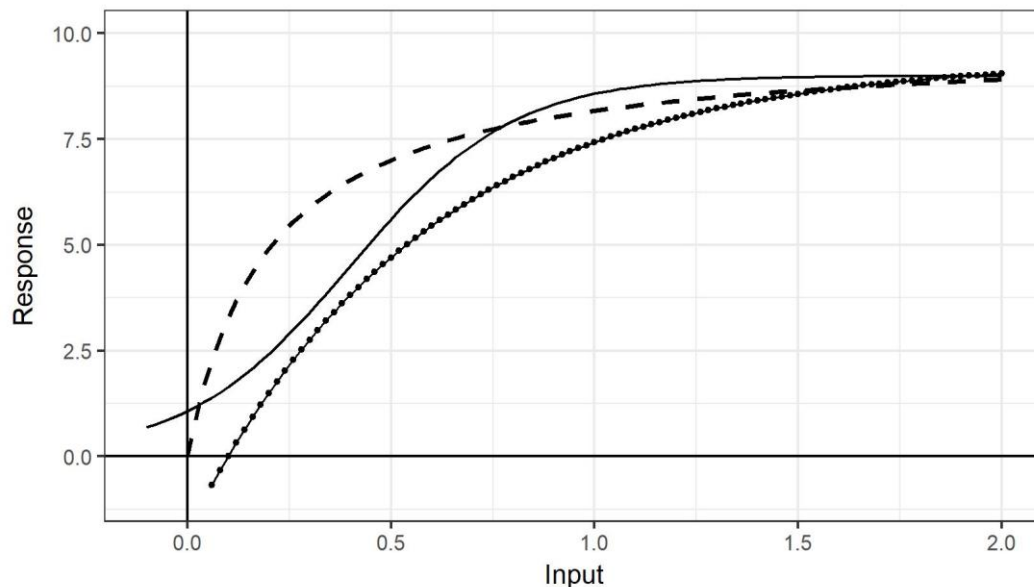
Figure 5.1. Examples of a Michaelis-Menten (dashed line), Logistic (continuous line) and Asymptotic-with-offset (dotted-continuous line) functions reaching similar asymptotic responses towards high values of input. The slope of the curves, that is the growth rate at which the asymptote is reached, could be different in each case.

Most previous non-linear light-growth studies have assumed the same response curve for trees of different size by using the relative growth rate, that is by scaling the absolute growth by the tree size (e.g. Pacala *et al.* 1996). However, relative growth rate usually decreases with increasing tree size due to biological and geometrical issues (Paine *et al.* 2012). Photosynthetic efficiency is also expected to change with tree height: taller trees can have an advantage in better exploiting light resources, but that ability comes with higher respiration maintenance costs (Givnish 1988; King 1990). Claveau *et al.* (2002) reported that the way in which tree size

affects light-growth responses has not been widely studied, and they suggested incorporating it as a predictor in future studies. The presence of intra-regeneration competition could be another factor significantly affecting the light-growth response. Intra-regeneration competition was found to significantly affect growth either only at higher light levels (Duchesneau *et al.* 2001), only the radial but not the height growth (Collet & Chenost 2006; van Couwenberghe *et al.* 2013), only if the trees were overtopped (Hasenauer & Kindermann 2002; Ligot *et al.* 2013), or not at all (Monserud & Ek 1977; Grassi & Giannini 2005). As far as I am aware only Ligot *et al.* (2013) used specific non-linear models where tree size and intra-regeneration competition were included as additional variables modifying the asymptote of the functions, albeit not the growth rate to reach it.

Interspecific differences in shade tolerance significantly affect stand dynamics (Finzi & Canham 2000). As mentioned in Chapter 3, of the three species studied in this thesis, western hemlock was considered the most shade-tolerant by all authors, while Sitka spruce was found to be either more than, less than or equally shade-tolerant to Douglas fir (Minore 1979; Malcolm, Mason & Clarke 2001; Mason, Edwards & Hale 2004). Shade tolerance, the ability to grow and survive under low levels of light, is an elusive property; ecologists have not yet agreed on a standardized method for its quantification (Lusk & Jorgensen 2013), and many characteristics have been used to define a shade tolerance ranking amongst species. More shade-tolerant species usually show a relatively faster growth at low light and a slower growth at high light than less shade-tolerant species, although this trade-off is not necessarily clear-cut (e.g. Pacala *et al.* 1996). Usually shade-tolerant species also show a complementary trade-off between higher capacity for surviving at low light with lesser growth at high light (Kobe & Coates 1997). Other authors define as more shade-tolerant the species that reach the whole-plant compensation point at lower light levels (Lusk & Jorgensen 2013). Crown plasticity is another characteristic usually associated with shade tolerance. More shade-tolerant trees growing under low light levels can modify their crown architecture to a more efficient shape for light absorption, by expanding it more horizontally than vertically, and by limiting the number of living lower branches, which are generally more shaded (Lieffers *et al.* 1999; Williams, Messier & Kneeshaw 1999; Claveau *et al.* 2002). In more shade-tolerant trees this would result in a reduction in the apical dominance ratio (ADR), the ratio between the length of the leader and of the lateral shoots of the same year, and also a reduction in the live crown ratio (LCR), the ratio between the height of the live crown and the tree height. In other words, more shade-tolerant trees tend to form an "umbrella-shaped" crown under low levels of light

(e.g. O'Connell & Kelty 1994), which allow them to survive long periods of shading from the overstorey.

5.1.1 Objectives

The general aim was to expand the knowledge of the light-growth response of Sitka spruce, western hemlock and Douglas fir in the understorey and to provide modelling tools for forestry operators interested in CCF. To do so, I investigated regenerating trees growing under canopy cover to evaluate:

1) The species-specific light-growth responses (in both height and diameter), under the range of light regimes encountered in CCF systems, comparing different non-linear models that include also tree size and intra-regeneration competition;

2) The species-specific crown plasticity (in terms of apical dominance ratio and live crown ratio) under different light levels, and how this process is affected by tree size and intra-regeneration competition;

3) If the above light-growth and crown plasticity responses can be used to identify a shade tolerance ranking.

5.2 Methodology

5.2.1 Data collection

The study areas included a wide range of forests across the UK, divided into various stands dominated by different overstorey species (see Table 5.1 for more details). For each stand, I laid out ten plots with a random-systematic approach. I drew random non-parallel transects on a desktop map and placed on them evenly-spaced plots, later located in the field using a GPS receiver. The distance between plots varied with the size of the stand. For each plot, I selected the closest Sitka spruce (SS), western hemlock (WH) and/or Douglas fir (DF) naturally regenerating tree, excluding trees with evident sign of browsing or other kinds of damage. Trees were classified into broad height classes, and for subsequent plots I chose trees belonging to a different class to ensure a balanced sample range. However, the patchy occurrence of natural regeneration forced me frequently to have to walk away from the planned transects. Recent silvicultural management in each stand varied from no intervention to thinning of different intensity and type, but purposely I selected no stand thinned in the last two years. I also relocated plots that fell in areas with recent windblow events if possible; otherwise, I discarded them. While all SS and WH seedlings were natural regeneration, one-third of the DF seedlings measured were artificially under-planted (all those in Clocaenog and some of those in Wykeham). Data collection was carried out from February to November 2016.

On each selected tree, I measured the height growth (Hg) as the length of the last complete leader shoot, and the tree height previous to that growth (Hp) as the total height minus the height growth. I calculated the apical dominance ratio for SS and DF (not for WH due to its different canopy architecture) as the ratio between the corresponding leader and lateral shoots for both the last complete vegetative season and the previous one (called respectively ADR and ADRp). I calculated the live crown ratio (LCR) as the ratio between the length of the stem from the top to the lowest live green branch and the total height. In all cases I discarded from the measurements any incomplete shoots found if the survey was carried out during spring/summer. The tree measurement schematics are displayed in Figure 5.2. For SS and WH trees, I collected a stem sample at 10 cm above the root collar, unless the tree presented an evident swelling, a common occurrence for large saplings, in which case no sample was collected. For SS trees, I also collected a stem sample at breast height (130 cm) if the height of the previous year was above that height; otherwise no sample was collected. For DF, I could not collect any stem samples due to particular forest management prescriptions. For each stem sample, I measured with an optical microscope the diameter growth as twice the width of the last annual wood ring (called respectively DRCg for the diameter at 10 cm above root collar and DBHg for the diameter at breast height), and the diameter previous to that growth (respectively DRCp and DBHp), as the total diameter under bark minus the diameter growth. As above, I discarded from the measurements any incomplete rings if the survey was carried out in spring/summer. I took all the measurements in two directions (the shortest and longest diameter for each sample) and averaged the values.
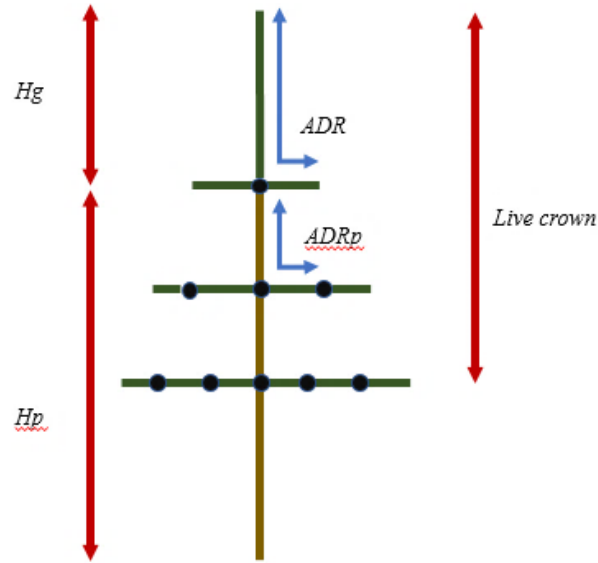
Figure 5.2. Schematics of tree height and crown measurements. Hg, height growth; Hp, tree height before that growth; ADR and ADRp, the apical dominance ratio respectively of the current vegetative season and of the previous one (the two arms of the arrows show which leader and lateral shoots were considered). Live crown ratio (LCR) was calculated as the ratio between live crown and total height.

I considered neither the relative growth rate, because of the problems identified in the introduction, nor the average of the leader length of more than one season, sometimes used to smooth possible yearly variations, (e.g. Grassi & Giannini 2005). The last leader length is the variable best correlated with the present stand characteristics (Page et al. 2001). Preliminary results (not shown) confirmed that the correlation between past leader lengths and current light availability was lower.

I assessed the intra-regeneration competition by counting the number of regenerating trees of all species around the subject tree. If the subject tree was under 130 cm height, to count the competition I used a circle of 80 cm radius from its stem (around 2 m^2), if 130-250 cm height, a circle of 120 cm radius (around 4.5 m^2), and if above 250 cm height a circle of 160 cm (around 8 m^2). I then added one and log-transformed the number, to create the variable *comp*. While circular 2 m^2 plots have been previously used for seedlings 20-180 cm (van Couwenberghe *et al.* 2013), I decided to compensate for the increasing crown radius of bigger trees by using larger circles based on empirical observations on the ground (i.e. a circle of radius 80 cm centred on a stem of a 5 m tall tree in most cases did not extend beyond its crown).

5.2.1.1 *Hemispherical photography*

At the top of the selected trees, I took hemispherical photography (HP) images using a Nikon Coolpix (4500 or 990 model), equipped with Nikon FC-E8 183˚ FOV Fish-Eye Converter Lens.

I carried out the circular HP image acquisition on windless days, under overcast sky conditions or after sunset (Fournier *et al.* 1996). In stands with the presence of broadleaved trees, I acquired the images during summer to have the full foliar development of the overstorey. I positioned the camera on a telescopic pole, oriented to the North using a compass and upwards to the zenith using a level. I took one picture using the automatic exposure and then some more in quick succession with reduced exposure bias to obtain at least one picture with good contrast (Hale et al. 2009). For image processing, I used the protocol of Bianchi *et al.* (2017). I automatically thresholded the pictures using the function *enhanceHemiphoto* of the package *Caiman* (Diaz & Lencinas 2015) from the R Statistical Software (R Core Team 2017). Using CIMES-FISHEYE (Gonsamo, Walter & Pellikka 2011), I estimated: Canopy Openness (CO), the unobstructed fraction of the sky hemisphere viewed from a single point (Gonsamo, Walter & Pellikka 2011); Indirect Site Factor (ISF) and Direct Site Factor (DSF), respectively the transmittance through the canopy of the diffuse light from an overcast sky (considering a Standard Overcast Sky model) and of the direct light from a clear sky (Hale *et al.* 2009). I calculated the Global Site Factor (GSF), the total radiation that comprises both those components, as shown in Equation 6.1.

$$Equation\ 6.1 : GSF = 0.65 * ISF + 0.35 * DSF$$

Table 5.1. Details of study areas and tree measured. Values of light (GSF, Global Site Facto) and size are given as minimum-mean-maximum. Height, height before the last growth season, DRC, diameter at 10 cm above root collar; DBH, diameter at breast height; n, the sample size. Larch, Larix spp.; Spruce, Picea abies and Picea sitchensis, Douglas fir, Pseudotsuga menziesii, Scots pine, Pinus sylvestris; mixed broadleaves, Acer spp, Fagus sylvatica and Quercus spp.

Forest	Coordinates (WGS84)	Canopy species	Light (GSF)	Sitka spruce						Western hemlock				Douglas fir	
				Height (cm)	n	DRC (mm)	n	DBH (mm)	n	Height (cm)	n	DRC (mm)	n	Height (cm)	n
Aberfoyle (Scotland)	56° 13' N 4° 21' W	Larch, spruce	0.13-*0.25*-0.39	25-*151*-410	31	2-*14*-25	19	3-*18*-38	10	-	-		-	-	-
Clocaenog (Wales)	53° 04' N 3° 24' W	Spruce, Larch	0.12-*0.41*-0.95	21-*184*-607	89	1-*12*-30	34	4-*33*-76	27	27-*108*-407	20	2-9-27	18	61-*116*-230	18
Coed-Y-Brenin (Wales)	52° 48' N 3° 53' W	Douglas fir, mixed broadleaves	0.13-*0.18*-0.25	-	-	-	-	-	-	112-*137*-188	4	17-*21*-26	4	31-*137*-322	18
Gwydyr (Wales)	53° 05' N 3° 48' W	Douglas fir, mixed broadleaves, Scots pine	0.07-*0.18*-0.38	45-*124*-200	16	-	-	-	-	83-*138*-190	10	-	-	41-*76*-133	11
Kielder (England)	55° 13' N 2° 27' W	Spruce	0.16-*0.24*-0.38	15-*87*-241	49	3-*10*-27	33	4-*12*-30	8	75-*175*-271	6	5-*13*-24	6	-	-
Lakes district (England)	54° 30' N 3° 09' W	Douglas fir	0.12-*0.24*-0.83	34-*133*-243	18	3-*15*-31	5	3-9-15	2	79-*175*-271	5	12-*14*-16	3	29-*130*-301	25
Mortimer (England)	52° 21' N 2° 45' W	Mixed broadleaves, Douglas fir	0.07-*0.15*-0.34	-	-	-	-	-	-	91-*191*-376	10	11-*23*-45	9	34-*170*-286	13
Wykeham (England)	54° 16' N 0° 33' W	Larch, Scots pine, spruce	0.11-*0.28*-0.53	16-*113*-320	30	2-*12*-33	26	2-*13*-34	8	33-*157*-422	11	2-*13*-35	11	41-*113*-272	16
Total			**0.07-*0.40*-0.95**	**15-*140*-607**	**187**	**2-*12*-33**	**117**	**2-*23*-76**	**55**	**27-*145*-422**	**66**	**2-*12*-45**	**51**	**29-*125*-322**	**101**

5.2.2 Statistical analysis

I carried out all the analyses with the package *nlme* (Pinheiro *et al.* 2016) of the R Statistical Software (R Core Team 2017).

5.2.2.1 *Height and diameter growth models*

I modelled *growth*, either Hg (for all species), DRCg (for SS and WH) or DBHg (for SS), as a function of *light*, the GSF estimated from HP, comparing three asymptotic non-linear functions based on the Michaelis-Menten (Equation 6.2), the 3-points Logistic (Equation 6.3), and the Asymptotic-with-offset (Equation 6.4).

$$\text{Equation 6.2: } Growth = \frac{r + Asym * light}{xmid + light}$$

$$\text{Equation 6.3: } Growth = \frac{r + Asym}{1 + e^{(xmid - light)/scale}}$$

$$\text{Equation 6.4: } Growth = (r + Asym) * (1 - e^{-exp(lcr)*(light - cp)})$$

Where:

$$Asym = (A + A2 * comp) * size^{Pa}$$

$$xmid = \frac{K - K2 * comp}{size^{Pk}}$$

$$lcr = (K + K2 * comp) * size^{Pk}$$

$$scale = \frac{S}{size^{Ps}}$$

$$cp = \frac{C}{size^{Pc}}$$

In all equations, *Asym* indicates the asymptotic maximum growth that is reached at high light levels, and *xmid* and *lcr* how fast the growth reaches this asymptote (i.e. the growth rate). In Equation 6.2 and 6.3, *xmid* represents the value of light about which the growth is half of the asymptotic growth, or simply half-maximum-growth. Then, *scale* in Equation 6.3 represents the steepness of the curve around the sigmoid inflection point, and *cp* in Equation 6.4 the compensation point, the level of light corresponding to zero growth. I included *size*, either the height or diameter before the growth (Hp, DRCp, or DBHp), in each of those terms, with an effect mediated by the coefficients *Pa*, *Pk, Ps* and *Pc*. I included competition (*comp*), only in the terms related to the asymptotic growth and the growth rate, with an effect mediated by *A2* and *K2*. I did not include a competition effect for *scale* in Equation 6.3 since it would not have had any biological validity, or for *cp* in Equation 6.4 for computational simplicity. I included

r, a random factor at forest level affecting the value of asymptotic growth, to take into consideration the possible auto-correlation of the plots in the same forest due to the site fertility or local climatic conditions. It must be noted that the growth rate increases with lower values of *xmid*, and the opposite for *lcr*. In other words, the asymptote is reached faster in Equations 6.2 and 6.3 for lower values of *xmid*, and in Equation (6.4) for higher values of *lcr*. The sign on the K2 parameter and the inclusion of *size* (as multiplicator or dividend) were adjusted to ensure a consistent direction of response for the *xmid* and *lcr* variables. The summary of the biological implications of each coefficient is shown in Table 5.2. I also tested equations in which *size* had opposite effects on *xmid/lcr*, *scale*, and *cp* than indicated on the table but the models did not fit.

Table 5.2. Summary of the biological effects of the various coefficients used in the non-linear functions

Asym	**All equations**	**A**	Value of maximum growth (in cm or mm).
		A2	Effect of competition on the maximum growth: if 0, it is null; if negative, it decreases the maximum growth.
		Pa	Effect of tree size on the maximum growth: null at 0, then increases the maximum growth with a stronger effect as this parameter increases.
xmid/lcr	**All equations**	**K**	Correlated to the growth rate to reach the maximum growth: for *xmid*, the higher the value, the slower the rate; for *lcr*, the opposite. Also, different scale for the different equations.
		K2	Effect of competition on the growth rate: if 0, it is null; if negative, it decreases the growth rate, both in *xmid* and *rate*.
		Pk	Effect of tree size on the growth rate: null at 0, then increases the growth rate with a stronger effect as this parameter increases, both in *xmid* and *lcr*.
scale	**Logistic**	**S**	Positively correlated to the steepness of the sigmoid curve.
		Ps	Effect of tree size on the steepness of the sigmoid curve: null at 0, then increases the steepness with a stronger effect as this parameter increases.
cp	**Asymptotic-with-offset**	**C**	Light level (GSF) equivalent to null growth (compensation point).
		Pc	Effect of tree size on the compensation point: null at 0, then decreases the compensation point with a stronger effect as this parameter increases.

For each combination of growth and species, I tested the three base functions, and all their possible combinations where some or all the main coefficients (*A*, *K*, *S* and/or *C*) were not affected by size (setting *Pa*, *Pk*, *Ps* and/or *Pc* to 0) or by competition (setting either *A2* and/or

K2 to 0). Preliminary results showed that when the competition was affecting both asymptotic growth and growth rate (by setting both *A2* and *K2* to non-zero values) it led to unrealistic biological responses, so I discarded such models. There were 12 models belonging to the family originated from the Michaelis-Menten function, and 24 each for the Logistic and Asymptotic-with-offset, a total of 60. To consider the heteroscedasticity of the data, I modelled the variance as a power of the fitted values, with the power determined during model fitting.

For each combination of species and type of growth, I pooled together all the models belonging to the different families. I selected as candidates the model with the lowest Akaike Information Criterion (AIC) and those within two AIC units. Then, I chose the best model as the one with the highest parsimony (fewest parameters affected by size and competition), and in one case of a tie, with the best prediction performance (lowest AIC) and better biological validity (by observing the simulated growth pattern). For each best model, I calculated the Pearson's correlation coefficient *r* between simulations and observations, and the simulation errors in terms of Root-Mean-Square-Error (RMSE), Mean Absolute Error (MAE), and Mean Absolute Percentage Error (MAPE), that is the MAE relative to the observed growth (Hyndman & Koehler 2006).

To compare growth patterns across species, I also calculated the light level necessary to obtain the half-maximum-growth for all best models. In case of the Michaelis-Menten and the Logistic, that was directly equal to the coefficient K, considering the influence of K2 and/or Pk. For the Asymptotic-with-offset, it was calculated empirically by observing the maximum value of the predictions at full light and estimating the light level necessary for its half growth.

5.2.2.2 Apical Dominance Ratio (ADR) and Live Crown Ratio (LCR) analyses

Using a dataset where all species were combined, I calibrated Generalized Linear Mixed Models (GLMMs) for ADR (only for SS and DF) and LCR. In both cases I used as predictor variables species, light (GSF), size (Hp) and competition (*comp*), including two-ways interaction terms between all variables. I included a random intercept effect at forest level to account for spatial autocorrelation. After observations of the data distribution and preliminary modelling results, I decided to use log-transformed GSF and Hp for a better fit. From the global model with all variables, I then tested structures with fewer fixed effects, and selected as the best model the one with lowest AIC. In the cases where models had differences of less than 2 points, I chose the model with fewer explanatory variables.

I then modelled the height growth (Hg) as a function of the previous year's apical dominance ratio (ADRp) and tree height (Hp). For DF, I used a GLMM including both those predictors and a two-way interaction term. I included a random intercept effect at forest level for spatial autocorrelation, and carried out a model selection procedure as above. For SS I observed a different data distribution, and after preliminary modelling results, I used a simplified version of Equation 6.2 without the competition effect, as shown in Equation (6.5).

$$\text{Equation 6.5: } Hg = \frac{r + A * Hp^{Pa}}{1 + e^{(K-ADRp)/S}}$$

5.3 Results

5.3.1 Growth models

For SS, I selected as best a model from the Logistic family in all cases (height, DRC and DBH); for WH, from the Michaelis-Menten in both cases (height and DRC); and for DF/Height, from the Asymptotic-with-Offset. Table 5.3 presents the coefficient values of those models, showing the main model components (asymptotic growth, growth rate, scale and/or compensation point) affected either by the tree size (if Pa, Pk, Ps and/or Pc $\neq$ 0) or by the intra-regeneration competition (if A2 or K2 $\neq$ 0). The estimated growth patterns for each model versus the observations are shown in Figure 5.3. See Annex I for the AIC values of all the models fitted, and supplementary information on the results. In all cases but for the WH/Height model, tree size affected the asymptotic growth (Pa > 0) and consequently, the absolute growth was higher for bigger trees at all light levels. Absolute growth was higher for taller trees also for the WH/Height model, even if Pa = 0, due to Pk > 0. However, the smaller data range in terms of light availability may have affected the model fit (i.e., the curve did not reach an asymptote within the data range for this case). For SS/Height and WH/Height, tree size also affected the growth rate (Pk > 0): bigger trees had a higher growth rate than smaller trees, more markedly at lower light levels. Trees growing at GSF 0.5 reached a growth that was equal to 70-75% of the maximum growth at full-light in the WH/Height model (increasing with tree height), 75% in the SS/DRC, 80% in the WH/DRC and DF/Height, and more than 95% in the SS/Height and SS/DBH models. Note that the growth at full-light (GSF 1) in all cases was considered as the one estimated by the models.

Only for DF/Height was the best model based on the Asymptotic-with-offset, with the same compensation point around GSF 0.08 for trees of all sizes. Since both the WH models were based on Michaelis-Menten, the compensation point was set at zero light for that species. Sitka spruce, since Logistic was selected for all the best models, had an estimated positive growth at

zero light in all cases. While this effect was almost negligible in the SS/DRC and SS/DBH models, it was more evident in the SS/Height model (see Figure 5.3).

Table 5.3. Best growth model for each case, showing the family of the equation. SS, Sitka spruce; DF, Douglas fir; WH, western hemlock; H, height; DRC, diameter above root collar; DBH, diameter at breast height. Empty cell: the coefficient was excluded in the best model. NA: the coefficient does not appear in the equation used. Then, r is the Pearson correlations coefficient between simulations and observations; RMSE, the Root-Mean-Square-Error (in cm for height and mm for diameter); MAE, the Mean Absolute Error (in cm for height and mm for diameter); MAPE, the MAE relative to the observations.

Model	Coefficient													
	A	K	A2	K2	C	S	Pa	Pk	Ps	Pc	r	RMSE	MAE	MAPE
SS/HEIGHT (n=187) - Logistic														
Value	5.624	0.340	-	-0.043	NA	0.117	0.430	0.101	-	NA	0.88	9.5	7.1	37.6%
p-value	0.003	0.003	-	0.014	NA	0.000	0.000	0.106	-	NA				
SS/DRC (n=117) - Logistic														
Value	2.406	0.369	-0.369	-	NA	0.118	0.581	-	-	NA	0.94	0.9	0.6	39.0%
p-value	<0.001	<0.001	<0.001	-	NA	<0.001	<0.001	-	-	NA				
SS/DBH (n=55) - Logistic														
Value	4.561	0.210	-	-0.025	NA	0.078	0.252	-	-	NA	0.81	2.5	1.8	42.9%
p-value	<0.001	<0.001	-	0.039	NA	<0.001	<0.001	-	-	NA				
WH/HEIGHT (n=66) - Michaelis-Menten														
Value	170.9	7.033	-	-	NA	NA	-	0.476	NA	NA	0.79	11.6	8.8	27.0%
p-value	0.005	0.048	-	-	NA	NA	-	<0.001	NA	NA				
WH/DRC (n=51) - Michaelis-Menten														
Value	1.936	0.308	-0.161	-	NA	NA	0.666	-	NA	NA	0.76	1.5	1.1	32.5%
p-value	0.003	0.055	0.070	-	NA	NA	<0.001	-	NA	NA				
DF/HEIGHT (n=101) - Asymptotic-with-offset														
Value	10.809	1.219	-	-	0.083	NA	0.390	-	NA	-	0.84	12.5	9.6	61.6%
p-value	0.061	0.010	-	-	<0.001	NA	<0.001	-	NA	-				

-
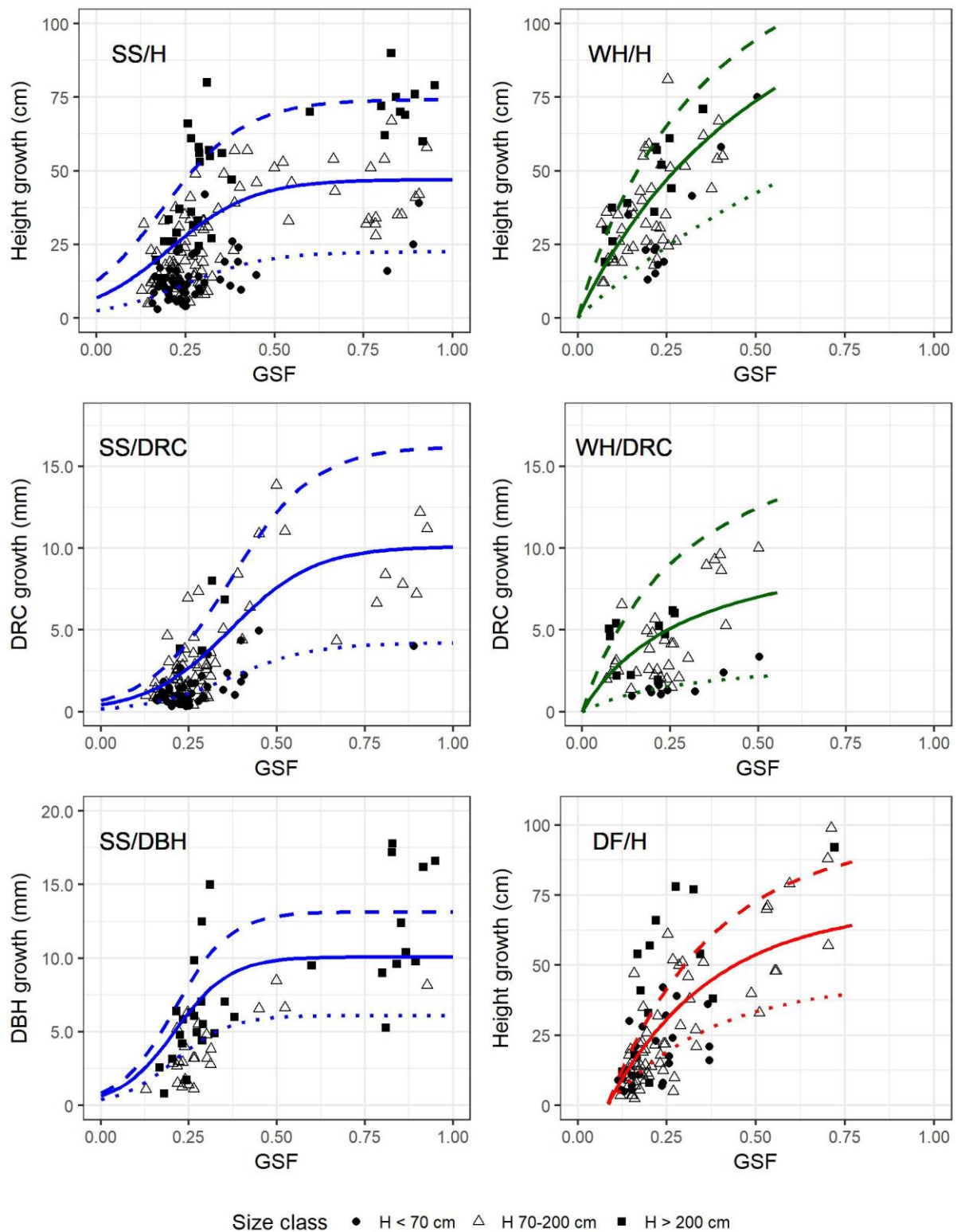
Figure 5.3. Simulated (lines) and observed (points) growth as a function of light (GSF, Global Site Factor), for trees of different sizes and in the absence of competition. SS, Sitka spruce; DF, Douglas fir; WH, western hemlock; H, Height; DRC, Diameter above Root Collar; DBH, Diameter at Breast Height. In each graph: top dashed line, simulated growth for a tree having size (height or diameter) equal to the 95% quantile of the population, medium continuous line, to the mean, and bottom dotted line, to the 5% quantile.

Table 5.3 presents the Pearson correlation coefficient between simulations and observations (quite high for all models), and the various measured errors. In Figure 5.4 and Figure 5.5 the standardized residuals of the simulations are plotted versus the observations, and the model predictors (tree size, light availability, and competition, even if the latter was not included in all models). There were some signs of heteroscedasticity in all models when the residuals were plotted versus the observations, specifically a tendency of decreasing accuracy and underprediction towards high values of observed growth. Considering the residual distribution versus the model predictors, there were fewer signs of heteroscedasticity: overprediction only for the biggest trees for SS/Height and SS/DRC; underprediction for SS/DRC and WH/DRC at mid-light availability; and underprediction towards higher light for WH/Height and DF/Height. A closer inspection of the residuals showed that, often, the underpredictions towards high values of observed growth happened for medium/large-sized trees growing at low/medium levels of light. Some of those trees showed a considerable growth, comparable to trees either of bigger size or growing at higher light availability, that was underpredicted by the models. The resulting values of Mean Absolute Percentage Error (MAPE) were lowest for the western hemlock models (27% and 32% for height and DRC), then higher for the Sitka spruce models (38-39% for height and DRC, and higher for DBH, 43%), and highest for the Douglas fir height model (62%). It must be noted that the MAPE was influenced in all cases by few but very large relative errors for the trees showing limited growth.
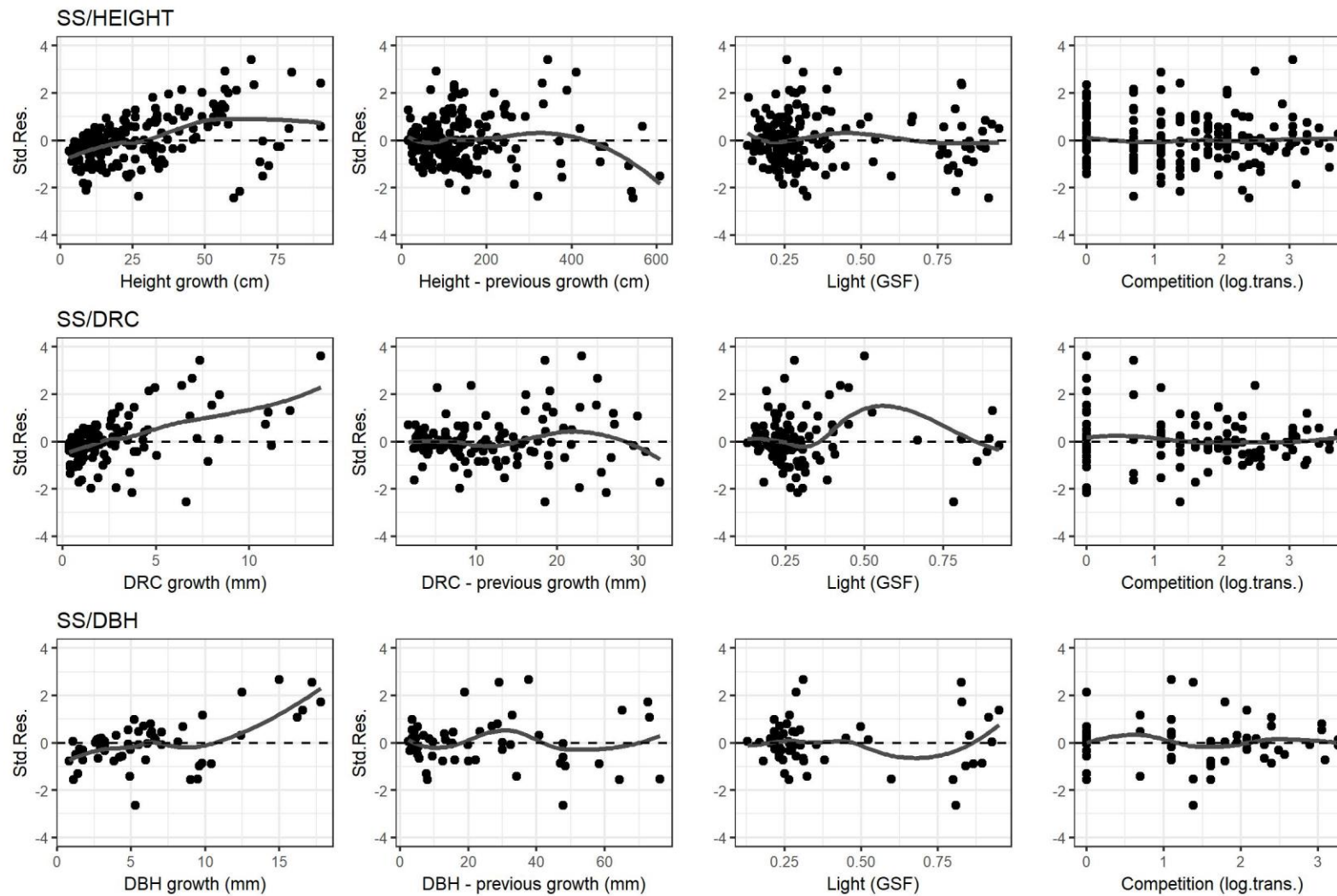
Figure 5.4. Standardized residuals plotted against the observed growth, the size previous to the growth, the light availability (GSF, Global Site Factor) and the intra-regeneration competition (log-transformed plus 1). SS, Sitka spruce; DRC, diameter above root collar; DBH, diameter at breast height. Continuous lines, LOESS (Locally Weighted Scatterplot Smoothing) curves.
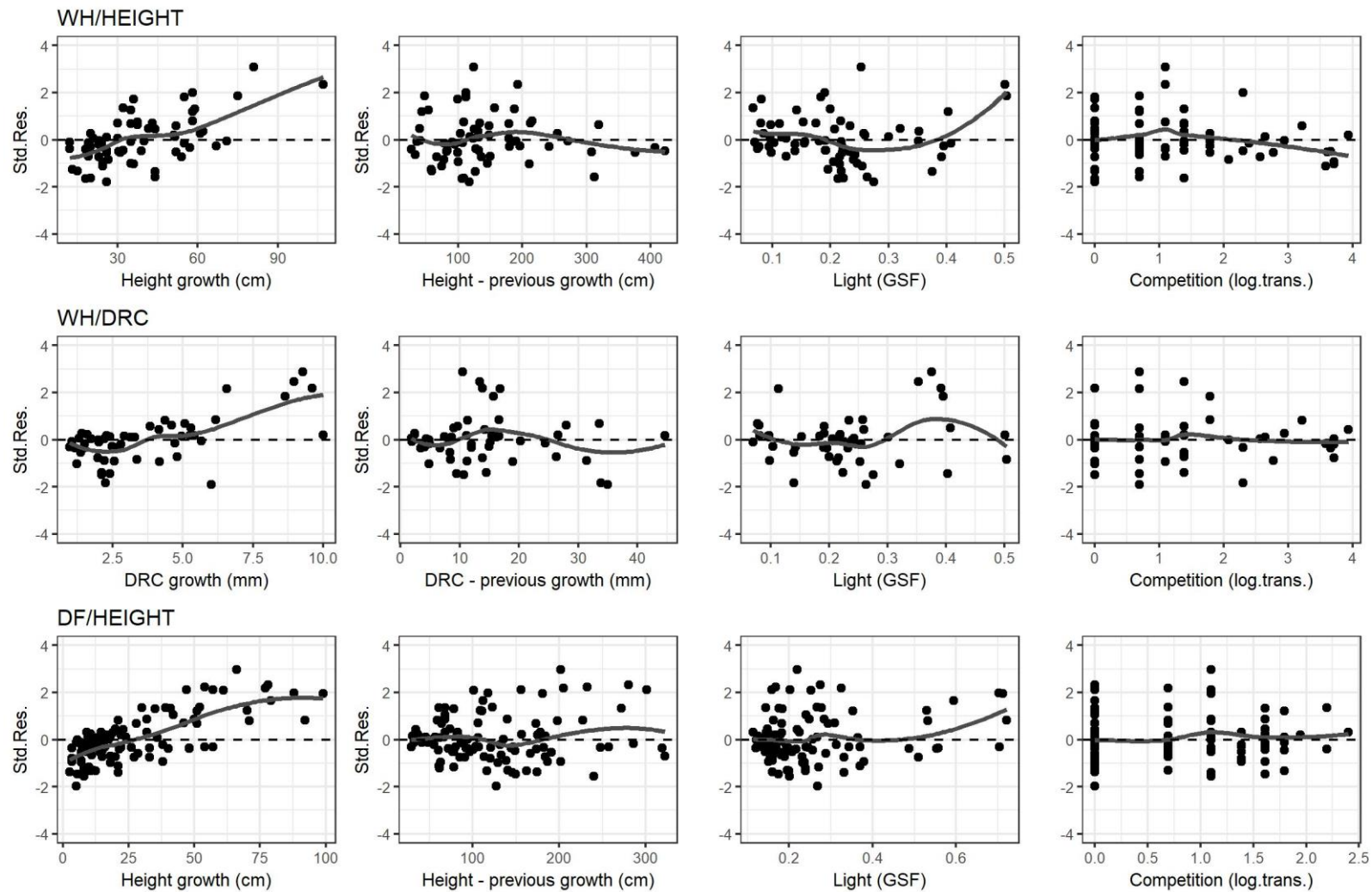
Figure 5.5. Standardized residuals plotted against the observed growth, the size previous to the growth, the light availability (GSF, Global Site Factor) and the intra-regeneration competition (log-transformed plus 1). DF, Douglas fir, WH, western hemlock; DRC, diameter above root collar; DBH, diameter at breast height. Continuous lines, LOESS (Locally Weighted Scatterplot Smoothing) curves.

Intra-regeneration competition was included in four models, affecting the growth rate for the SS/Height and SS/DBH models ($K2 < 0$), and the asymptotic growth for the SS/DRC and WH/DRC models ($A2 < 0$) (see Figure 5.6). The resulting effect in the first two models was to decrease the absolute growth especially at lower light levels, with a reduced impact as the light availability increases, while in the last two models the reduction was the same in relative terms across all light levels. It must be noted that in all the diameter growth models, the effect of competition in reduction either of the asymptotic growth or of the growth rate had a very low impact on the AIC (see Supplementary Information) and the other statistical diagnostics, but a more drastic impact on the shape of the light-growth curve.
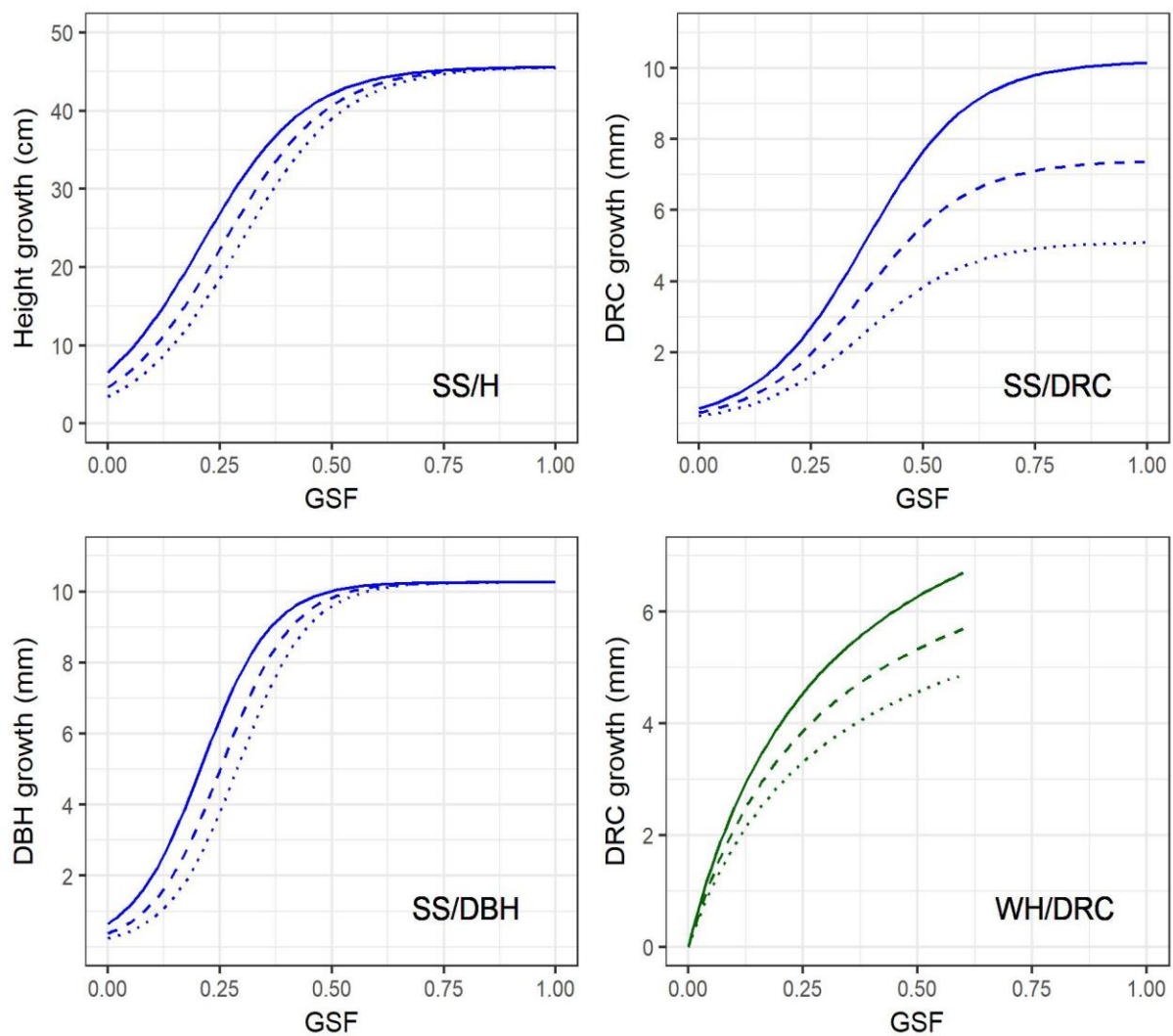
Figure 5.6. Predicted values of growth as a function of light (GSF, Global Site Factor) under different competition levels. SS, Sitka spruce; WH, western hemlock; H, Height; DRC, Diameter above Root Collar; DBH, Diameter at Breast Height. For height growth, a tree of height of 130 cm was considered; for DRC growth, of DRC 12 mm; for DBH growth, of DBH 25 mm. Continuous lines, no competition; dashed lines, low competition (5 trees/plot); dotted lines, high competition (25 trees/plot).

Figure 5.7 shows the species-specific differences in absolute growth at low and high light, simulating values for a medium-sized tree (height = 130 cm, DRC = 12 mm) in the absence of competition (a and b), or under strong competition, 25 trees per plot (c and d). For height growth, WH had the highest absolute values at almost all light levels for both scenarios. In the absence of competition, for height SS had higher absolute growth below GSF 0.2 than DF, while above it was the opposite; for DRC, WH had higher absolute growth than SS below GSF 0.4, and the opposite above. With strong levels of competition, at low light the advantage in height growth of SS over DF decreased markedly, and at high light the advantage in DRC of SS over WH totally disappeared. For trees of increasing sizes, SS had a slightly increasing advantage for growth at low light over Douglas fir (results not shown).
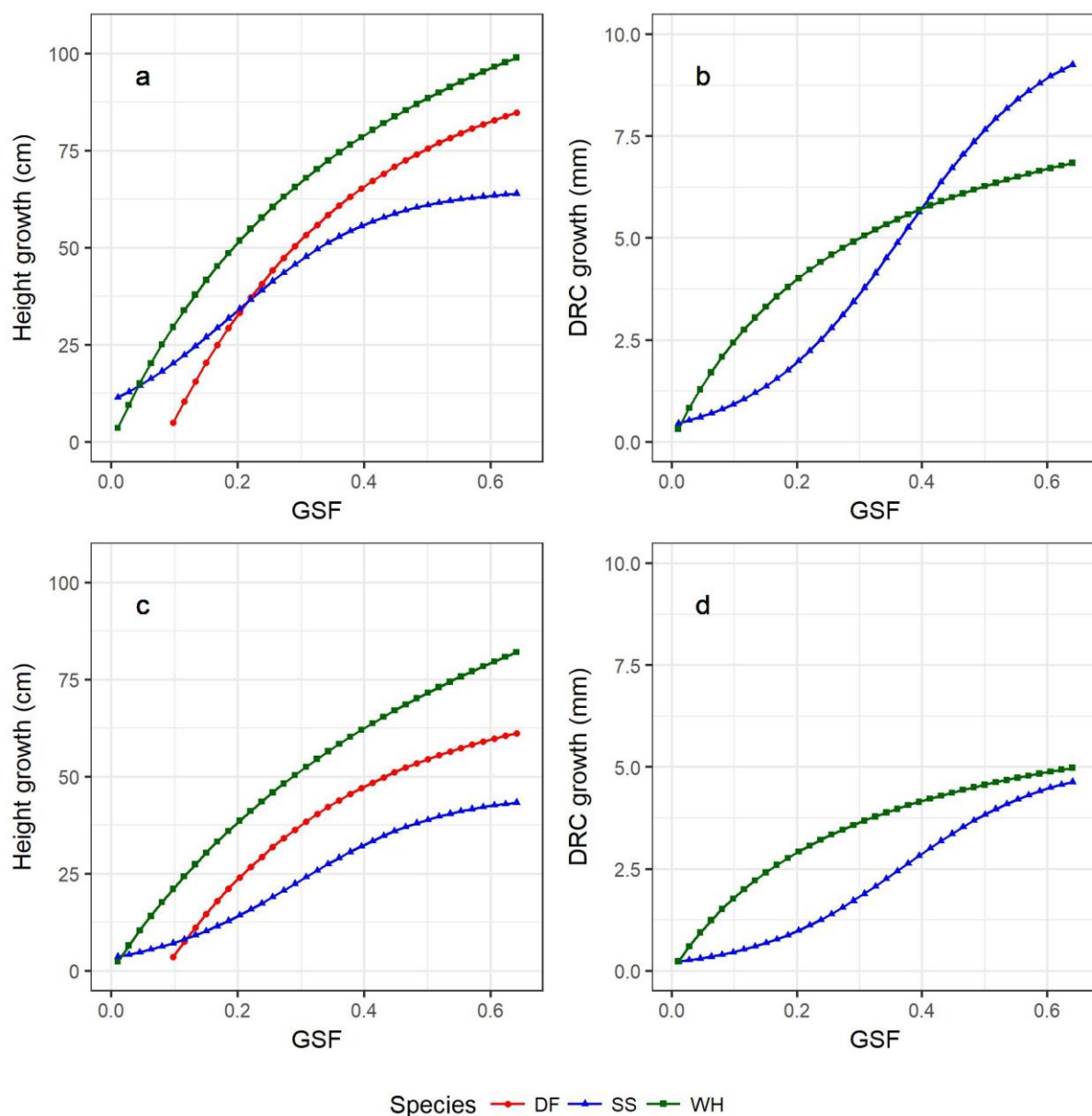
Figure 5.7. Comparison of species-specific simulated growth as a function of light (GSF, Global Site Factor), in the absence of competition (a and b) and under strong competition (25 trees/plot, c and d). DF, Douglas fir; SS, Sitka spruce; WH, western hemlock. The height growth was simulated for trees of 130 cm height; the diameter above root collar (DRC) growth for trees of DRC 12 mm.

Figure 5.8 shows how tree size affected the growth rate in the height models for all species, by plotting the light level necessary to reach the half-maximum-growth in the absence of competition. For SS/Height and WH/Height, this light level decreased with increasing tree size because of the effect of Pk. For Sitka spruce, it decreased from around GSF 0.25 for a small (20 cm height) tree, to GSF 0.18 for a big (400 cm height) tree. For western hemlock, from around GSF 0.35 for a small tree, to around GSF 0.20 for a big tree, always higher than for Sitka spruce. The analysis for western hemlock could have been biased due to the lack of sampled trees growing at high light levels and of an asymptote within the data range. For

DF/Height, SS/DRC, SS/DBH and WH/DRC, the light necessary for half-maximum-growth was respectively GSF 0.27, 0.37, 0.21 and 0.17, in the absence of competition, for trees of all sizes.
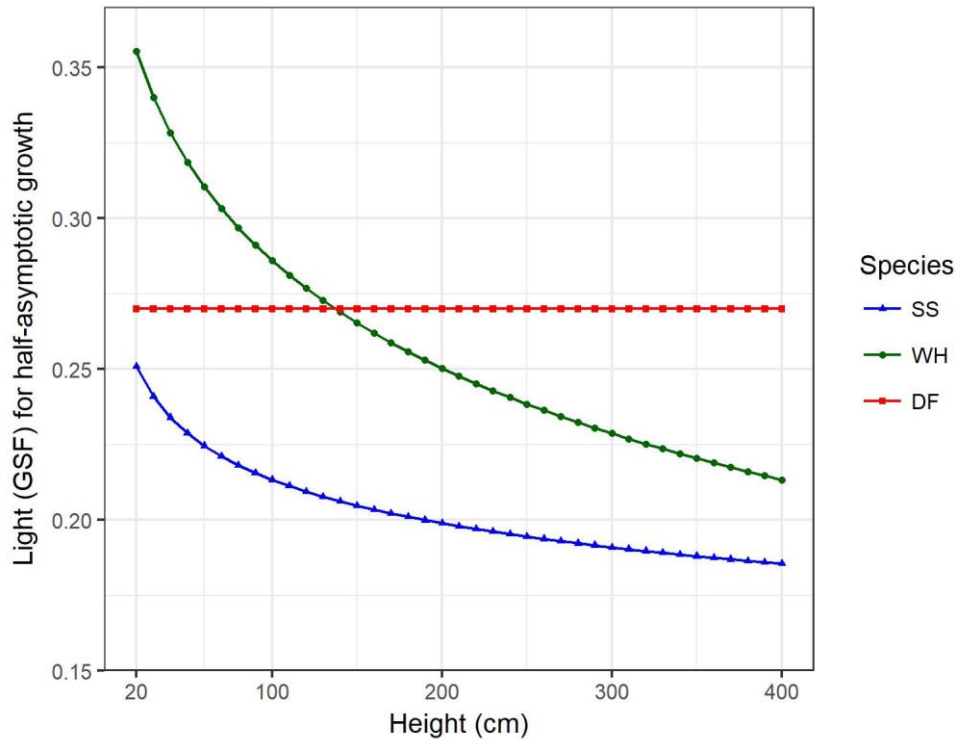
Figure 5.8. Light level (GSF, Global Site Factor) necessary for height growth equal to half the maximum growth, as a function of tree size. DF, Douglas fir; SS, Sitka spruce; WH, western hemlock.

5.3.2 Crown plasticity analyses

Table 5.4 presents the best models describing ADR and LCR as a function of light. The final model for ADR included only light availability with a positive effect (Figure 5.9, graph a). There were no significant differences between SS and DF, so the same model was fitted to both species. The threshold of 20-25% of full light indicated in the literature for good growth of Sitka spruce would correspond to an ADR of 1.2-1.4. For the LCR model (Figure 5.9, graph b), light had again a positive effect, but that was mediated by species-specific differences (a significant interaction term between light and species). WH had the highest LCR values, and LCR had a practically flat relationship with light. SS had significantly higher LCR than DF, but the difference decreased towards higher light levels.

Table 5.4 also presents the details for the species-specific models simulating height growth as a function of the previous year's apical dominance ratio (ADRp). The resulting GLMM for DF also included tree height as an interaction term, although its fit was relatively poor (Figure 5.9,

graph c). Better results were found for the non-linear model fitted for SS, where again the height growth significantly increased with ADRp and tree height (Figure 5.9, graph d). The model shows that trees of ADRp around 1.2 (the value of the coefficient K) had growth the following year equal to half the maximum growth at full light.

Table 5.4. Details for the models describing (a) apical dominance ratio (ADR) as a function of light (GSF, Global Site Factor); (b) Live Crown Ratio (LCR) as a function of light and species; (c) and (d), the height growth respectively of Douglas fir and Sitka spruce as a function of ADR of the previous year (ADRp). It is indicated whether the model is based on a Generalized Linear Mixed Model (GLMM) or on the non-linear Logistic equation. Hp, is the height of the tree in the previous year, SS is Sitka spruce, WH is western hemlock.

(a) ADR = f(light) (n=284) - GLMM				
Coefficient	Intercept	log(GSF)		
Value	2.254	0.641		
p-value	<0.001	<0.001		
(b) LCR = f(light) (n=331) - GLMM				
Coefficient	Intercept	log(GSF)	log(GSF):SS	log(GSF):WH
Value	0.921	0.121	-0.043	-0.123
p-value	<0.001	<0.001	<0.001	<0.001
(c) DF/Height = f(ADRp) (n=180) - GLMM				
Coefficient	Intercept	ADRp	ADRp:Hp	
Value	5.247	9.033	0.035	
p-value	0.060	<0.001	<0.001	
(d) SS/Height = f(ADRp) (n=180) - Logistic				
Coefficient	A	K	S	Pa
Value	4.033	1.232	0.582	0.501
p-value	<0.001	<0.001	<0.001	<0.001
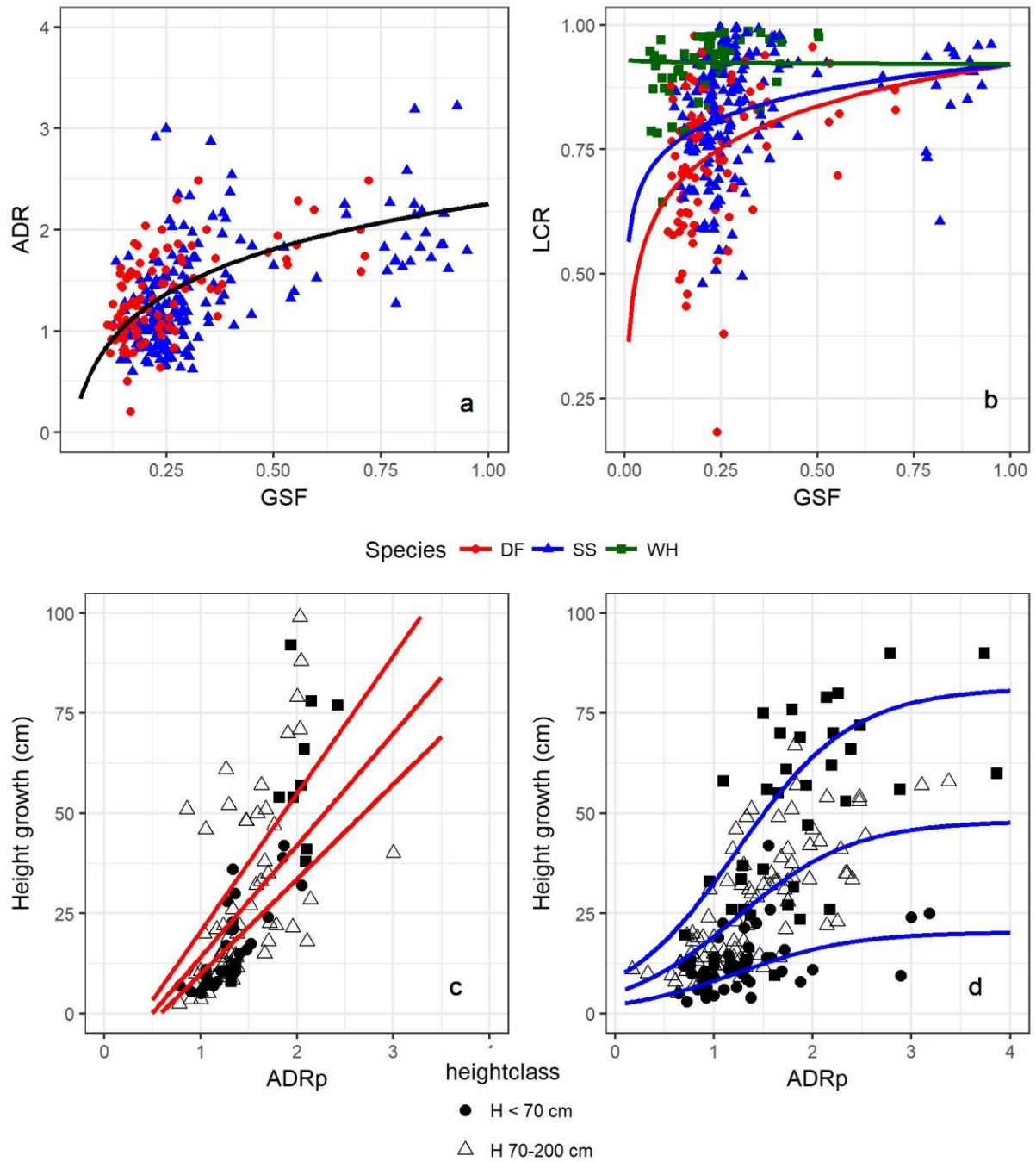
Figure 5.9. Predictions (lines) and observations (points) for: graph a, Apical Dominance Ratio (ADR) as a function of light availability (GSF, Global Site Factor), the continuous black line is for both Douglas fir (DF) and Sitka spruce (SS); graph b: Live Crown Ratio (LCR) as a function of light availability (GSF, Global Site Factor) and species; graphs c and d, respectively for Douglas fir and Sitka spruce height growth as a function of Apical Dominance Ratio of the previous year (ADRp), from top to bottom in both graphs, the lines are for trees respectively having height equal to the 95% quantile of the population considered, to the mean, and to the 5% quantile.

5.4 Discussion

Objective 1. To evaluate the species-specific light-growth responses (both height and diameter), under the range of light regimes encountered in continuous cover forestry systems, comparing different non-linear models that include also tree size and intra-regeneration competition.

The growth models presented here can be used to support planning in CCF management, by simulating the potential growth response of natural regeneration to different levels of light under a canopy. The use of light availability as the main predictor makes these models suited to describing the regeneration growth in those future uneven-aged, mixed-species forest stands that could be the result of continuous cover forestry management in the UK. The simulated values of each model were biologically sound and fitted well the observations, although in all models there was a tendency to under-predict the growth of medium/large-sized trees growing at low/medium levels of light. I demonstrated that different non-linear structures are best suited to simulating different species-specific light-growth relationships. These relationships may also vary for the height and diameter growth in the same species.

For western hemlock, and to some extent also for Douglas fir, there was lack of data on seedling growing at full light, which especially for the former may have affected the analysis. However, I covered the critical range of low-medium light levels most likely to be encountered in continuous cover forestry stands, and where the growth performance is more influenced by light and less by other environmental factors (Carter & Klinka 1992). It was observed in other studies that the net photosynthesis in western hemlock and Douglas fir, already reached saturation towards light levels of 30-40% full sunlight (Leverenz & Jarvis 1980; Carter & Klinka 1992; Grossnickle & Arnott 1992). All the models in this research already predicted values close to maximum growth at light levels equal to half of full sunlight. For the Sitka spruce height model only, the final structure based on the Logistic function showed an unlikely positive growth at zero light, even if it was very limited. I did not sample Sitka spruce trees growing at very low levels of light, but due to the sampling design followed I cannot conclusively state that there were none growing and surviving in those conditions. A more thorough sampling at those critical levels of light would be necessary to improve the model. It must also be noted that hemispherical photography has been shown to be a poor predictor of light transmitted through dense canopies, i.e. at values of GSF 0.1 and less (Hale *et al.* 2009).

The inclusion of tree size as an additional predictor always improved the fit, and had a significant effect in increasing the maximum growth in all models, both for height and

diameter. Larger trees as a consequence had a greater absolute growth at all light levels, due mostly to an increased capacity for light absorption and partly to an increased efficiency of light use (Binkley *et al.* 2013). I observed that for height growth in Sitka spruce and western hemlock, bigger trees compared to smaller trees had an even more marked higher growth at low light than at high light. However, according to Givnish (1988), maintenance and construction costs should increase with plant height because taller plants have a higher proportion of non-photosynthetic tissues, and this should result in a disadvantage for bigger trees especially at low light (when the effect of competition is excluded). It is possible that shade-tolerant species could still build large crowns with increased light absorption capacity and efficiency (see also the results on the live crown ratio) without being overburdened by maintenance costs, or that the effect described by Givnish (1988) applies only to trees above the dimensions I considered. Larger regenerating trees have been also observed to be able to use their accumulated reserves to survive short periods of reduction in light when compared to smaller ones (Delagrange *et al.* 2004), and this could contribute to their growth advantage over small trees at low light.

Intra-regeneration competition significantly decreased the growth in all Sitka spruce height and diameter models, and in the western hemlock diameter model. The negative effect of competition in the Sitka spruce height and diameter at breast height models decreased at higher light levels, consistent with the findings of Hasenauer & Kindermann (2006) and Collet & Chenost (2006), while for both the Sitka spruce and western hemlock diameter above root collar models the growth was reduced similarly at all light levels. The results suggest that height growth of seedlings may be less affected by competition than diameter growth (Collet & Chenost 2006; van Couwenberghe *et al.* 2013). Trees growing in dense patches but with almost full sunlight above them may have vertical growth that is not affected by competition while reducing their radial growth. I am aware of studies where only the radial and not the seedling height growth was affected by intra-regeneration competition (Collet & Chenost 2006; van Couwenberghe *et al.* 2013), but not of the contrary. However, the inconsistency between diameter above root collar and at breast height for Sitka spruce does not have an obvious explanation. On the question of why some combinations of species and growth were affected by competition and others not, the results did not shed more light on the already mixed review presented in the introduction. Further work, such as improving the measure of competition by considering the size, distance and species of the competitors, is needed to clarify the effects of intra-regeneration competition.

Objective 2. To evaluate the species-specific crown plasticity (in terms of apical dominance ratio and live crown ratio) under different light levels, and how this process is affected by tree size or the intra-regeneration competition

For Douglas fir and Sitka spruce, both the apical dominance ratio and the live crown ratio increased with increasing light, with a pattern similar to that observed for other conifer species by Duchesneau *et al*. (2001) and Grassi & Giannini (2005). This confirmed the ability of these species to react to low light levels by changing their crown architecture. I did not observe species-specific differences between Sitka spruce and Douglas fir when modelling the apical dominance ratio as a function of light availability. However, there were significant differences in the live crown ratio: Douglas fir maintained a shorter crown than Sitka spruce especially at lower light levels. Conversely, western hemlock seemed almost unaffected by light availability and maintained a full live crown at all levels of light. Grassi & Giannini (2005) suggested that the apical dominance and live crown ratio patterns may shift as the trees gain in size, but this was not observed in this study, consistent with the results of Williams *et al.* (1999). I found intra-regeneration competition significant neither for the apical dominance nor for the live crown ratio.

For both Douglas fir and Sitka spruce, I could fit models of height growth as a function of the apical dominance ratio of the previous year, even if for the former the results were not very accurate. For Sitka spruce, a value of apical dominance ratio of 1.2 corresponded to half of the maximum potential height growth in the next year. This result is similar to those of Grassi & Giannini (2005) (for *Picea abies* and *Abies alba*) and Page *et al.* (2001) (for Sitka spruce), who considered trees with an apical dominance ratio equal to or less than 1 to be "in check". Applying the threshold (Mason 2015) of 20-25% of full light for good growth in Sitka spruce to the model of apical dominance ratio as a function of light gives an apical dominance ratio of 1.2-1.4. I thus suggest using as a quick assessment tool in the field an apical dominance ratio of 1.5 (more conservative and simpler to measure) for identifying Sitka spruce seedlings with an adequate growth potential.

Objective 3: To evaluate if the above light-growth and crown plasticity responses can be used to identify a shade tolerance ranking.

Overall, observing all the parameters considered in this study, I define a shade tolerance ranking as Douglas fir ≤ Sitka spruce < western hemlock, similar to the one identified by Mason *et al.* (2004). However, considering only one parameter could be misleading.

Douglas fir compared to Sitka spruce had only slightly slower growth at low light but more evident faster growth at high light. Western hemlock had the greatest hight growth at all light levels, maybe due to an intrinsic difference in the canopy architecture: a very thin, drooping, and elongated leader, with no clear lateral shoots. Kunstler *et al.* (2005) also showed that a more shade-tolerant species (*Fagus sylvatica* L.) had height growth higher at all light levels than a less shade-tolerant one (*Quercus pubescens* Willd.). When comparing the diameter growth, the higher shade-tolerance of western hemlock was evident: it had a faster radial growth than Sitka spruce at low light and the opposite at high light, as observed in their natural range (Minore 1979; Taylor 1990). The fact that under high intra-regeneration competition the Sitka spruce advantage at high light disappeared may be another indication of higher shade tolerance in western hemlock, which can better resist the lateral shading from other regenerating trees.

For the three species, the best growth models belonged to different families, reflecting their different growth patterns. Only for Douglas fir was the Asymptotic-with-offset equation selected, showing a compensation point at around 8% of full light, indicative of lower shade tolerance than Sitka spruce and western hemlock (even if, as discussed already, some lack of sampling at very low light levels may have affected the analyses).

According to traditional shade tolerance definitions (e.g Messier *et al.* 1999), the observed pattern for the apical dominance ratio as a function of light availability would indicate a increasing shade tolerance ranking from Douglas fir (with lower live crown ratio a low light) to Sitka spruce to western hemlock (with higher live crown ratio at low light). On the contrary, the results of the present study indicate that at low light the more shade-tolerant species (western hemlock and then Sitka spruce) could maintain a longer live crown than the less shade-tolerant Douglas fir. This is likely to be because the former suffered less from self-shading and their shade-acclimated lower branches managed to maintain a positive carbon-balance, at least in the light range analysed in this study. The observations of the apical dominance ratio did not suggest any difference in shade tolerance between Sitka spruce and Douglas fir.

Considering the light level necessary for half-maximum-growth, the results for western hemlock in terms of height were likely affected by the lack of asymptote in the range of light considered (up to Global Site Factor 0.5). Excluding that case, the comparison of height growth suggested a shade tolerance ranking of Douglas fir < Sitka spruce, and for the diameter (above root collar) growth, a ranking of Sitka spruce < western hemlock. For Sitka spruce, the light

levels necessary for half-maximum-growth for both height and diameter at breast height were consistent with the 20-25% light threshold identified by Mason (2015), but a much higher value (Global Site Factor 0.37) was identified for the diameter above root collar.

All the species, however, seem to thrive relatively well at the light levels that can be commonly achieved in conifer stands managed with shelterwood systems (GSF 0.20-0.30). Foresters aiming at mixed-species stands in the UK could obtain an adequate regeneration growth of all these species at the same time, even considering the higher light requirements of Douglas fir when compared to western hemlock. It is likely that successional dynamics in a mixed-stand of species with such similar light requirements may be affected more crucially by variations in regeneration occurrence and survival (Wright *et al.* 1998), which could not be addressed in this study

6 Rapid assessment of forest canopy and light regime using smartphone hemispherical photography

In this chapter, I present a novel method for carrying out hemispherical photography analyses with smartphone cameras. I collected images with a smartphone and a traditional camera both equipped with fish-eye lenses. I processed the smartphone images with different protocols, and compared their results with the traditional camera pictures.

The study has been published as: "Bianchi S., Cahalan C., Hale S., and Gibbons J.M. (2017). Rapid assessment of forest canopy and light regime using smartphone hemispherical photography. *Ecology and Evolution*. DOI: 10.1002/ece3.3567". I present the same text, tables, figures of the published paper in this chapter, and the supplementary information for the online version in Annex II.

The study has been designed also with the objective of engaging citizen scientists within this thesis. If the methods were adequate, I would have tried to recruit volunteers across all the country for a crowd-sourced data collection campaign. More details about this are in Annex III.

6.1 Abstract

Hemispherical photography (HP), implemented with cameras equipped with "fisheye" lenses, is a widely used method for describing forest canopies and light regimes. A promising technological advance is the availability of low-cost fisheye lenses for smartphone cameras. However, smartphone camera sensors cannot record a full hemisphere. We investigate whether smartphone HP is a cheaper and faster but still adequate operational alternative to traditional cameras for describing forest canopies and light regimes.

We collected hemispherical pictures with both smartphone and traditional cameras in 223 forest sample points, across different overstory species and canopy densities. The smartphone image acquisition followed a faster and simpler protocol than that for the traditional camera. We automatically thresholded all images. We processed the traditional camera images for Canopy Openness (CO) and Site Factor estimation. For smartphone images, we took two pictures with different orientations per point and used two processing protocols: (i) we

estimated and averaged total canopy gap from the two single pictures, and (ii) merging the two pictures together, we formed images closer to full hemispheres and estimated from them CO and Site Factors. We compared the same parameters obtained from different cameras and estimated generalized linear mixed models (GLMMs) between them.

Total canopy gap estimated from the first processing protocol for smartphone pictures was on average significantly higher than CO estimated from traditional camera images, although with a consistent bias. Canopy Openness and Site Factors estimated from merged smartphone pictures of the second processing protocol were on average significantly higher than those from traditional cameras images, although with relatively little absolute differences and scatter.

Smartphone HP is an acceptable alternative to HP using traditional cameras, providing similar results with a faster and cheaper methodology. Smartphone outputs can be directly used as they are for ecological studies, or converted with specific models for a better comparison to traditional cameras.

KEYWORDS

canopy openness, light regime, site factors, total gap fraction

6.2 Introduction

Solar radiation is fundamental in forest ecosystems as it drives plant photosynthesis, morphogenesis, and fluxes of carbon, water and energy between soil, vegetation, and the atmosphere (Ligot & Balandier 2014). The analysis of the light intercepted by the tree crowns has been the basis for various ecological studies, especially for the dynamics of the vegetation growing under canopy cover (e.g. Pacala et al. 1996; Finzi & Canham 2000; Duchesneau et al. 2001; Coates et al. 2003). Evans & Coombe (1959) started using hemispherical photography (HP) for light analysis in forest research after they discovered the "ingenious 'fish-eye' camera" developed by Hill (1924) for cloud observations. Later, Anderson (1964a; 1964b; 1966) made a crucial contribution to the computation of light transmittance through tree crowns by using such photographs. HP is now considered the most widely-used ground-based method for describing both canopy characteristics and forest light regimes (Promis *et al.* 2011; Chianucci & Cutini 2013). It is an indirect method for measuring the light transmittance with an associated level of error that can occasionally be substantial (Ligot & Balandier 2014). However, its advantage over instantaneous light measurement is that its results do not inherently vary with time of day, time of year, or cloud cover. Direct measurements of light, such as quantum sensors, can be heavily affected by the conditions at the time of the

observations (Anderson 1966), requires longer and more expensive data collection and are more difficult to be linked to stand conditions (Čater, Schmid & Kazda 2013). Another photographic method used in forested environments is cover photography, which does not use a fish-eye lens and is focused more on canopy parameters analysis such as the leaf area index (Macfarlane, Grigg & Evangelista 2007; Chianucci & Cutini 2013).

Hemispherical photography is commonly implemented with analogue or digital cameras equipped with 180° field-of-view (FOV) "fish-eye" lenses pointing upwards. The first processing step is to estimate the amount of sky visible through the canopy, by classifying each pixel of the photo as belonging either to the sky or to any blocking element from the vegetation (canopy, leaf, branches or stems) (Gonsamo, Walter & Pellikka 2011). This is usually carried out by thresholding the image, which is done by selecting a brightness value and considering the image pixels above this as belonging to the sky and below to vegetation. Thresholding can be manual, if the operator visually decides the best brightness value to use, or automatic, if software-based techniques are applied to make the process objective and reproducible (Nobis & Hunziker 2005). Photo exposure, by affecting the quality of the image, can strongly affect the thresholding process (Rich 1990). Specifically, over-exposure can lead to overestimation of the sky fraction, but there are various methods available to tackle this issue (Beckschäfer *et al.* 2013).

From a thresholded HP image, various methodologies and software have been developed to estimate several variables, sometimes leading to a confusion in terminology (see Gonsamo et al. 2013). For canopy structural characteristics, canopy openness (usually defined as proportion of sky visible from a point) is one of the most common parameters estimated with this technology. The light transmittance of the canopy has been described largely using the Site Factor definition from Anderson (1966): the percentage of incident solar radiation at a given site compared to the total incident solar radiation in the open over the same period. This analysis requires the knowledge of the position of each gap on the hemisphere and the geographical location of the photo so that the sun track can be superimposed onto the hemisphere.

Film handling and processing constraints slowed the widespread adoption of HP until digital photography and computer software become available, leading to an increase in the use of this methodology (Chianucci & Cutini 2012). Today, another potential technological advance in this field is the availability of low-cost fish-eye lenses for smartphone and tablet cameras. One published case has already shown that for canopy cover analysis, the proportion of the forest

floor covered by the vertical projection of the tree crowns (Korhonen *et al.,* 2006), smartphone HP is comparable to HP using traditional cameras (Tichý 2015). However, that study involved the use of a specific smartphone app (GLAMA - Gap Light Analysis Mobile Application) that is useful for on-the-fly analysis in the field but less so for larger-scale studies, due to reduced processing options. Another smartphone app, HabitApp (McDonald & McDonald 2016; Deichmann *et al.* 2017) allows a quick analysis of canopy cover but again with limited processing options.

Cameras traditionally employed for HP record circular photos, while smartphone cameras take only diagonal photos, following the definition of Schneider *et al.* (2009) (Figure 1). Circular HP records the full hemisphere visible from the lens, while the diagonal photos consider a smaller rectangular area.
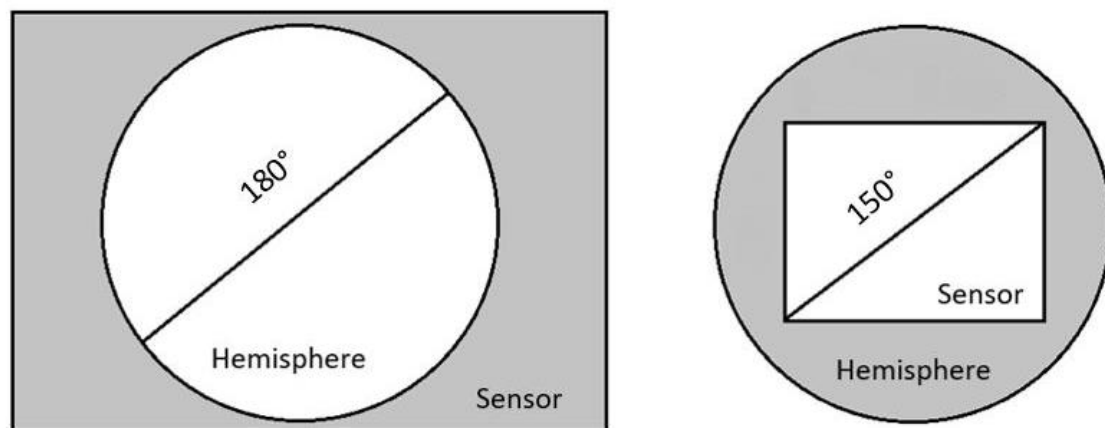
Figure 6.1. Circular HP with a full-frame camera (left) versus diagonal smartphone HP (right). Adapted from Schneider, Schwalbe & Maas (2009)

The fish-eye lenses available for smartphones at the beginning of this study only provided a FOV of up to 160°, thus reducing even further the view compared to circular HP. Both these issues will surely lead to different estimations of canopy openness between the cameras. The bias is expected to be towards higher values of openness in the smartphone HP since it excludes some of the peripheries of the image, the areas of the hemisphere usually more prone to be obscured. We are not aware of any studies where Site Factors are calculated from diagonal pictures. A sun track could be still laid on the pictures but there will be portions of the hemisphere where the computation of the light transmittance will not be possible. However, in circular HP studies the area at higher zenith angles (closer to the horizon) has sometimes been excluded from either canopy openness or light transmittance computations, for exactly the reason that is more likely to be obscured (Machado & Reich 1999) or because is prone to many

sampling and optical errors (Gonsamo, Walter & Pellikka 2010). Sky areas located at the periphery have also less luminosity and a lower contribution to the Site Factor than areas located close to the zenith (Anderson 1964a). Thus, it is possible that even if less accurate, smartphone diagonal HP could provide adequate information and in more quantity on both canopy structure and Site Factors, and, if a bias is present, it could be individuated and corrected. The challenge is to verify that the potential reduced accuracy of such measurements does not outweigh the benefits of using a cheaper, faster, less encumbering, more wide-spread technology with internet connectivity. With smartphone HP, every forestry practitioner (or citizen scientists following the recent trends) could carry out quick canopy or light analysis without the need for extra tools other than a small fish-eye lens that fits in a pocket. This could potentially lead to an amount of data substantially larger than in the traditional studies with smoothing of the probable errors present in the single measurements.

The main objective of the present research is to determine if smartphone HP is an adequate operational alternative to traditional circular HP in describing canopy structural parameters and the light regime under canopy cover. For smartphone images, we will take two pictures with different orientations per sample point and use two processing protocols: i) we estimate total canopy gap from the two single pictures, and average the values; ii) by merging the two pictures together, we form images closer to full hemispheres, so that we will be able to estimate from them canopy openness and Site Factors as in circular HP. We verify if smartphone values can be directly compared to circular HP ones, or, if a bias is present, whether models can be applied to transform and remove the bias. The values estimated from traditional circular HP images will be considered in our study the "ground truth" data against which we compare the smartphone HP estimates.

6.3 Methodology

6.3.1 Canopy and light parameter definitions

Of the various structural canopy parameters, we considered in this study: *Canopy Openness* (CO), the area fraction of the sky hemisphere that is unobstructed by canopy or other blocking elements when viewed from a single point; and *Total Gap* (TG), the ratio of the number of sky pixels to the total number of pixels in a hemispherical image (Gonsamo, Walter & Pellikka 2011). The difference between the two parameters is that the Canopy Openness calculation weights the gaps according to their position on the hemisphere, due to the geometric distortion produced by the fisheye lens (Gonsamo, Walter & Pellikka 2011). This process assigns a lower

weight to sky pixels located in the portions of the hemisphere with lower zenith angles, which are closer to the top of the hemisphere. For light regime measurements, we considered the *Indirect Site Factor* (ISF) as the transmittance through the canopy of the diffuse solar radiation generated by an overcast sky, the *Direct Site Factor* (DSF) as the transmittance of the direct solar radiation from a clear sky, and the *Global Site Factor* (GSF) as the total radiation that comprises both those components (Hale *et al.* 2009). All the Site Factors were considered averaged over one-year period. Indirect Site Factor is thus independent of the location and orientation of the photo: it is necessary only to know the zenith angle of the gaps (Anderson 1966). To calculate DSF and subsequently GSF, a sun track is overlaid on the photo to analyse how each gap interacts with the direct sunlight at different moments of the day and of the year (Anderson 1964a). In all cases, the values range from zero (fully closed canopies and no light) to one (no canopy cover and full light).

6.3.2 Study sites

We collected data from 223 sample points distributed in 24 stands located in eight forests across the UK to consider different species, overstorey and geographical conditions (see Table 1). For each stand, we laid out ten sample points with a random-systematic approach. We drew random transects on a desktop map and placed on them evenly-spaced points, later identified in the field using a GPS receiver. The distance between points varied with the size of the stand. Since most of the stands were originated by artificial planting, transects were not laid out parallel to each other to avoid following the planting lines. When carrying out the field survey, if a sample point fell in an open gap with no overstorey we relocated it under canopy cover if possible, otherwise it was discarded (thus some stands had less than 10 sample points).

Table 6.1. Overview of the study sites

Forest	Location (WGS84)	Overstorey type	No. of stands	No. of sample points
Clocaenog (Wales)	53° 04' N, 3° 24' W	spruce	4	39
		larch	1	10
Kielder (England)	55° 13' N, 2° 27' W	spruce	4	37
Aberfoyle (Scotland)	56° 13' N, 4° 21' W	larch	2	20
		spruce	1	9
Treborth (Wales)	53° 13' N, 4° 10' W	broadleaves	1	10
Newborough (Wales)	53° 09' N, 4° 20' W	pine	2	20
Mortimer (England)	52° 21' N, 2° 45' W	broadleaves	1	8
		douglas	1	9
Coed-Y-Brenin (Wales)	52° 48' N, 3° 53' W	douglas	2	17
Wykeham (England)	54° 16' N, 0° 33' W	pine	4	36
		spruce	1	8
Total			24	223

We assigned to each compartment a categorical variable named OV according to the overstorey main species, with the following levels: "broadleaves" for mixed stands composed mainly of European beech (*Fagus sylvatica* L.) and oaks (*Quercus petraea* (Matt.) Liebl. and *Q. robur* L.); "douglas" for Douglas fir (*Pseudotsuga menziesii* (Mirb.) Franco), sometimes associated with broadleaves; "larch" for European and Japanese larch (*Larix kaempferii* (Lamb) Carr. and *L. decidua* Mill.); "pine" for Corsican and Scots pine (*Pinus nigra* subsp. *laricio* Maire and *P. sylvestris* L.); and "spruce" for Sitka spruce (*Picea sitchensis* (Bong.) Carr.).

6.3.3 Data collection

At each sample point we took circular hemispherical colour photos in quick succession, under overcast sky or beneath a clear sky after sunset (Fournier *et al.* 1996). We employed either a Nikon Coolpix 4500 or a Nikon Coolpix 990 equipped with Nikon FC-E8 183° Fish-Eye Converter Lens with azimuthal equidistant projection. Of the 223 sample points, in 145 we took hemispherical photos at a fixed height of 130 cm, while in 78 points (the ones in Newborough, Mortimer and Wykeham forests) we took them above a regenerating seedling or sapling which varied from 30 cm to 200 cm, as part of another research (data unpublished).

The camera was positioned on a tripod and oriented to the North using a compass and upwards to the zenith using a level. We took a picture using the automatic exposure and then three more with respectively -0.3, -0.7 and -1 Exposure Values (EV) to obtain at least one picture with good contrast between sky and canopy (Hale *et al*. 2009). The Nikon Coolpix 4500 recorded pictures of 2048 x 1536 pixels, the Nikon Coolpix 990 pictures of 2272 x 1704 pixels. Due to this difference, we had to keep the pictures separated during some of the processing steps, but the results (see later) did not differ between the two cameras, simply called "circular HP" from here onwards.

In the same spot as each circular HP, and at the same height, we collected diagonal hemispherical colour photos with a Samsung Galaxy Grand Prime smartphone, equipped with a built-in CMOS 8.0 MP camera and a 150° Aukey fish-eye lens with azimuthal equidistant projection. We took the pictures immediately after reaching the point and with fewer precautions regarding the sky conditions (i.e. sometimes we waited for overcast sky conditions for the circular HP acquisitions, but never for the smartphone). We held the smartphone by hand, keeping it levelled and pointing upwards as best as we could. We took two pictures, once aligning the smartphone North-South and once East-West with the aid of a compass, always using the automatic exposure. The smartphone pictures had pixel dimensions of 3264 x 1836. We purposely followed a faster protocol and used less equipment (no tripod and no level) for collecting the smartphone HP.

6.3.4 Image processing

We automatically classified all the circular HP images using two systems. The first was the Ridler & Calvard (1978) iterative selection method applied to the blue channel of the pictures, where differences between sky and vegetation pixels are most evident. We used this method with the function IsoData from the software Fiji (Schindelin *et al.* 2012). For the second method, we used the colour-based algorithm *enhanceHemiphoto* (from now on called EnhanceHP) from the package *Caiman* (Diaz & Lencinas 2015) in R (R Core Team 2017). The EnhanceHP function combines the Ridler & Calvard (1978) method with a fuzzy pixel-based classification based on the colour attributes of hue, lightness and chroma, working more efficiently where differences between sky and vegetation pixels are less evident. More documentation is available in Diaz & Lencinas (2015). We applied the CIMES-FISHEYE software package (Gonsamo, Walter & Pellikka 2011) to the outputs of both classification methods. We extracted the gap fraction information for each portion of the hemisphere with the function GFA, using a grid of 24 azimuth sectors and 18 zenith annuli. This information

was the input for the following functions of the package: OPENNESS to obtain the Canopy Openness, PARSOC for the Indirect Site Factors (using the Standard Overcast Sky model) and PARCLR for the Direct Site Factor. Using the same procedure as Hale *et al*. (2009), which in turn followed the recommendations of the Met Office (2006), we calculated the Global Site Factor as in Equation 6.1.

Equation 6.1: $GSF = 0.65 \times ISF + 0.35 \times DSF$

We repeated the above estimations simulating a FOV of 150° by considering all the area comprised between the zenithal angles 75°-90° as obstructed, and obtained the same parameters, named CO150, ISF150, DSF150, and GSF150.

For processing the smartphone pictures, we used two approaches. The first was to obtain Total Gap separately from the East-West (E-W) and North-South (N-S) pictures in each sample point. After classifying each image with both the IsoData and EnhanceHP functions as above, we used the package *Raster* (Hijmans 2016) of the R Statistical Software to calculate Total Gap as the ratio of white pixels (gaps) to the total pixels. We estimated Total Gap for both the N-S and E-W smartphone photos, and then the average for each pair.

The second approach was to merge the two original pictures in each sample point and create a new one with the largest possible visible portion of the full hemisphere. We merged the images with the open source software 'Hugin', which automatically aligns and blends two or more images. The main use of Hugin is producing panoramic views but we developed scripts to batch process our canopy photos. Minor deviations from the N-S and E-W axes were frequent with the handheld smartphone, and we arbitrarily decided to use the E-W picture as the reference image for correct alignment. We thresholded all merged images with both the IsoData and Enhance function as above.

Using CIMES-FISHEYE as above, we estimated COsm, ISFsm, DSFsm and GSFsm ("sm" for smartphone) for each picture and each classification method. We carried out the calculations considering a full 180° FOV hemisphere, by setting up the GFA function of CIMES to extract the gap fraction of a larger circle than just the area covered by the merged images. Given that the diagonal length of one smartphone HP corresponds to 150°, we used a circle having a diameter equal to the diagonal length multiplied by the ratio 150°/180°. The software considered the portions of the hemisphere not covered by the merged images as obstructed (specifically, the area between the zenithal angles 75°-90° and the corners not covered by

merging the two pictures; in total around half of a full circular HP image. See online supplementary information for more details).

We carried out all the image processing with automatic and repeatable batch scripts. Figure 2 shows the workflow of the image processing. The original and merged pictures were JPG format and were transformed during the thresholding into TIFF. The free software IrfanView was then used to batch convert all the files to BMP format for CIMES-FISHEYE. The online supporting information shows examples of the circular, single smartphone and merged smartphone HP images, highlighting the corresponding coverage.
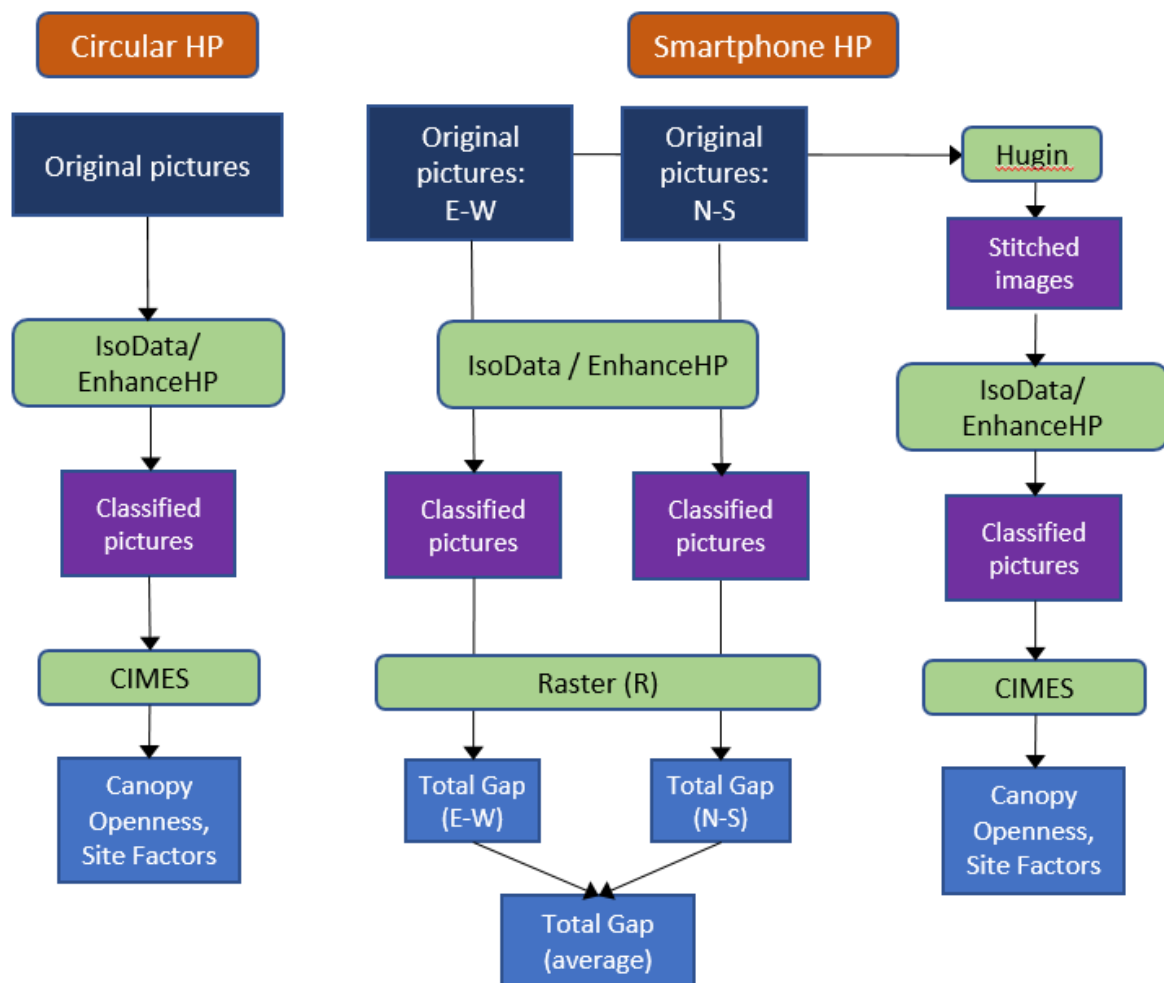
Figure 6.2. Simplified workflow of the various steps of image processing, from the original pictures to the output values.

6.3.5 Statistical analysis

To determine if there were significant differences between the thresholding methods, we compared the TG and CO estimations of the two methods when applied to the same camera pictures. To assess the differences between the estimations from circular images when different FOV were considered, we compared the respective CO and Site Factor estimations.

Then we compared the following parameters estimated from the different cameras but using the same thresholding method: CO from circular HP images (only FOV 180°) and TG from smartphone HP images (both single orientation and average values); CO, ISF, DSF, and GSF from circular HP images (only FOV 180°) and from merged smartphone HP images. We estimated Generalized Linear Mixed Models (GLMMs) of circular HP parameters as functions of the corresponding smartphone HP values. We tested as fixed effects the overstorey type both as a main term and as an interaction, to account for differences between species. We also included terms related to the different circular camera ("camera_type", with the values of either "N990" or "N4550") and the data collection methodology ("height_from_ground", with the values of either "130cm" or "variable"), to verify if such differences were significantly affecting the relationship. We used a random effect of compartments nested within forests, to account for the sampling structure. From a global model including all the above effects, we then assessed reduced models with fewer effects using the Aikake Information Criteria (AIC), and selected the one with the lowest AIC as the best model for each analysis (Symonds & Moussalli 2011). We carried out all analyses using the packages *nlme* (Pinheiro *et al.* 2016) and *stats* in R (R Core Team 2016).

6.4 Results

Figure 3 shows the value distribution for GSF calculated from the circular HP images, using the EnhanceHP method, to provide a reference for the range of data. The areas surveyed in this research varied from low light transmittance (GSF around 0.05) to medium-high level of transmittance (GSF around 0.60), with most of them falling in the range GSF 0.20-0.30. However, the range was not even across different overstorey types.
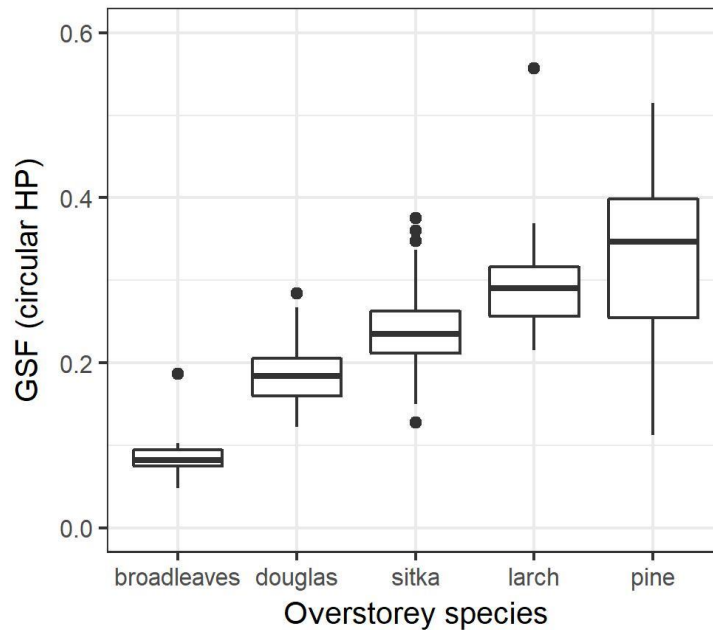
Figure 6.3. Boxplots of Global Site Factor (GSF) from circular HP images for different overstorey species. The horizontal line shows the median value, the boxes the values between the first and third quartile, the vertical lines are an additional 1.5 Inter Quartile Range above and below them.

6.4.1 Comparison of thresholding methods

Canopy parameters estimated from the pictures taken by the same camera (respectively the averaged Total Gap for smartphone and Canopy Openness for circular HP images), but classified with the different methods, were slightly lower for the EnhanceHP method than the IsoData (mean of differences respectively -0.023 for TG and -0.027 for CO, p-value < 0.001 for both). This means that more pixels were classified as canopy elements with EnhanceHP. A visual analysis of the thresholded images confirmed that EnhanceHP correctly identified as vegetation many elements that were mistaken for sky by the IsoData method. That was true not only in the few obvious cases of high exposure images but also for small vegetation elements under good contrast. Since all the following analyses showed better correlations between the values from the circular and smartphone cameras when EnhanceHP was applied to both rather than the IsoData method, we present here only the former. Additional results for the IsoData method can be found in the online supporting information.

6.4.2 Comparison of different FOVs for circular HP

Values of CO, DSF and GSF when estimated from circular HP images with FOV 150° were significantly lower than from FOV 180° (p < 0.001) although the difference was very small in absolute terms: the mean of the differences between the different FOV estimations were,

respectively, -0.001 (standard deviation, st.dev., 0.009), -0.013 (st.dev., 0.022) and -0.004 (st.dev., 0.010). No significant difference was present for ISF.

6.4.3 Comparison of circular HP with non-merged smartphone HP

The comparison of Canopy Openness from circular HP images and Total Gap from smartphone HP images (averaged between the two pictures), using the EnhanceHP method, is shown in Figure 4. TG values from the smartphone pictures were higher than CO values from circular HP images: mean of differences 0.12, st.dev. 0.04. In relative terms, TG values from the smartphone pictures on average were 165% of the CO values from circular HP images. The GLMM structure with lowest AIC maintained overstorey type only as interaction term, while both the differences in the circular camera type and the height from the ground did not affect the relationship. See Table 2 for the AIC comparison between model structures, and Table 3 for more details of the selected model. The effect of the overstorey type was that for the same increase in the values of observed TG, the predicted CO values increased more rapidly for larch and pine than for broadleaves, with Sitka spruce and Douglas fir having an intermediate effect.
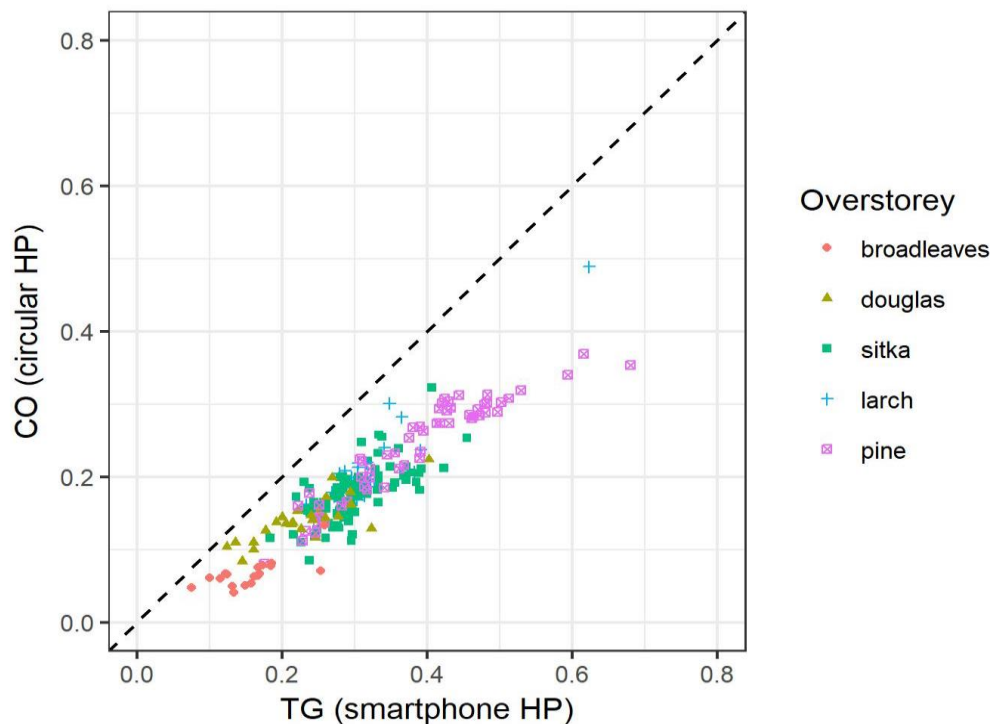
Figure 6.4. Scatterplot of Canopy Openness (CO) from circular image with Total Gap (TG) from smartphone, showing the line of identity (dashed black line), both estimated using the EnhanceHP method. Smartphone values were obtained by averaging the single images results for each plot

Table 6.2. Aikake Information Criteria comparison between different generalized linear mixed model structures for all analyses. TG is Total Gap, CO is Canopy Openness, ISF, DSF and GSF are respectively Indirect, Direct and Global Site Factor ("sm" for smartphone HP). In the formulas, y and x are the respective circular HP and smartphone HP parameter considered, OV is the overstorey type, camera is the type of Nikon Coolpix used for circular images, and HFG is the height from the ground at which the pictures were taken (see Methodology). The lowest AIC values are shown in bold.

Model	CO ~ TG	CO ~ COsm	ISF ~ ISFsm	DSF ~ DSFsm	GSF ~ GSFsm
y ~ x + x:OV + OV + camera + HFG	-984	-980	-852	-761	-877
y ~ x + x:OV + OV + camera	-991	-988	-861	-768	-885
y ~ x + x:OV + OV	-999	-997	-869	-776	-894
y ~ x + x:OV	**-1019**	**-1016**	**-891**	-792	**-916**
y ~ x + OV	-990	-980	-869	-780	-894
Y ~ x	-1009	-997	-885	**-795**	-908

The TG values from Smartphone pictures taken with different orientation in the same point, both classified with EnhanceHP, were not statistically significant ($p = 0.53$). However, when we used the TG values estimated only from the E-W and N-S pictures, instead of the averages, in the above model the results were slightly less accurate in both cases, although better for the E-W than the N-W pictures (results not shown).

6.4.4 Comparison of merged Smartphone HP with circular HP

The comparisons between the outputs estimated from the circular and the merged smartphone HP images, using the EnhanceHP method, are shown in Figure 5. The smartphone values were on average significantly different from the circular ones ($p < 0.05$ in all cases): mean of differences respectively 0.004 for CO (st.dev. 0.031), 0.042 for ISF (st.dev. 0.037), -0.012 for DSF (st.dev. 0.047), and 0.023 for GSF (st.dev. 0.040). In relative terms, the smartphone values on average were respectively the 102% (for CO), 115% (for ISF), 93% (for DSF), and 109% (for GSF) of the values of the circular HP values. For the CO, ISF and GSF models, the GLMM structure with lowest AIC maintained overstorey type as interaction term, while for the DSF both the main and interaction term were dropped. In all cases, the differences in the circular camera type and the height from the ground did not affect the relationship. See Table 2 for the AIC comparison between model structures, and Table 3 for more details of the selected models. When the effect of the overstorey type was present, it meant again that for same increase in the values of observed smartphone HP values, the predicted circular HP values increased more

rapidly for larch and pine than for broadleaves, with Sitka spruce and Douglas fir having an intermediate effect.
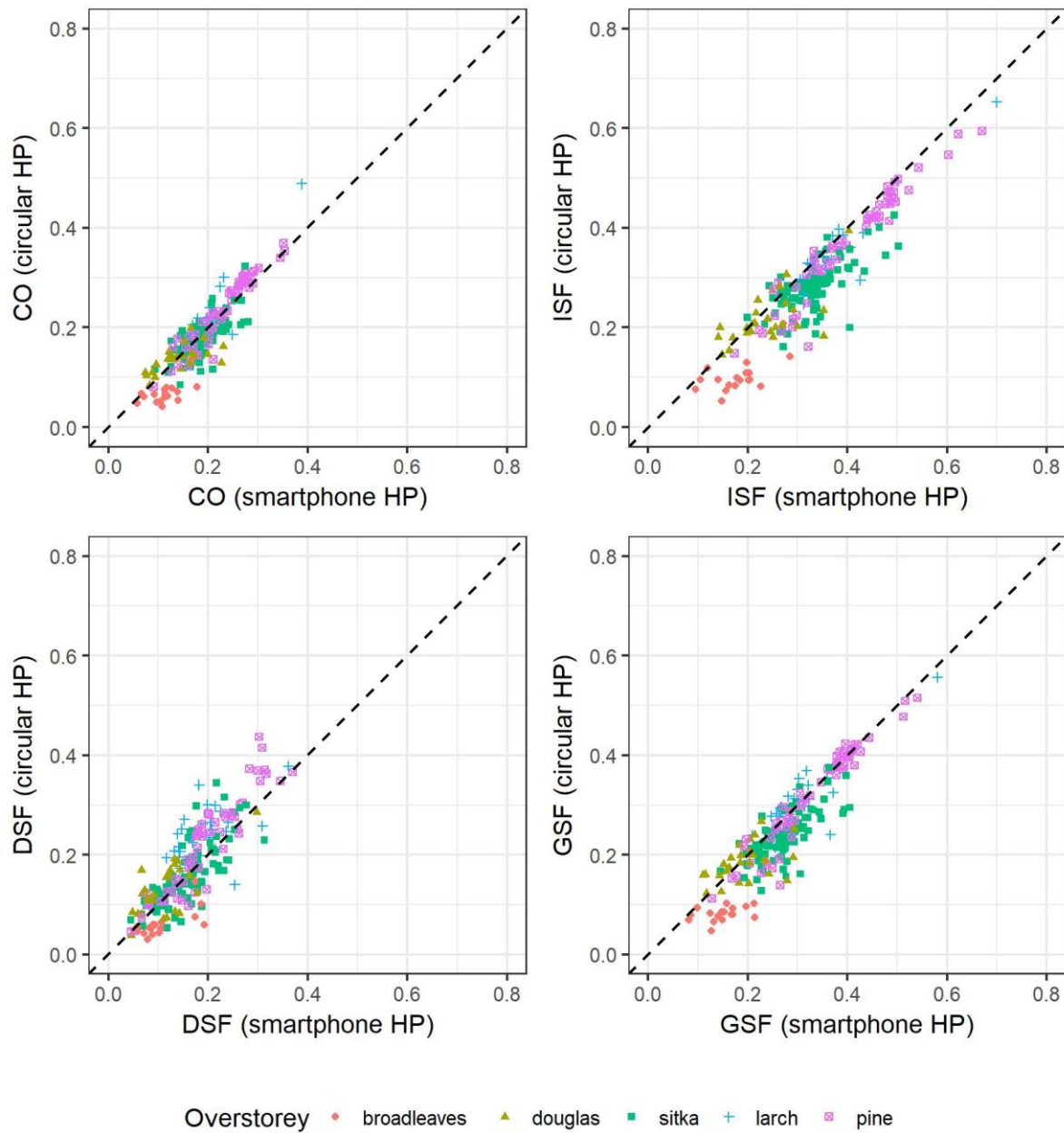
Figure 6.5. Scatterplots of Canopy Openness and Site Factors (respectively ISF for Indirect, DSF for Direct, and GSF for Global Site Factor) estimated from different cameras, using EnhanceHP method, showing the line of identity (dashed black line). Smartphone values were obtained from merged images.

Table 6.3. Results of generalized linear mixed models between the outputs estimated by circular and smartphone HP pictures, using the EnhanceHP method. CO is Canopy Openness, TG is Total Gap, ISF, DSF and GSF are respectively Indirect, Direct and Global Site Factor ("sm" for smartphone outputs). For the fixed effects, "x" indicates the smartphone HP parameter used in the model, and OV is the overstorey type.

	CO ~ TG			CO ~ COsm			ISF ~ ISFsm			DSF ~ DSFsm			GSF ~ GSFsm		
Fixed Effects	Value	St. Err	p-value	Value	St. Err	p-value	Value	St. Err	p-value	Value	St. Err	p-value	Value	St. Err	p-value
(Intercept)	0.025	0.010	0.013	0.032	0.009	0.001	0.042	0.012	0.000	0.049	0.011	0.000	0.049	0.011	0.000
x	0.275	0.082	0.001	0.309	0.118	0.009	0.355	0.095	0.000	0.764	0.046	0.000	0.292	0.104	0.002
x:OV(douglas)	0.197	0.080	0.014	0.386	0.120	0.002	0.347	0.094	0.000	-	-	-	0.376	0.107	0.001
x:OV(sitka)	0.228	0.081	0.005	0.437	0.112	0.000	0.341	0.086	0.000	-	-	-	0.384	0.097	0.000
x:OV(larch)	0.398	0.083	0.000	0.694	0.118	0.000	0.471	0.090	0.000	-	-	-	0.542	0.101	0.000
x:OV(pine)	0.267	0.081	0.001	0.610	0.113	0.000	0.487	0.088	0.000	-	-	-	0.560	0.096	0.000
Random Effects (Intercept)	Standard Deviation			Standard Deviation			Standard Deviation			Standard Deviation			Standard Deviation		
Forest	0.018			0.012			0.008			0.000			0.009		
Stand (in Forest)	0.011			0.012			0.019			0.038			0.019		
Residual	0.020			0.020			0.031			0.034			0.028		

6.5 Discussion

The results of the study suggest that smartphone-based hemispherical photography can be used as a faster and cheaper alternative to traditional camera sets. We demonstrate methods to obtain canopy structural parameters and Site Factors with the advantage of less expensive equipment and faster data collection time. We purposely carried out the smartphone image acquisition with a simpler protocol that does not need extra tools (such as a tripod or a level) or to wait for the best sky conditions. The rationale was to test a methodology that could be applied by any forest practitioner in a speedier way, potentially obtaining a higher amount of data. In this case study, a smartphone is used only for the image acquisition, while the processing is done subsequently in a computer. Thus, for example, in a crowd-sourcing project various operators can acquire the images in the field and, using other smartphone applications, upload them to a central server where the more advanced processing here described can take place.

While we carried out the smartphone pictures acquisition with fewer precautions, generally the images showed an acceptable quality in terms of exposure and contrast between sky and canopy and in turn the thresholding process gave good results. This is likely due to a combination of factors. The new sensors and in-camera processing of the smartphones are likely better than the now almost 20-years-old Nikon Coolpix. The smaller FOV of the smartphone fisheye lens may have reduced the direct sunlight hitting the sensor. The generally favourable sky conditions of the UK (high latitude, cloudy climates) have likely also played an important role, so that in other geographical areas the same precautions regarding direct sunlight may have to be applied also to smartphone hemispherical photography. However, where sub-optimal contrast between sky and canopy occurred in some of our smartphone pictures, the EnhanceHP function from the *Caiman* package gave good results during the thresholding. This method was designed to work with sub-optimal images, while the IsoData function requires good contrast pictures.

The small differences between parameters estimated from circular HP images with a FOV of 150° and 180° demonstrate that the reduced FOV of the smartphone fisheye lens could not be the main source of difference between the two cameras, which most likely are the diagonal character of the camera sensors and the lower quality of the images. New smartphone camera sensors and lenses are likely to be developed continuously, influencing both issues due to changes in the resolution of sensors and the quality and FOV of the lens, and then in turn affecting the analyses carried out in this study with our particular combination of smartphone and fish-eye lens. However, given that the same fisheye lens is used, the smartphone camera

88

used can be considered representative of the average sensor resolution and quality nowadays available, and if only new sensors will have likely better characteristics. In any case, we suggest verifying the real FOV of the conversion lens.

Total Gap, obtained from the simple processing protocol of single smartphone pictures, was consistently higher than the Canopy Openness values from circular hemispherical images, as expected. The bias between those values in this study was consistent and with a reduced deviation, suggesting that there is still potential to use Total Gap from smartphone pictures in ecological study as a substitute to traditional circular camera analysis, either as it is or transformed by using the model provided. Taking two pictures in the same point and averaging the results improved the results without significantly increasing the time required for data collection and processing, so we advise this operation for future studies.

Through the more advanced merging protocol we obtained processed smartphone pictures that could be used for estimation of Canopy Openness and Site factors. The mean differences and standard deviations between the parameters from different cameras were relatively small. This suggests that the smartphone camera outputs could be used in place of those from a circular camera. As already discussed, the areas close to the horizon not covered by the smartphone HP images did not greatly affect the Canopy Openness and Indirect Site Factor estimation. However, the different coverage was expected to give poorer results in the estimation of Direct Site Factor, which is a function also of the location of the gaps in relation to the sun track. Particular gaps with a large contribution to this Site Factor in circular hemispherical images might be excluded from merged smartphone images. In addition, the handheld alignment of the smartphone in the field are likely to have introduced additional errors in the sun track overlay. However, for the Direct Site Factor the mean difference between the circular and smartphone cameras were even lower than for other parameters. For the Global Site Factor, which in the UK depends more from the Indirect than Direct Site Factor, the differences between cameras were similar to the former. The best model structures for Canopy Openness, Indirect and Global Site Factor, included the overstorey type as interaction term, i.e. the relationship was affected by the different species' foliar and crown architecture. Overstorey type was not included in the model for Direct Site Factor, which is likely more affected by large gaps falling around the sun track, and less by the overall fine gap structure. However, there were few replicates for some classes (i.e. only two broadleaved stands out of 24), and the range of canopy openness sampled within classes was not equal (i.e. for broadleaved stands it was lower than for pine and larch stands).

In conclusion, we believe that the cheaper and faster methodologies here described for smartphone-based hemispherical photography provide reliable parameters that can be used as substitutes for those estimated from circular cameras. Smartphone outputs could be employed as they are in forest ecology studies, such as for assessment of different sites or as inputs for ecological modelling, or converted with specific transformation models for a better comparison between cameras. The range of application of the models provided here outside the forest and sky conditions and smartphone specifications considered in this study has not been tested. Since we first designed this study, new smartphone fish-eye lenses promising wider angles (up to 180° and even more) are available on online marketplaces, providing different but hopefully more accurate results when applying the methodologies here described. Due to rapid technological development, smartphone hemispherical photography could potentially gain increasing importance in future years.

6.6 Acknowledgments

6.7 Conflict of interest

None declared.

6.8 Data accessibility

The dataset used for this study is stored on the Dryad Digital Repository https://doi.org/10.5061/dryad.f6506 together with the main scripts used for the processing of the smartphone hemispherical images with R Statistical software and Hugin.

6.9 Authors' contribution

Simone Bianchi designed the original work and methodology, carried out the data acquisition, analysis and interpretation, and prepared the manuscript. Christine Cahalan and Sophie Hale critically contributed to the data interpretation and manuscript revision. James Gibbons critically contributed to the methodology development, the data analysis and interpretation, and manuscript revision.

7 Simulations of Diameter at Breast Height growth for Sitka spruce regenerating trees

In this chapter, I investigate some challenges related to DBH growth modelling for Sitka spruce regeneration, necessary for the integration of the regeneration models presented previously into the framework of MOSES_GB.

7.1 Introduction

MOSES_GB follows the same structure of the original MOSES: trees with DBH above 7 cm belong to the overstorey class, and below to the regeneration class (Hasenauer, Kindermann & Steinmetz 2006). To integrate the regeneration models described in the previous Chapters into MOSES_GB, the models should simulate the growth of regenerating trees until they reach 7 cm at which point the trees would be moved to the overstorey class.

First, the problem of the starting DBH must be solved. The models for regeneration occurrence described in Chapter 4 generates trees with height less than 130 cm, so DBH is null. After a tree grows above that height, or if for any reason a tree is manually added to the simulation, a DBH value must be assigned to it. Using the trees measured for the previous chapter, a total height-total DBH relationship, or *total H-DBH*, can be built. This relationship can be used to generate a starting DBH value as a function of height for all trees that surpass the height threshold of 130 cm at the end of any growing cycle.

Second, both the height and DBH growth for each new growth cycle must be modelled until the tree reaches the threshold of 7 cm DBH. For the height, the light-growth model presented in Chapter 5 can be used. For the DBH, there are three different possible approaches.

1) Use the light-DBH growth model presented in Chapter 5;
2) After estimating the height growth as above, simulate the DBH growth as a function of the height growth;
3) After estimating the height growth as above, assign a new total DBH as a function of the new total height.

The second and third approach are height-driven. Their rationale is that height growth for seedlings and saplings is the most crucial developmental force as trees compete for light and vertical growing space, which in turn determines the diameter growth (Crookston & Dixon 2005). For approach 2, it is necessary to build a new height growth-DBH growth relationship, or *growth H-DBH*, again using the trees measured for the previous chapter. For approach 3, the same total H-DBH model aforementioned can be used.

The specific objectives of this chapter were: i) to build a total H-DBH function, simulating the DBH of Sitka spruce regenerating trees taller than 130 cm as a function of total height; ii) to build a growth H-DBH function, simulating the DBH growth of Sitka spruce regenerating trees as a function of height growth; and iii) to compare the three different aforementioned approaches for modelling the DBH growth.

7.2 Methodology

7.2.1 Tree measurements

For each Sitka spruce tree assessed for DBH in Chapter 5 (n=55), I took additional measurements following the same methodology described there. On each tree, I measured the leader shoots of two additional past vegetative seasons, all called Hg_i (height growth at year *i*), as long as the beginning of the shoots were above 130 cm height. On each DBH stem section, I measured the corresponding growth rings of those additional vegetative seasons (on two diameters and averaged the values), all called $DBHg_i$ (DBH growth at year *i*). Then I assessed the corresponding total tree height and diameter at the end of each growth period (Ht_i and $DBHt_i$ respectively total height and total DBH at year *i*). See Figure 7.1 for a summary of the tree measurement schematics. I created new datasets for each analysis with the replicated measurements on each tree, keeping track of the tree identity and the year of the corresponding growing season. I used the Hg_i and $DBHg_i$ data for the growth H-DBH model (n=127), and the Hg_t and $DBHg_t$ for the total H-DBH relationship (n=182). From the 55 original individual trees, I obtained more data points for the latter since I could use the measurements from an extra past growing season (*i*-3).
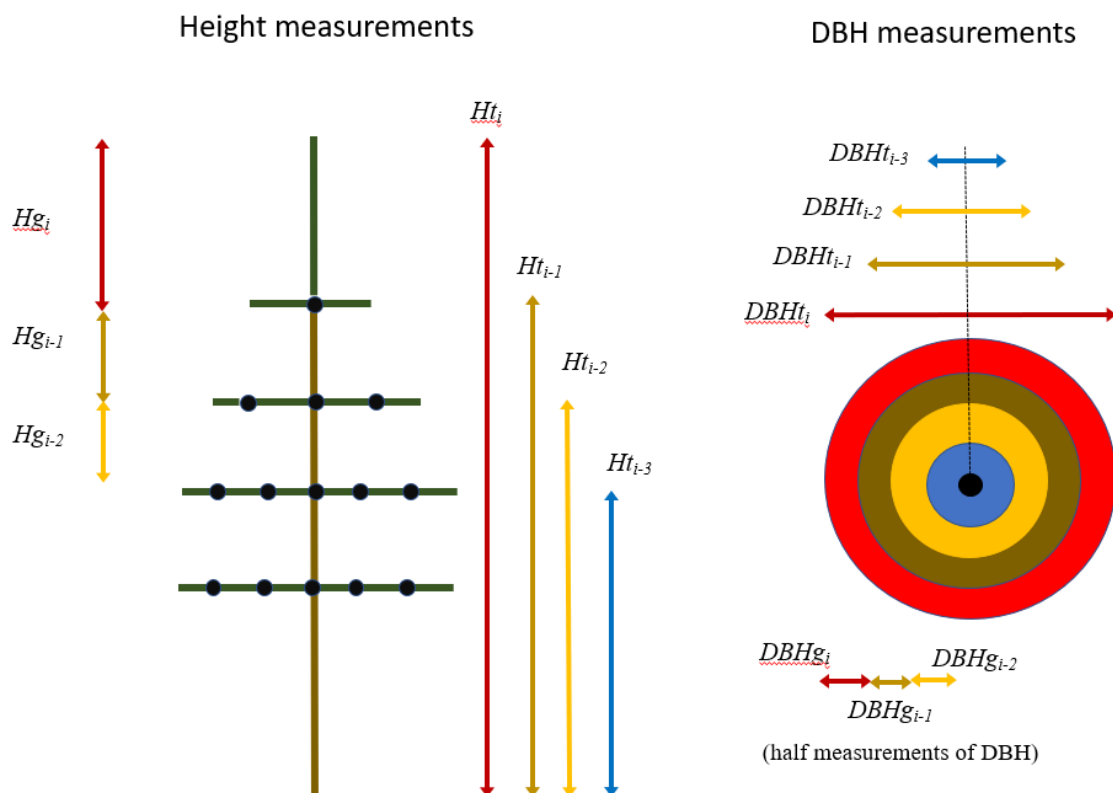
Figure 7.1. Schematics of tree height and diameter measurements. Hgi is the height growth at year i; Hti is the total height at year i; DBHgi is the diameter at breast height growth at year i, DBHti is the total diameter at breast height at year i. Please note that the arrows for DBHgi indicate the extent of the radius, thus half the diameter growth. DBHgi has been measured on two different diameters and the result averaged.

7.2.2 Statistical analysis

I carried out all the analyses using the package *nlme* (Pinheiro *et al.* 2016) from R Statistical Software (R Core Team 2017).

7.2.2.1 Height-DBH relationships

I estimated Generalized Linear Mixed Models (GLMMs) fitted by maximum likelihood of DBH (growth or total) as a function of height (growth or total), intra-regeneration competition (as estimated in the previous Chapter), and a 2-way interaction term between height and competition. I included as a random effect the tree ID, to account for repeated measurements being taken on the same individual. After a preliminary observation of the data and of the Akaike Information Criteria (AIC) results of preliminary models, I decided to include tree ID as a random intercept in the growth H-DBH model, and as a random slope in the total H-DBH. I excluded light availability as a fixed effect since I could not be sure if and how it changed in the last 3-4 years. The correlation between light availability, estimated at the time of the survey,

and both height & diameter growth decreased going from the current season to the previous ones (results not shown). Preliminary results showed that neither a spatial autocorrelation effect due to the stand or forest surveyed, or a temporal autocorrelation effect due to the year of the growing season significantly improved the AIC, so they were excluded. To better model the heteroscedasticity of the data, I considered the variance as a function of the fitted values. Then, from both the global growth H-DBH and total H-DBH models with all the variables, I tested all the possible nested sub-models with fewer fixed effects and selected as the best model the one with the lowest AIC. In case there were models with differences of less than 2 AIC units, I chose the one with fewest explanatory variables.

7.2.2.2   Comparisons of DBH growth simulation approaches

I estimated the accuracy of the three modelling approaches for DBH growth by cross-validating the light-DBH growth model calibrated in Chapter 6, and both the growth H-DBH and total H-DBH models calibrated as above.

I used the same dataset with the original 55 Sitka spruce trees measured for DBH. First, using the light-height growth model described in Chapter 5, I simulated the height growth of the last growing season (Hg) and added it to the observed height previous to the growth (Hp) to simulate the total Height (Ht). Then, I applied the following procedures:

1) Using the light-DBH growth model described in Chapter 5, I simulated the DBH growth of the last growing season (DBHg) and added it to the observed DBH previous to the growth (DBHp) to simulate the total DBH (DBHt).

2) Considering the simulated Hg as input, I used the growth H-DBH model to simulate DBHg, then added it to DBHp to simulate DBHt.

3) Considering the simulated Ht as input, I used the total H-DBH model to simulate directly DBHt.

I used a cross-validation technique during all the simulations steps, specifically a *leave-one-out cross-validation* (LOOCV), which has been shown to provide an almost unbiased estimate of the true generalisation ability of a model (Cawley & Talbot 2004). When using any of the models indicated in the above procedures for a certain tree (either the light-height growth, the light-DBH growth, the growth H-DBH or the total H-DBH model), I recalibrated it beforehand without the data from that tree and then predicted the values for that tree. I compared the results of the total DBH simulations from the three approaches with the observed values using scatterplots and calculating the residual errors. The summary of the validation process

procedures is shown in Figure 7.2. For the light-DBH growth and growth H-DBH approaches, I also calculated the residuals of the DBH growth simulation obtained during the intermediated steps, and plotted against the observed values.
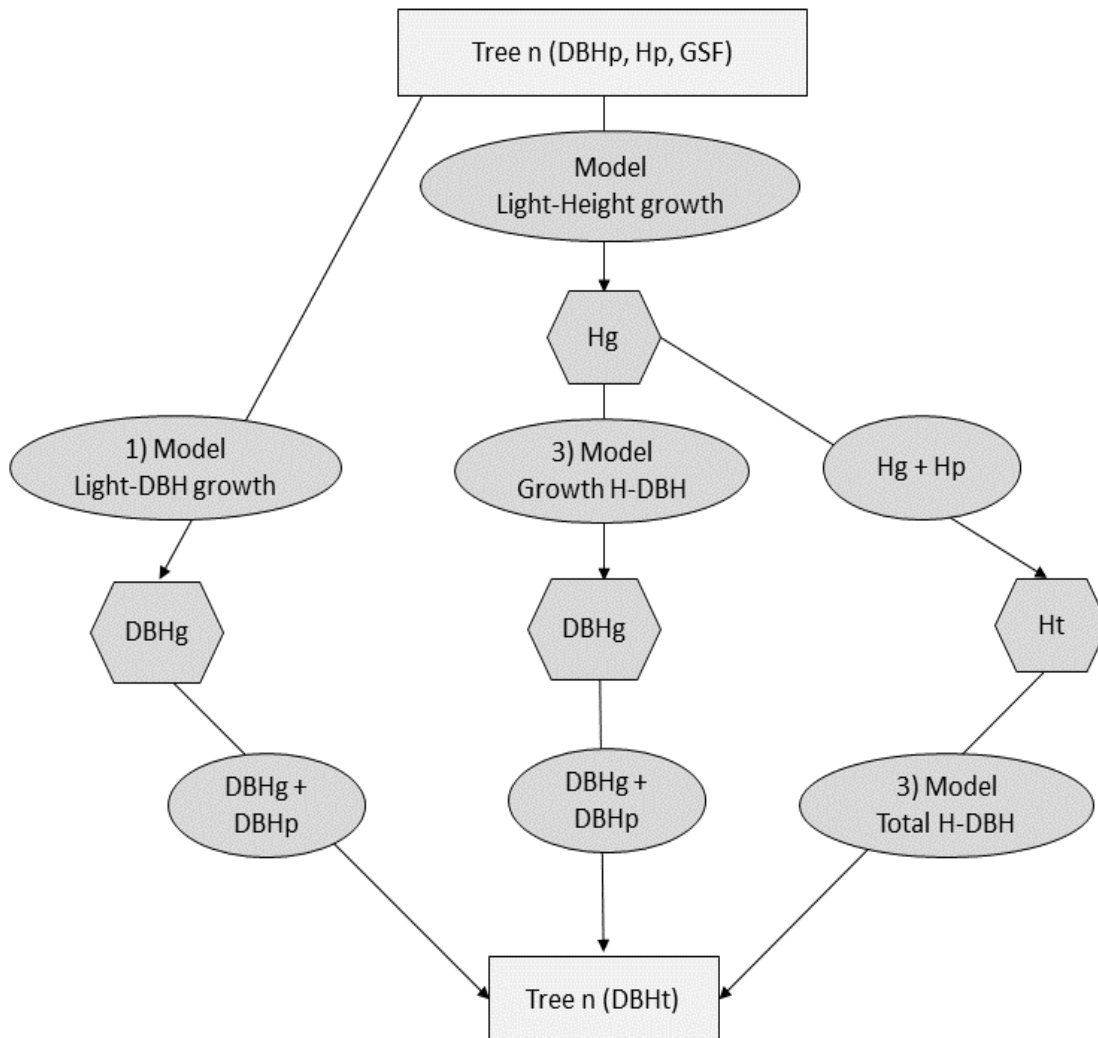
Figure 7.2. Summary of the validation procedures for the three approaches for DBH growth simulation. DBHp, diameter at breast height previous to the growth; Hp height previous to the growth; GSF (Global Site Factor), light availability. Circles, the models used during the process for each tree with a leave-one-out cross-validation process, or simple algebraic operations. Exagons, outputs of such models or operations (DBHg and Hg are respectively DBH and height growth). DBHt, the final simulated total DBH for a certain tree n.

7.3 Results

7.3.1 Height-DBH relationships

The best model (lower AIC, least explanatory variables) for both the growth H-DBH and the total H-DBH relationships included only height growth as a fixed term (see Table 7.1). Competition and the two-way interaction term were excluded in both cases. Figure 7.3 shows the simulated versus the observed values for both models, and the standardized residuals plotted against the fitted values, which were both homogenously distributed.

Table 7.1. Details for the fixed and random effects of the best growth H-DBH and total H-DBH models.

growth H-DBH model			
Fixed terms	**Value**	**Standard Error**	**p-value**
(Intercept)	0.901	0.310	0.005
Height growth	0.125	0.008	<0.001
Random terms (Intercept)	**Standard Deviation**	**Residual**	
tree.id	0.972	0.290	
total H-DBH model			
Fixed terms	**Value**	**Standard Error**	**p-value**
(Intercept)	-17.868	1.010	0.000
Height	0.154	0.005	<0.001
Random terms (slope)	**Standard Deviation**	**Residual**	
tree.id	0.034	0.305	
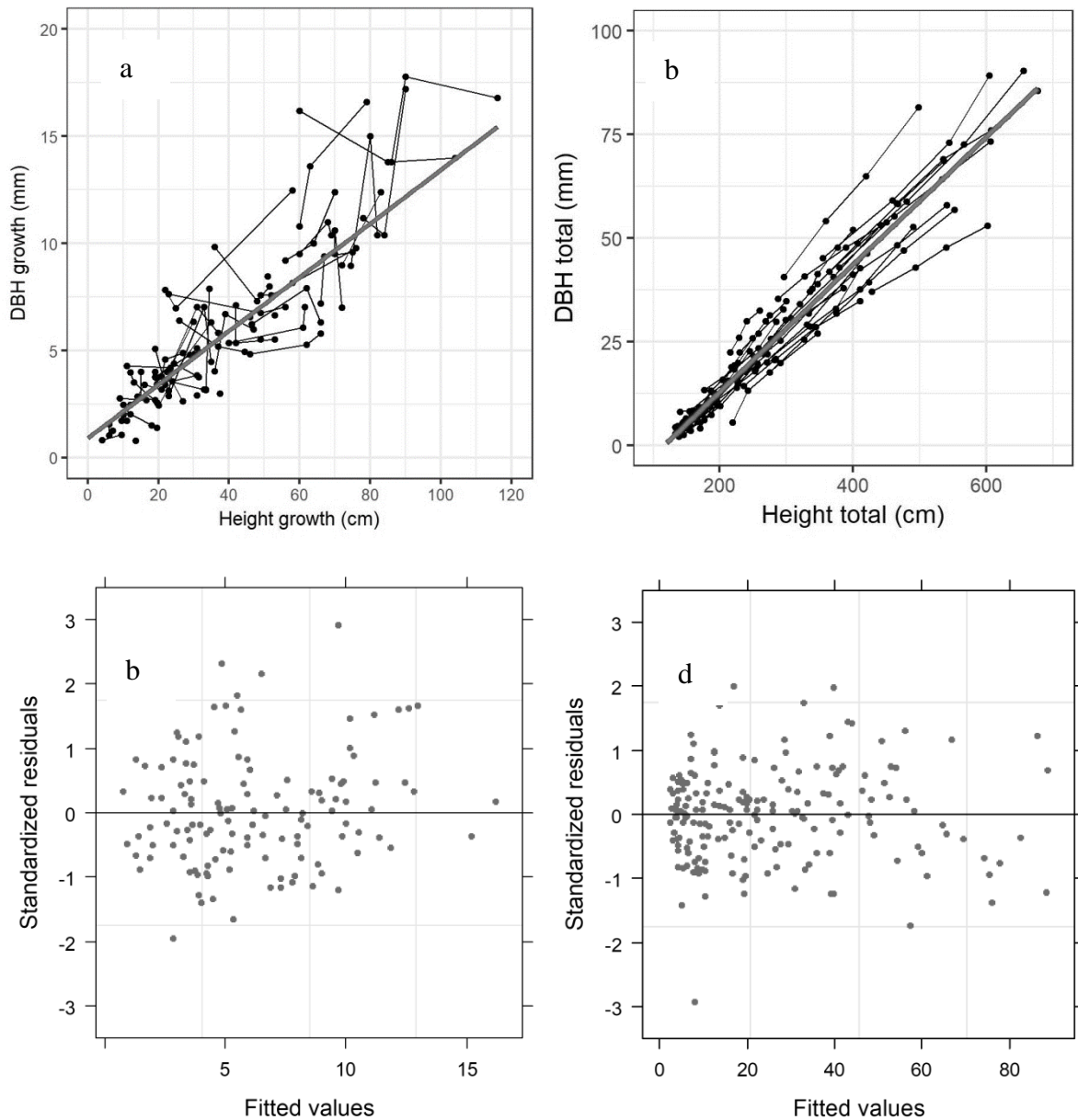
Figure 7.3. Graph a and b, observed values (points, tree measurements on the same tree are connected by lines) versus simulation results (grey lines), respectively for the growth H-DBH model and the total H-DBH model. Graph c and d, standardized residuals plotted against the fitted values respectively for the growth DBH-Height model and total H-DBH model.

7.3.2 Comparisons of DBH growth simulation methods

The results of the cross-validation procedures for all methods are summarised in Figure 7.4, which displays the simulated versus observed DBH values, and in Table 7.2, which shows the Root-Mean-Square-Error (RMSE), the Mean Absolute Error (MAE), and the Mean Absolute Percentage Error (MAPE). The light-DBH growth and the growth H-DBH approaches were the most accurate, and very similar in their error distribution, while the total H-DBH was the least accurate.

Table 7.2. Summary of the errors (in mm) for the total DBH after the cross-validation procedure for each approach. RMSE is the Root-Mean-Square Error. MAE is the mean absolute error. MAPE is the MAE relative to the observed total DBH.

	RMSE	MAE	MAPE
Light-growth DBH	2.75	2.01	0.09
Growth H-DBH	2.82	2.04	0.11
Total H-DBH	6.46	4.15	0.16
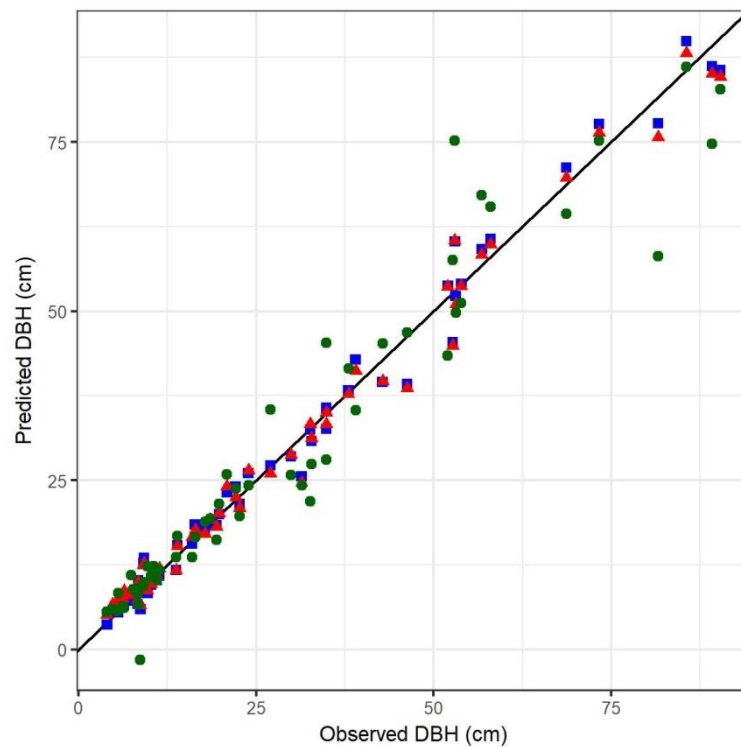
Figure 7.4. Scatterplot of the predicted versus observed total DBH for each approach. Blue square, using approach 1 (DBH light-growth); red triangles, approach 2 (growth H-DBH); dark green circles, the approach 3 (total H-DBH).

Moreover, when using the total H-DBH model, all trees would reach the 7 cm DBH threshold at the same height (around 580 cm). On the other hand, with the growth H-DBH model, trees would reach 7 cm DBH at different total heights according to their growth history. Specifically, a tree growing faster in height would reach 7 cm DBH at a higher total height than a tree growing slower in height (see an example in Figure 7.5). Similarly, in the case of the light-DBH growth model, each tree would reach 7 cm DBH at a different height according to its specific growth history, influenced not only by light availability but also by the competition.
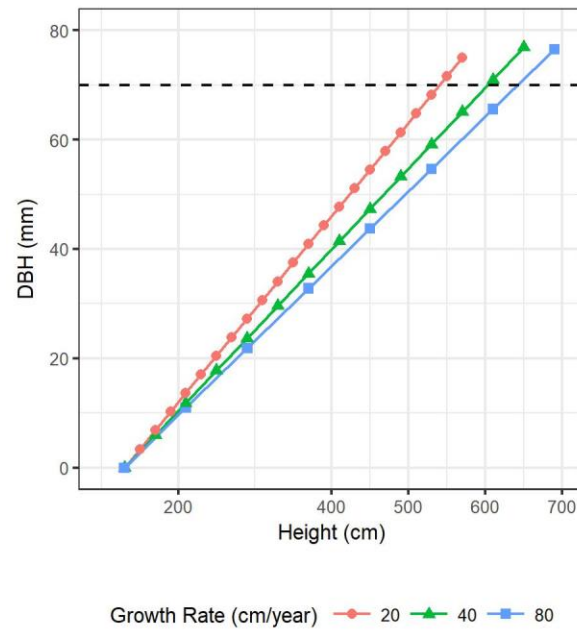
Figure 7.5. Simulation of DBH as a function of height for trees growing at different and constant yearly rates, using the growth H-DBH model. The horizontal dashed line is the 7 cm DBH threshold, each point on the line corresponds to one growing season.

Figure 7.6 shows the residuals analysis of the simulated DBH growth for the light-DBH growth and growth H-DBH approaches, plotted against the observed DBH growth. The same tendency of decreasing accuracy for higher growth values observed in Chapter 5 for the light-DBH growth model, was here observed for both approaches.
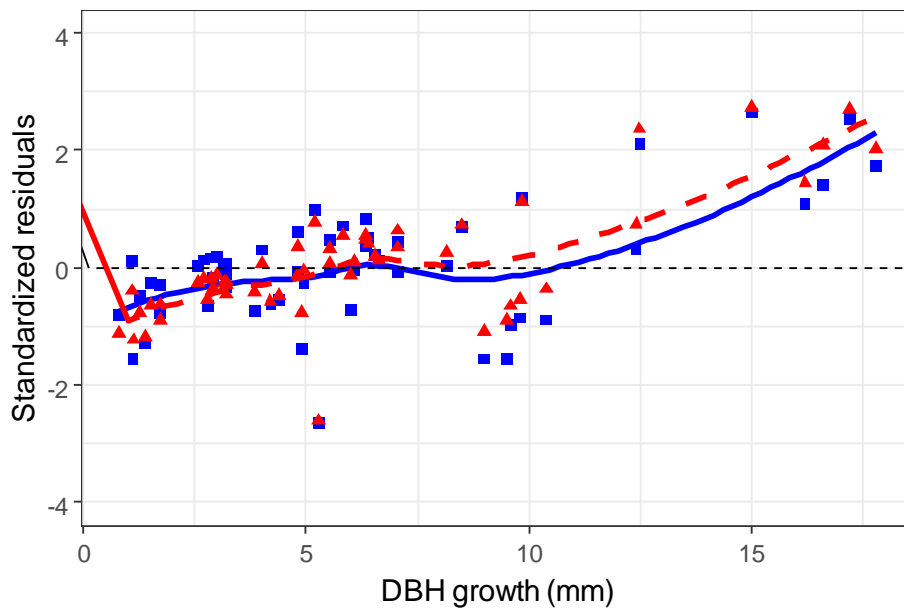
Figure 7.6. Standardized residuals of the light-DBH growth (blue squares and blue line) and growth Height-DBH (red triangles and red dashed line) models after the cross-validation process, plotted against observed values of DBH growth. The lines are LOESS smoothers.

99

7.4 Discussion

I prepared here some tools necessary for the DBH growth simulation and the integration of the regeneration models presented so far in this thesis into a forest growth simulator such as MOSES_GB. I calibrated a model of total DBH as a function of total height, which can be used to simulate the initial DBH of Sitka spruce trees surpassing the 130-cm height threshold during the regeneration development simulation, or that are manually added by an operator.

After comparison of the different approaches for simulating the DBH increment, the light-DBH growth and the growth Height-DBH models were found to be very similar in accuracy. This confirms a close relationship between height and diameter growth. The results were interesting especially since the two modelling steps necessary for the growth Height-DBH approach were expected to introduce more errors. The total Height-DBH approach showed errors of a greater magnitude which is likely to be because it was predicting a new total DBH value (a parameter with relative larger variability), instead of starting from the known DBH of the previous year and adding the DBH growth (a parameter with relative smaller variability). Moreover, when using the total Height-DBH approach, all trees of a certain height would automatically have 7 cm DBH, regardless of their growing history. This would not happen in any of the other approaches.

Therefore, discarding the total Height-DBH model, the remaining two approaches both seem suitable to the same degree for modelling DBH growth. However, due to the small number of trees measured for DBH in this thesis (n=55), and the tendency towards lower accuracy at higher values of DBH growth in both approaches, there could be the need to expand the sample size to improve the models. This study suggests that in such a case, the growth Height-DBH approach would require a simpler data collection: only height and diameter growth sampling, with the possibility of repeated measurements on each tree, and without the need of assessing the light availability.

8 Integrating the Sitka spruce natural regeneration models into MOSES_GB

In this chapter, I investigate the integration of the regeneration models for Sitka spruce prepared so far (Chapters 4, 5 and 7) into MOSES_GB. I compare different modelling options, and test them under different forest characteristics and silvicultural managements.

8.1 Introduction

It is important for this thesis, to test the feasibility of integrating the regeneration models I prepared so far into a forest growth simulator that includes an overstorey trees layer, so that the continuous stand development desired in CCF scenarios could be modelled (Miina & Saksa 2006). To do so, I decided to simulate the development over many years of an overstorey layer by using MOSES_GB, together with a regeneration layer by using the models prepared in this thesis. The regeneration layer is affected by the characteristics of the overstorey layer and in turn, provides information on if, when and how many new trees are recruited to the overstorey. However, the lack of long-term regeneration studies in the UK made it impossible to validate the results of such a simulation with existing data.

I focused on verifying the sensitivity of the regeneration simulation when all the components were brought together into MOSES_GB. I considered two different stands each under two different thinning regimes. In each of the above cases, I tested two different modelling approaches in terms of spatial information. The overstorey components of MOSES_GB are non-spatially-explicit, that is even if a complete tree tally with spatial information is provided, the simulation considers a competition effect for each tree that is independent of its location in the stand (it is based only on the number and size of all trees larger than the subject tree at stand level). For the regeneration components, I compared a non-spatially-explicit approach as above (all regeneration was affected by a homogenous overstorey competition) with a spatially-explicit approach. In the latter the positions of both the overstorey and regenerating trees were known, and within-stand variations affected the regeneration processes at local level, as recommended by Miina *et al*. (2006). For the eight different scenarios (two stands × two thinning regimes × two simulation approaches), I determined when and how many regenerating trees were recruited into the overstorey after a medium-term simulation.

8.2 Methodology

8.2.1 General workflow of the simulation

I considered two virtual one-hectare Sitka spruce pure stands, both of mature age but with different tree densities and past management. The first, Clocaenog or stand A, was based on a structure already on the way to transformation to CCF, with a relatively low tree density due to a past thinning regime aimed at achieving natural regeneration. The second, Grizedale or stand B, represented a more traditional stand, not recently managed and with a higher tree density. The characteristics of both stands were obtained from Chapter 4 (more details are given there on the survey methodologies employed), specifically age (in years), years after last thinning, moss cover (in %), basal area (BA, m^2 ha^{-1}), stems per hectare (SPH, n ha^{-1}), and DBH distribution (Table 8.1). As described in Chapter 4, I assigned to both stands a Thinning Class, as a numeric value and homogenous at stand level, according to the years since the last thinning: TC1, 1-5 years; TC2, 6-10 years; TC3, 10+ years or never. I considered the moss cover also to be homogenous at stand level. I collected the data for Clocaenog, while the Grizedale data come from the dataset of Kerr *et al.* (2011).

Table 8.1. Summary of stands characteristics at the beginning of the simulation.

Forest name	Clocaenog (A)	Grizedale (B)
Area (hectares)	1	1
Age (years)	65	60
Years after last thinning	6	20+
Moss cover (%)	90	39
Basal area (m^2 ha^{-1})	38.2	84.4
Minimum DBH (cm)	40	8
Average DBH (cm)	49	33
Maximum DBH (cm)	57	57
Stems per hectare	200	900

For technical details on the MOSES_GB overstorey modelling components, see the prototype manual from Hale, Jenkins & Arcangeli (2012). I compared the application of two thinning regimes for each stand: no intervention, denominated "Control", and a thinning of 20% of the stems at the beginning of each five-year period, denominated "Thinned". MOSES_GB carried out a random selection of trees to be removed during each thinning. After each 5-year growth period, I updated the age and the Thinning Class for each scenario. I assumed the moss cover to be constant throughout the years.

The general workflow of the simulation, summarized in Figure 8.1, was as follows:

1) generate the stand characteristics at year 0;
2) generate a first Sitka spruce regeneration layer with the models of regeneration presence and density prepared in Chapter 4, using as inputs the corresponding stand characteristics;
3) simulate the overstorey growth and mortality after 5 years using MOSES_GB, with or without the thinning event;
4) estimate the average light availability under canopy cover for this five-year period (see later for model details and averaging methods);
5) simulate the regeneration growth in one-year steps for this five-year period according to the light availability, using the height and DBH growth models prepared in Chapter 5 and 7, and the regeneration mortality (see later for model details);
6) generate a new wave of regeneration, as in step 2 above;
7) check if any regenerating tree reached the 7-cm DBH threshold, and if so move it to the overstorey;
8) and then repeat from point 3 to 6 above for a new five-year period.

I simulated in this way three five-year periods, from year 0 to year 15. Figure 8.1 shows some of the main issues that were encountered during the simulation, for example the lack of a dedicated model for a step (namely for the starting regeneration height and the regeneration mortality), the lack of a proper validation for a model (namely for the light availability model), or uncertainties about when to activate a step (namely for step 6).
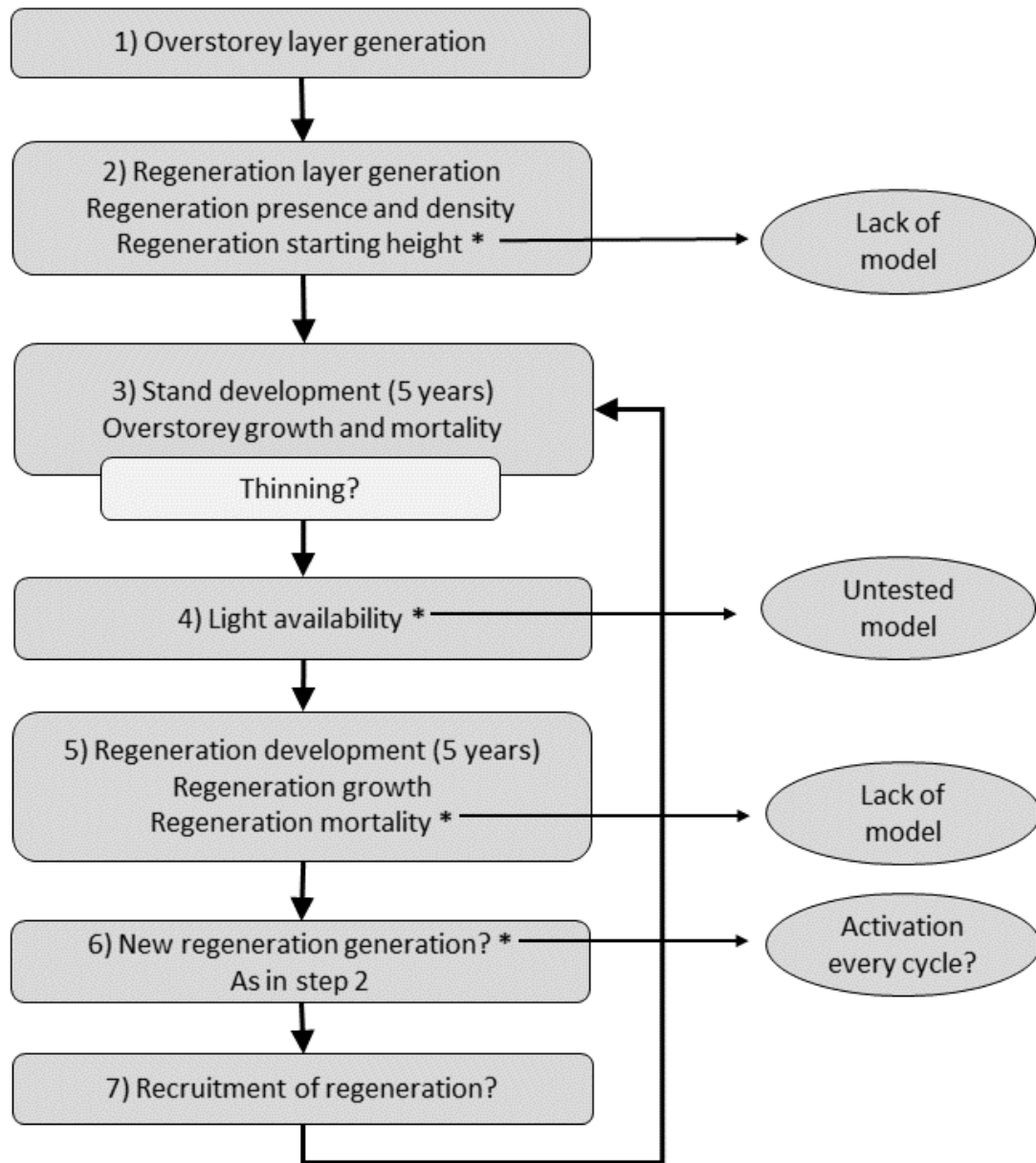
Figure 8.1. General workflow of the simulations, indicating some of the possible problems (circles).

To determine the light availability below canopy cover, I used Model 8.1 from Hale *et al.* (2009), which estimates the Global Site Factor (GSF) from stand characteristics in pure stands of Sitka spruce in the UK that originated as artificial plantations.

Model 8.1: $GSF = e^{-0.5710 - 0.0178 * \text{BA} - 0.0011 * \text{SPH}}$

The model was designed to estimate the average light availability at stand-level, and its use at plot level (see later in the spatially-explicit approach) was not tested in the original study. To verify the feasibility to use this model at plot-level, I carried an independent validation in Annex IV.

For the regeneration mortality, the only available growth-mortality relationship was from Butler (2016). He observed that the relative height growth (RHG, the height growth relative to the total height of the plant) for recently-deceased Sitka spruce seedlings was on average 15%, a value significantly lower than the average for the live seedlings in the same study area. However, he studied only seedlings ranging from 20 cm to 130 cm in height. For the trees sampled in Chapter 5, the average RHG decreased sharply with increasing height, almost threefold from seedlings 75 cm tall to saplings 600 cm tall (results not shown), indicating that this threshold could not be used for bigger trees. In any case, there was no information on the likelihood of seedlings dying when their growth was below that threshold. Arbitrarily, I decided that if a seedling (considered to have height ≤ 130 cm, and therefore DBH = 0) experienced a RHG below 15%, it had a 50% chance of mortality. For saplings (considered to have height > 130 cm, with DBH > 0), I used a density-induced mortality function like the one MOSES_GB applies to the overstorey. I calculated the Stand Density Index of regeneration (SDIr), applying Equation 8.1 to the regenerating trees.

Equation 8.1: $SDIr = \sum(\frac{DBHi}{25})^{1.6614}$

where *DBHi* is the DBH in cm of a certain sapling *i* present in the simulation unit. If the SDIr per hectare was higher than the maximum value of 1,476 (as used by MOSES_GB for Sitka spruce mature trees) at any given time, the number of regenerating trees was reduced until the maximum SDIr was obtained.

I considered harvesting damage to happen immediately after each thinning, with rates based on the study from Stokes, Kerr & Ireland (2009). For simplicity, I considered only the mortality for regenerating trees less than 200 cm, as a 50% rate after each thinning event. It was assumed here that the damage to the bigger regenerating trees could not lead to mortality and removal of the trees from the simulation.

More details on how I carried out all the above steps in the non-spatially-explicit and spatially-explicit approaches are described in the next sections. I used the base tools of R Statistical Software (R Core Team 2017) for all steps involving the regeneration modelling, and the packages *raster* (Hijmans 2016), *rgdal* (Bivand, Keitt & Rowlingson 2017) and *rgeos* (Bivand & Rundel 2017) for the spatially-explicit analyses. Due to the stochastic methods employed in the regeneration presence and density models (see later), I employed the same set of pseudo-randomly generated numbers for all the simulations.

8.2.2 Non-spatially-explicit approach:

Year 0. For step 1, I used the module STANDGEN (Kitterberger 2003) within MOSES_GB to create a tree tally that had the same total BA, same total SPH and same DBH distribution (in terms of standard deviation) of the original stand. The spatial location of the trees was ignored. I assumed that within each stand the characteristics (Table 8.1) were homogenous across all the area, in terms of age, TC, moss cover, BA and SPH.

For step 2, I used Model 4.1 to estimate the likelihood of regeneration presence (p_{regen}) at stand level, using as input the stand average characteristics. In each scenario, I considered the 1 ha stands to be divided into 2,500 virtual 4 m^2 regeneration plots (the simulation unit of the regeneration presence and density models). Again, their spatial location was ignored. Using a stochastic method, I checked the regeneration presence for each plot. To do so, I generated 2,500 pseudo-random values between 0 and 1. The number of virtual plots assigned as having regeneration was set to be equal to the number of pseudo-random values below p_{regen}. For each virtual plot with regeneration presence, I simulated the seedling density by generating a random number from the Weibull distribution functions presented in Chapter 4 (see Table 4.5), using the function for the specific TC in each scenario. Those functions generated density values per hectare that had to be transformed to seedlings per plot.

I considered all the seedlings in one plot to have the same height, determined by generating in each case a pseudo-random number from a normal distribution with mean 75 cm and standard deviation 15 cm (a distribution roughly encompassing the full seedling height range, 20-130 cm).

Year 5. For step 3, I used MOSES_GB to simulate the development of the overstorey trees for a five-year period (considering growth, mortality and, where appropriate, thinning), obtaining a new tree list for each scenario. From that I calculated the new stand-level values of SPH and BA at year 5, and updated age and TC as appropriate. In the thinned regime, I halved (rounded to the closest integer) the number of regenerating trees in all plots with height less than 200 cm, to account for the harvesting damage.

For step 4, I estimated the average light availability for this five-year period with Model 8.1, which was assumed to be homogenous across all the stand. I used the stand-level characteristics as inputs and applied the following averaging methods according to the thinning regime:

1) Control = average of light availability estimated at year 0 and at year 5.

2) Thinned = average of light availability estimated at year 0 *immediately after the thinning* (i.e. the tree removal) and at year 5.

For simplicity, I assumed that the light availability was constant throughout each year in both regimes, and that the thinnings were carried out at the very beginning of the five-year period. To estimate the light availability at year 0 and at year 5, I used the corresponding stand-level characteristics. For the light availability immediately after the thinning, I retrieved from MOSES_GB the list of trees cut during the thinning, removed the number of trees and the sum of their basal areas from the stand SPH and BA of year 0, and applied again Model 8.1.

For step 5, I used the above light availability as input for the regeneration height growth simulation in all virtual plots. I applied the light-growth Model 8.2 to each virtual plot five times in a row to represent each one-year simulation within the five-year period, updating every year the total height with the new growth (source: Chapter 5).

Model 8.2: $Hg_t = \dfrac{5.264 * H_t^{0.430}}{1 + e^{\frac{(0.339 + 0.043 * COMP) * H_t^{0.101} - GSF}{0.117}}}$

where Hg_t is the height growth in year t, H_t the height (before the growth) in year t, *COMP* the competition factor, *GSF* the light availability estimated by Model 8.1. I considered the competition for trees less than 130 cm height to come from half of the number of trees in each virtual plot, minus one to exclude the subject tree, to consider a 2 m^2 area as in Chapter 5. For taller trees, I considered the competition to come from the total number of trees in each virtual plot (a 4 m^2 area), again minus one. For trees taller than 250 cm, the 4 m^2 area was smaller than the one considered in Chapter 5, but this approach was the only one possible due to the lack of spatial information. In both cases, I log-transformed plus 1 the number of trees considered to obtain COMP, as in the method described in Chapter 5.

For trees that surpassed 130 cm height at the end of any one-year simulation, I used Model 8.3 to calculate their initial DBH as a function of the height (H) (source: Chapter 7).

Model 8.3: $DBH = -17.868 + 0.154 * H$

For trees that were already above 130 cm in height at the beginning of any one-year simulation, I calculated their DBH growth (DBHg) after their height growth (Hg) using Model 8.4 (source: Chapter 7).

Model 8.4: $DBHg = 0.901 + 0.125 * Hg$

The Live Crown Ratio (LCR), information that is used in MOSES_GB for modelling the growth of mature trees, was estimated for regenerating trees using Model 8.5 (source: Chapter 5, note that the coefficient for log(GSF) is adjusted for Sitka spruce).

Model 8.5: $LCR = 0.921 + 0.078 * \log(GSF)$

Since all the regenerating trees in the same plot had the same starting height, throughout the simulation they all grew in the same way and thus always have the same height, diameter and LCR.

For mortality, I used different methodologies for plots containing seedlings or saplings. For plots with seedlings (height < 130 cm), in each one-year simulation that they experienced an RHG less than 15%, half of the trees died (rounded down). For plots with saplings (height > 130 cm), every year I calculated the SDIr at plot-level using Equation 8.2, a modification of Equation 8.1, since all trees had the same DBH in a plot.

Equation 8.2: $SDIr = (n * 2500) * (\frac{DBH}{250})^{1.6614}$

where *n* is the number of trees in the plot (multiplied by 2,500 since SDIr is a per-hectare index) and *DBH* is in mm. If for any given year, the SDIr for any given virtual plot with saplings was higher than the maximum value of 1,476, the number of regenerating trees was reduced until a new SDIr value no higher than 1,476 was obtained. To do so, Model 8.7 was resolved for *n*, assuming SDIr was equal to 1,476 and DBH equal to the value for that plot. This value of *n*, the number of surviving trees, was rounded down to the nearest integer and considered the new number of saplings in the plot. For both seedlings and saplings, if a plot had no trees at the end of any given year, it was reset and considered empty.

For step 6, I checked if new regeneration would occur in the empty virtual plots. I re-assessed the regeneration probability using Model 4.1 with the new stand-level characteristics at year 5. Then, I used the same stochastic method as above for all the virtual plots without regenerating trees that were still alive (otherwise they were considered fully occupied and unavailable to new regeneration). If there were new virtual plots with presence of regeneration, I generated the tree density and height as above.

For step 7, at the end of the five-year period, I checked if there were regenerating trees that surpassed the 7 cm DBH threshold. If so, those trees were added to the overstorey tree list, maintaining their information on height, DBH and LCR, to be used for the next simulation

cycle with MOSES_GB. Any virtual regeneration plots with trees more than 7 cm DBH were then reset and considered empty.

Year 10 and 15. I repeated all the above simulations steps 3 to 7 for two more five-year periods.

8.2.3 Spatially-explicit approach:

Year 0. For step 1, I used the module STANDGEN as above, obtaining for both stands the same tree tallies as in the non-spatially-explicit approach. Additionally, I used STANDGEN to assign to each tree spatial coordinates within the 1 ha square. From the various options available I considered a regular tree distribution, since both the stands were originally artificial plantations. Note that this distribution is not perfectly homogenous but maintains a certain degree of randomness, creating areas with different tree densities and gaps of various sizes. I thus created tree maps for both stands, and overlaid them with a grid of 2 m × 2 m squares to create 2,500 spatially-located regeneration plots. For each plot, I calculated the local BA and SPH by identifying all the overstorey trees within 5.6 m from its centre (for BA, I summed up the BA of each tree, and for SPH, I counted the number of trees). I considered the same area used for the calibration of Model 4.1. However, the same values of age, TC and moss cover (Table 8.1) were assigned to all plots.

For step 2, I used Model 4.1 to estimate the likelihood of regeneration presence (p_{regen}) for each specific plot, using as inputs the stand-level values of age, TC and moss cover, and the plot-level values of BA. I generated, as in the non-spatially-explicit approach, a pseudo-random number for each plot to determine the regeneration presence. For all plots where the number was below the local p_{regen}, I generated the seedling density and height as above.

Year 5. For step 3, I used MOSES_GB as in the non-spatially-explicit approach, obtaining both a new tree list and a new tree map for each scenario (after the growth, mortality and, where appropriate, thinning). I then recalculated the BA and SPH values at plot level for year 5 using the new tree maps, and updated the stand-level age and TC as appropriate. In the thinned regime, I accounted for the harvesting damage as in the non-spatially-explicit scenario.

For step 4, I estimated the light availability for this period by applying Model 8.1 to each plot, using the plot-level values of BA and SPH, and the same averaging method depending on the thinning regime as in the non-spatially-explicit approach.

For step 5, I carried out all the modelling of growth and mortality (height growth, DBH development, LCR estimation, mortality) using the same methods as in the non-spatially-

explicit approach, but using as inputs for Model 8.2 and Model 8.5 plot-level values of light availability. Also in this case, all the regenerating trees in a plot had the same height, diameter and LCR throughout the simulation.

For step 6, I again checked if new seedlings would occur in empty plots, according to the new plot-level characteristics at year 5, and then generated seedling density and height as in step 2 above.

For step 7, at the end of the five-year period, I checked if there were plots with regenerating trees that surpassed the 7 cm DBH threshold, as above. If so, all those trees were added to the overstorey tree list for the next cycle of MOSES_GB, maintaining not only their information on height, DBH and LCR, but also the spatial coordinates. For simplicity, all the trees in a plot were assigned the spatial coordinates of the centroid of the regeneration plot. Any plots with trees more than 7 cm DBH were then reset and considered empty.

Year 10 and 15. I repeated all the above simulation steps 3 to 7 for two more five-year periods.

8.3 Results

Table 8.2 shows how many trees reached the 7-cm DBH threshold in each scenario at the end of every five-year period, and their contribution in terms of BA when recruited in the overstorey. There were differences between the simulation approaches (recruitment started earlier in the spatially-explicit simulation), thinning regimes (higher values for the thinned), and stands (higher values for stand A). However, in stand A, all scenarios after 15 years showed a relatively similar high number of regenerating trees recruited into the overstorey (around 1,500-2,000 trees per ha and BA 9-11 m^2 ha^{-1}) except for the non-spatially-explicit scenario, control regime, where it was very low. For stand B, only in one scenario (thinned regime, spatially-explicit approach) did regeneration recruitment occur, although very sporadic and almost negligible.

Table 8.2. Number of regenerating trees per hectare recruited in the overstorey for each scenario, and their total basal area (BA, m^2 ha^{-1}).

Method	Non-spatial							
Stand	Stand A				Stand B			
Thinning	Control		Thinned		Control		Thinned	
Value	*n*	*BA*	*n*	*BA*	*n*	*BA*	*n*	*BA*
Year 05	0	0	0	0	0	0	0	0
Year 10	0	0	0	0	0	0	0	0
Year 15	126	0.534	2,088	10.912	0	0	0	0
TOTAL	**126**	**0.534**	**2,088**	**10.912**	**0**	**0**	**0**	**0**
Method	Spatial							
Stand	Stand A				Stand B			
Thinning	Control		Thinned		Control		Thinned	
Value	*n*	*BA*	*n*	*BA*	*n*	*BA*	*n*	*BA*
Year 05	0	0	0	0	0	0	0	0
Year 10	466	2.206	571	2.674	0	0	0	0
Year 15	1,100	6.741	1,349	8.321	0	0	51	0.254
TOTAL	**1,566**	**8.947**	**1,920**	**10.995**	**0**	**0**	**51**	**0.254**

Figure 8.2 shows the development over time of the overstorey layer in each scenario. The BA and SPH (graphs a to d) for each stand were modelled in the same way with MOSES_GB in both simulation approaches; only the regeneration had a spatially-explicit approach. Thus, those characteristics were the same for the same stand and thinning regime in the two simulation approaches until regeneration was recruited to the overstorey. Only in stand A were these changes consistent.

Figure 8.2 (graphs e and f), shows the mean light availability below canopy at each stage for all scenarios, after the recruitment of the regeneration. For the non-spatially-explicit approach, the figure displays the homogenous stand-level estimate, while for the spatially-explicit approach, the mean of all local plot-level values is known. Due to the methods used for of the calculations (discussed later), for the same stand and thinning regime the average GSF was always slightly higher using the spatially-explicit than the non-spatially-explicit approach, until the regeneration was recruited to the overstorey layer. This effect was more evident for stand A, but it was present in both stands and thinning regimes. In the spatially-explicit tree maps, several gaps and the stands edges (the stands were considered surrounded by an open area) contributed with higher values of light availability (Figure 8.5). Note that even in the absence of any tree (BA and SPH equal to 0), Model (8.1) returns a maximum value of 0.56 GSF (see Annex IV). However, in the three scenarios which resulted in thousands of regenerating trees being recruited into the overstorey of stand A (both spatial scenarios, and the thinned non-

spatial), the light availability dropped to values less than 0.1, due to very high values of SPH then used in Model (8.1).
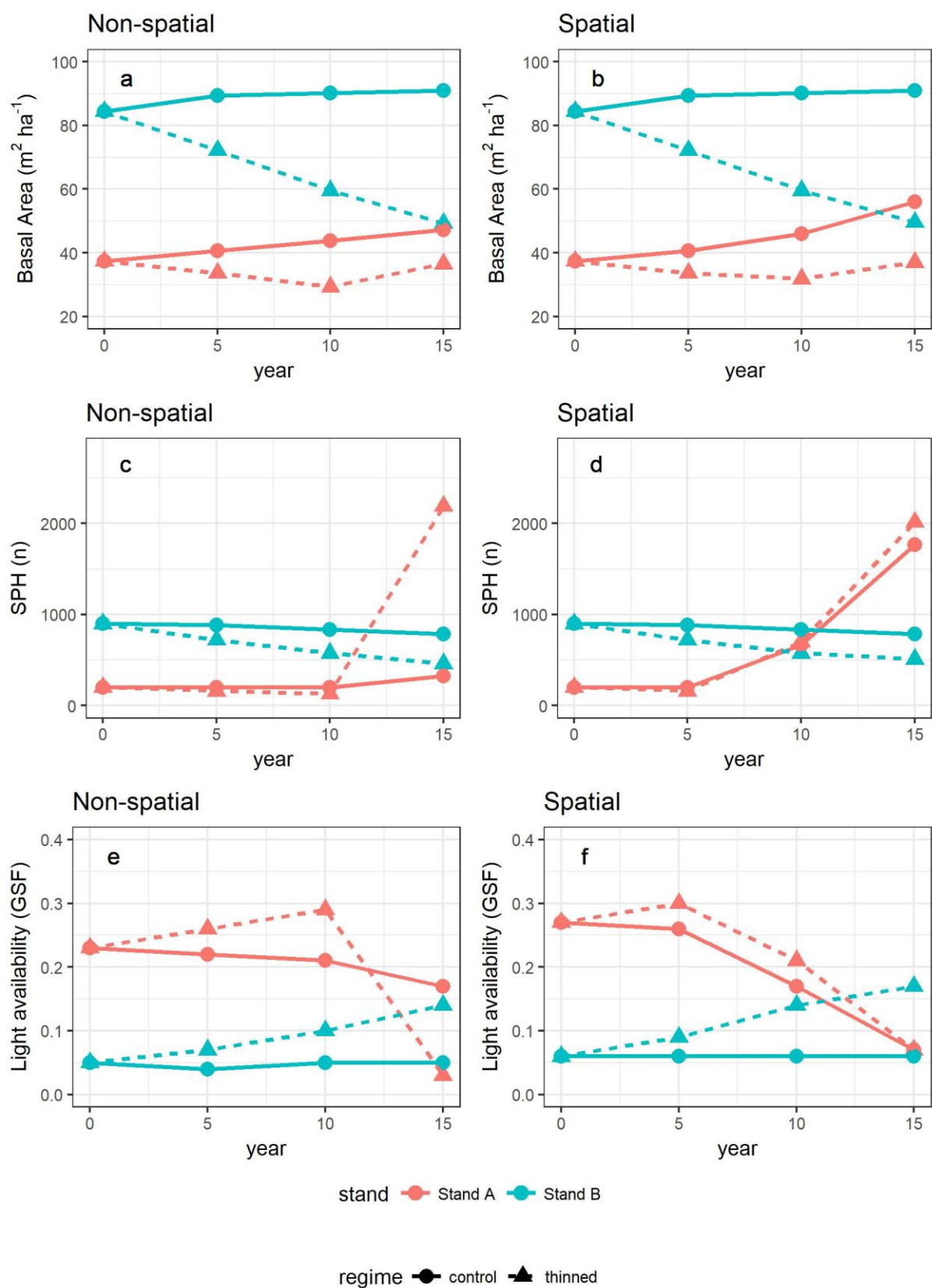
Figure 8.2. Stand basal area (BA, graph a and b), stems per hectare (SPH, graphs c and d), and mean stand light availability (GSF, Global Site Factor, graphs e and f), for each scenario, from year 0 to 15.

Figure 8.3 (graphs a and b) shows how the regeneration presence likelihood, averaged at stand level, changed in each scenario over time. There were only very small differences between the spatially-explicit and non-spatially-explicit approach for the same stand and thinning regime. In the control regime, the regeneration presence likelihood decreased sharply for stand A passing from TC2 to TC3 after the first five-year period, and then increased again due to the increasing age. For stand B, the regeneration likelihood was generally low throughout all the simulation, reaching a maximum of 0.31 only after 15 years due to the positive effect of age. In the thinned regime, the regeneration presence likelihood increased sharply in both stands after the first five-year period, when they both passed to TC1 for the rest of the simulation. Then it keeps increasing due to the increasing age, reaching almost 100% (almost all cells had regeneration of some size) even if there were hundreds of new trees recruited in the overstorey (in the case of stand A) or the values of BA were still high (in case of stand B). The effect of TC and age were the most important in determining the regeneration presence likelihood in all scenarios.

Figure 8.3 (graphs c and d) shows the total area within the stand with presence of regeneration for each scenario over time. Again, differences were generally small between the spatially-explicit and non-spatially-explicit approaches. Under the thinned regime, for both stands A and B, all the area became covered with regeneration in 15 years, due to the constantly high regeneration presence likelihood, even considering mortality and ingrowth. Stand A, control regime, showed the only difference between the different simulation approaches: at year 15, the coverage was lower in the spatially-explicit, due to higher regeneration ingrowth in this scenario.

Figure 8.3 (graphs e and f) shows the total regeneration density for each scenario over time. The higher number of regenerating trees in stand B than stand A under thinning, from year 5 and onwards, is due to their differences in the first regeneration layer (year 0). In stand A, the starting regeneration was generated using the Weibull distribution for TC2, resulting in most of the available plots being occupied with the relatively lower densities generated this way (almost 70% of the total area, see graph c), while stand B was practically devoid of regeneration, due the very low likelihood of regeneration. After the first thinning (year 5), in stand A, an additional 29% of the total area was covered with regeneration generated with the Weibull distribution for TC1 (which produces considerably higher densities), while around 75% of the total area for stand B. The high regeneration density of stand B however did not provide a high recruitment due to the low growth rates in all its scenarios. Seedling mortality

and ingrowth reduced the number of seedlings in each scenario, slightly more so in the spatially-explicit than in the non-spatially-explicit approach, consistent with the trends in the area covered.
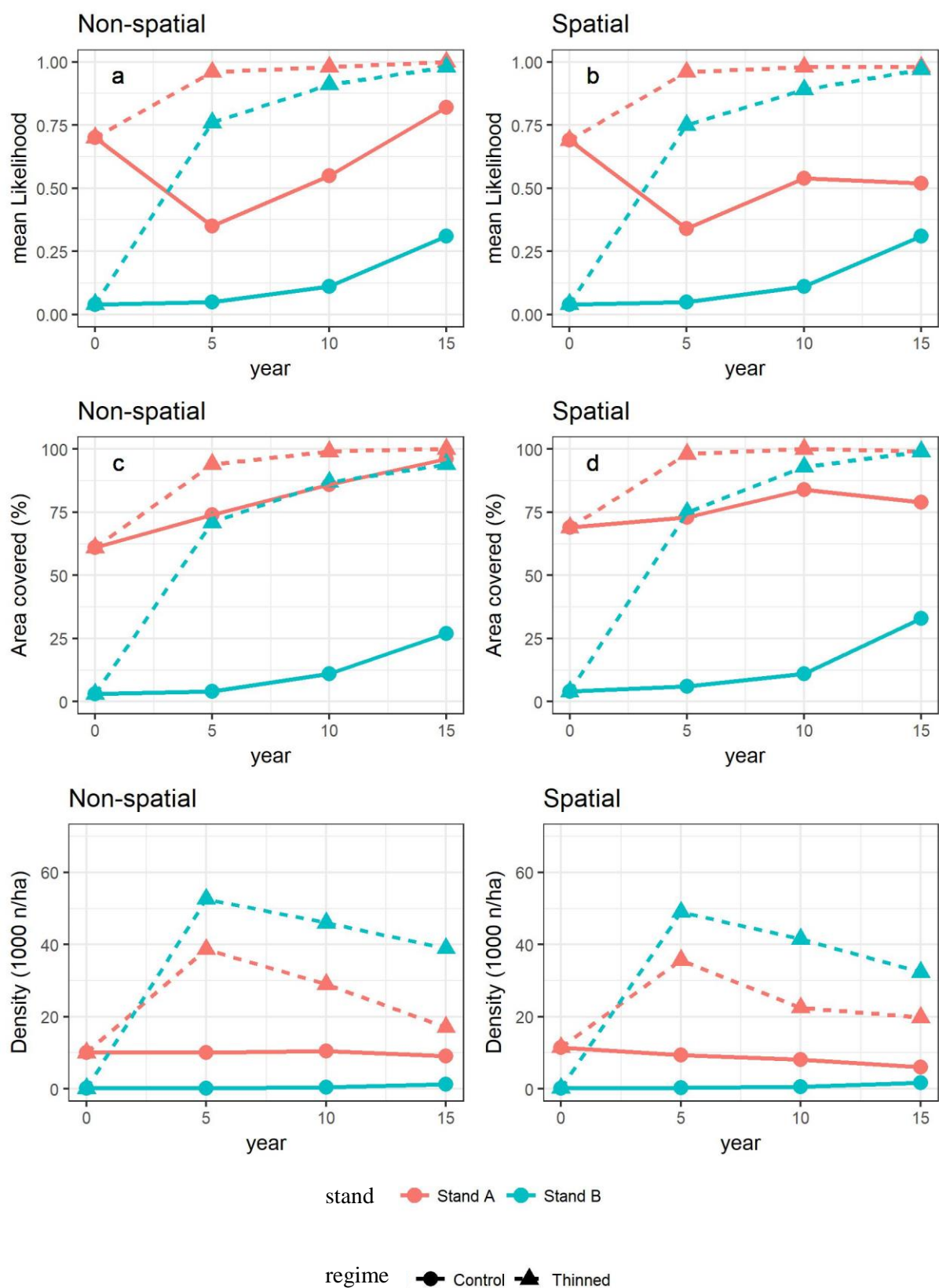
Figure 8.3. Regeneration characteristic at stand level for each scenario, simulated from year 0 to 15. Mean regeneration likelihood (graphs a and b), total area covered by regeneration (graphs c and d), total regeneration density (graphs e and f).

Figure 8.4 shows the regeneration size development for each scenario, in terms of mean DBH (graphs a and b) and maximum DBH (graphs c and d), only for saplings (height > 130 cm, DBH > 0). When comparing the different simulation approaches, the maximum DBH was higher in the spatially-explicit then in the non-spatially-explicit approaches due to the regeneration growing in the high-light gaps and edges considered in the former, for both stands and thinning regimes. The differences in the mean DBH were less evident: only in stand A was it slightly higher in the spatially-explicit approach, at least until year 10 when the recruitment process started. When comparing the different thinning regimes, few differences in mean DBH could be observed for both stands and approaches. The increase in DBH growth after thinning due to the higher light availability was counterbalanced by the higher presence of new trees with lower DBH values, hence the small differences in the means. Greater differences between the different thinning regimes (higher values in the thinned stands) were seen in the maximum DBH for all scenarios except the stand A, spatially-explicit approach. In this case, the similar values in the control and thinned regimes were due to trees originated in the same high-light (GSF 0.566) gaps and edges generated in the tree maps of year 0 for both cases, and which were then unaffected by the tree removals. In all other cases, tree removals increased light availability and so the regeneration maximum height. Particularly in stand B, for the spatially-explicit approach, some large gaps were created in the canopy that were instrumental in few regenerating trees reaching 7 cm DBH.
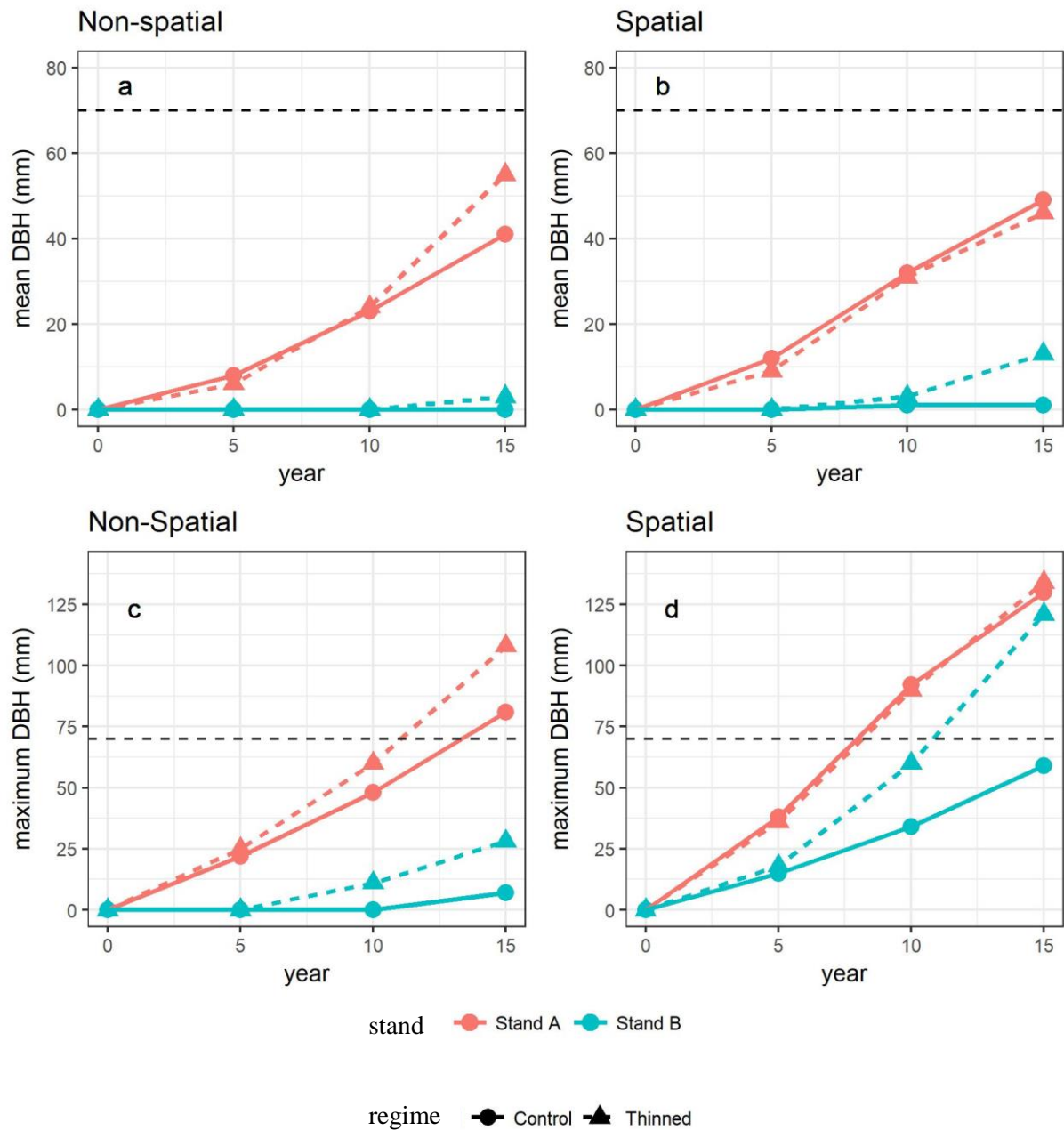
Figure 8.4. Development of regeneration DBH in all simulation scenarios. The dashed black horizontal line corresponds to the 7-cm threshold.

The starting random height of the regeneration crucially affected its growth. A tree of 20-cm height generated at year 0, with no competition, took a full five-year period to reach the height of 130 cm if growing at an average light level of GSF 0.34. During the same time, a tree generated with 130 cm height, with no competition and with the same light, was already 347 cm tall.

Another problem related to the starting height was identified when considering the regeneration generated at the end of the subsequent five-year periods. Such regeneration would have had no more than 4 growing seasons available to grow, if we consider at least a one-year delay for

seedling establishment (defined as reaching 20 cm, the entry point of the simulation). In other words, we must assume that if new regeneration is created at year 5, it would have passed the establishment phase and reached 20 cm height no earlier than year 1 (since it was absent at year 0), and then had no more than 4 years to grow. However, the new seedlings were created with the same random starting height distribution, possibly up to 130 cm. Only regeneration growing in canopy gaps with GSF > 0.50 could reach 130 cm in just 4-years, while new regeneration created at lower light should surely have had lower heights.

There were inconsistencies between the regeneration and overstorey growth models that led to unrealistic outcomes. For trees of the same size, the former tended to simulate much higher growth, especially for DBH. As an example, a tree 6 m tall and with DBH 7 cm, after 5 years in MOSES_GB with no competition at all, could grow to 9.7 m height and DBH 10.1 cm. The same tree with the regeneration growth models presented here, at GSF 0.56 (such as in a gap) and no intra-regeneration competition, could grow to 10.7 m height and DBH 13.3 cm in 5 years. The regeneration growth models were likely to be less accurate in this case because they were not calibrated for trees above 7 cm DBH. This problem was important in the simulations, since regenerating trees that reached 7 cm DBH before the end of a five-year cycle could not be moved immediately to the overstorey layer and modelled with MOSES_GB for the rest of the period. Figure 8.4 (graph c) shows a maximum DBH of more than 13 cm reached by the saplings in stand A at year 15, for the spatially-explicit approach in both thinning regimes, before being recruited in the overstorey. Those trees were saplings of just a few mm below 7 cm DBH at year 10 that grew more than 6 cm in the next five-year period, thanks to the high light environment in gaps. However, overstorey trees that were already recruited into the overstorey layer of stand A at year 10 (with a mean DBH of 7.7 cm for both thinning regimes), grew only 0.6 cm DBH in the control regime and 1.1 cm in the thinned regime in the same five-year period. On top of the aforementioned growth overestimation of the regeneration models, there was a stark contrast in the competition considered. When thousands of saplings moved to the overstorey layer at the same time, the non-spatial simulation of MOSES_GB considered all of them to be subject to a much higher competition than before (which was on average 1.8 trees per plot, for both thinning regimes).

The high density of seedlings per plot generated in both stands after a thinning (up to 30 seedlings per plot) decreased due to the combined use of the various mortality tools. Harvesting damage greatly was instrumental in stand A in reducing the number of trees recruited in the thinned regime to values more like the control regime. In all scenarios, when the regeneration

plots with trees above 7 cm DBH reached the recruitment stage at the end of a five-year period, they had on average around 2 saplings that moved to the overstorey (except for stand A, thinned, non-spatially explicit approach, where it was on average 1.2). However, I could not validate such mortality rates due to lack of existing data.

8.3.1 Spatially-explicit approach

The following maps show the within-stand variations considered in the spatially-explicit approach. Figure 8.5 displays how the local light availability changed in stand A, under the different thinning regimes. In year 0, before the first thinning happened, the situation was the same for both the control and thinning regimes (hence only one map is shown). It possible to identify the gaps in the canopy and the edge effect, which led to high values of light. With the passage of time, there was a negative effect of the local overstorey tree growth that led to higher BA values and so less light, and a positive effect of tree removals. In this simulation, gaps of any size did not ever close until the ingrowth of the regeneration, quite an unrealistic scenario. It is possible to note that most of the recruitment in year 10 (new trees present in the maps) happened in the gap and edge areas, as expected in a real situation.
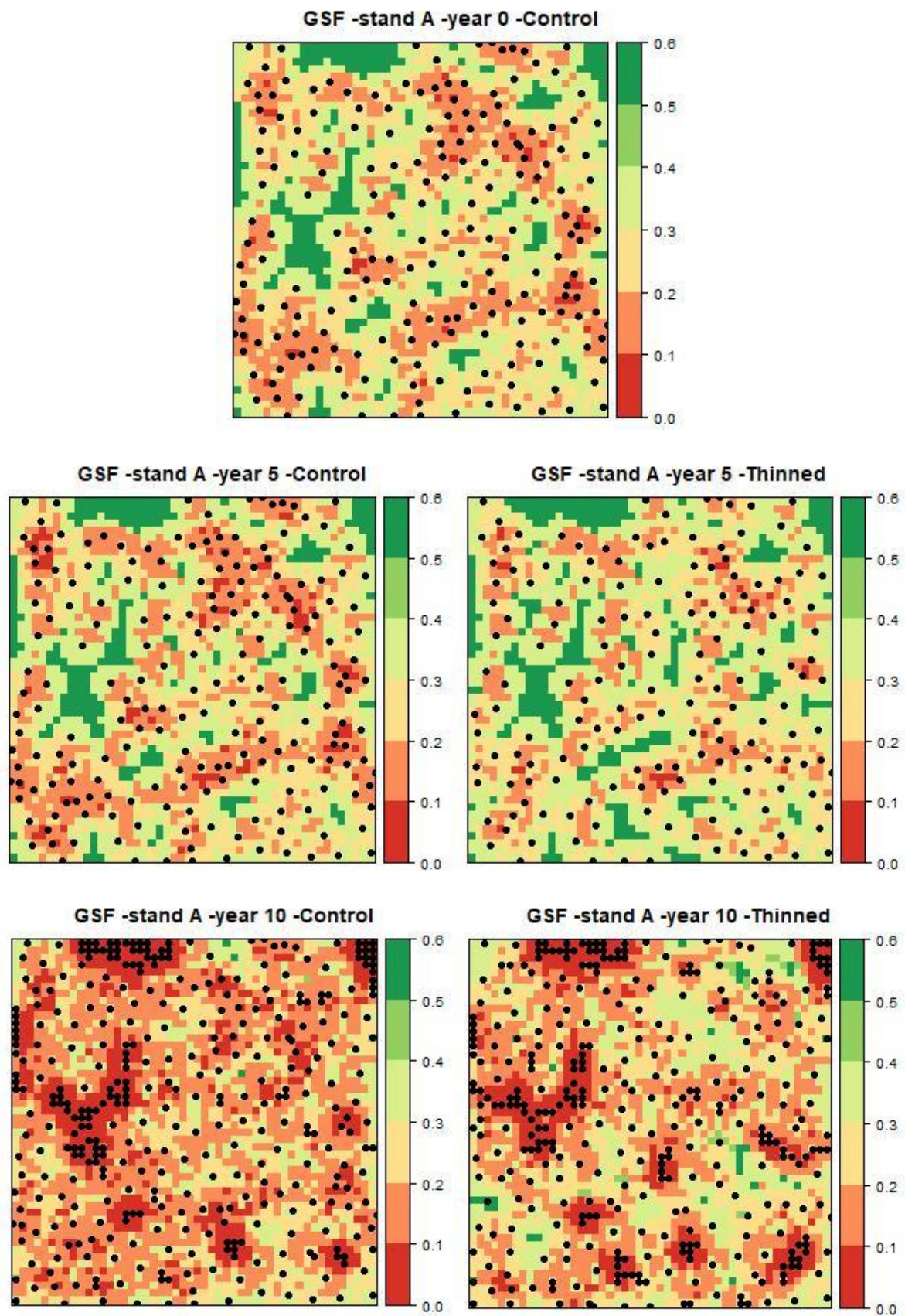
Figure 8.5. Maps of light availability (GSF, Global site factor) of stand A under different thinning regimes, from year 0 to 10, spatially-explicit approach. The legend is displayed in the scaled colour bar. The small squares represent the regeneration plots. The black points represent the overstorey trees, including those recruited from the regeneration.

121

Figure 8.6 displays how the local regeneration presence likelihood changed in stand A, under the different thinning regimes. In year 0, before the first thinning, the likelihood was mostly 0.6-0.8 (stand mean 0.69) in both regimes. Then, in year 5, control regime, the likelihood decreased to a stand mean of 0.34, with higher values in the gaps and edges (around 0.4-0.5), while with the thinning regime it was homogenously high in all the stand (stand mean 0.96). In year 10 the likelihood generally increased in the control regime to a mean of 0.53, again with some differences in the gaps and edges, while in the thinning regime stayed homogenously at values near 1. Note that in the maps for year 10 the new ingrowth trees in the overstorey layer are not displayed. In the simulation, the generation of a new wave of regeneration (step 6) happened before moving the regeneration recruit to the overstorey (step 7). Note also that these maps do not display which plots were actually occupied by regeneration.
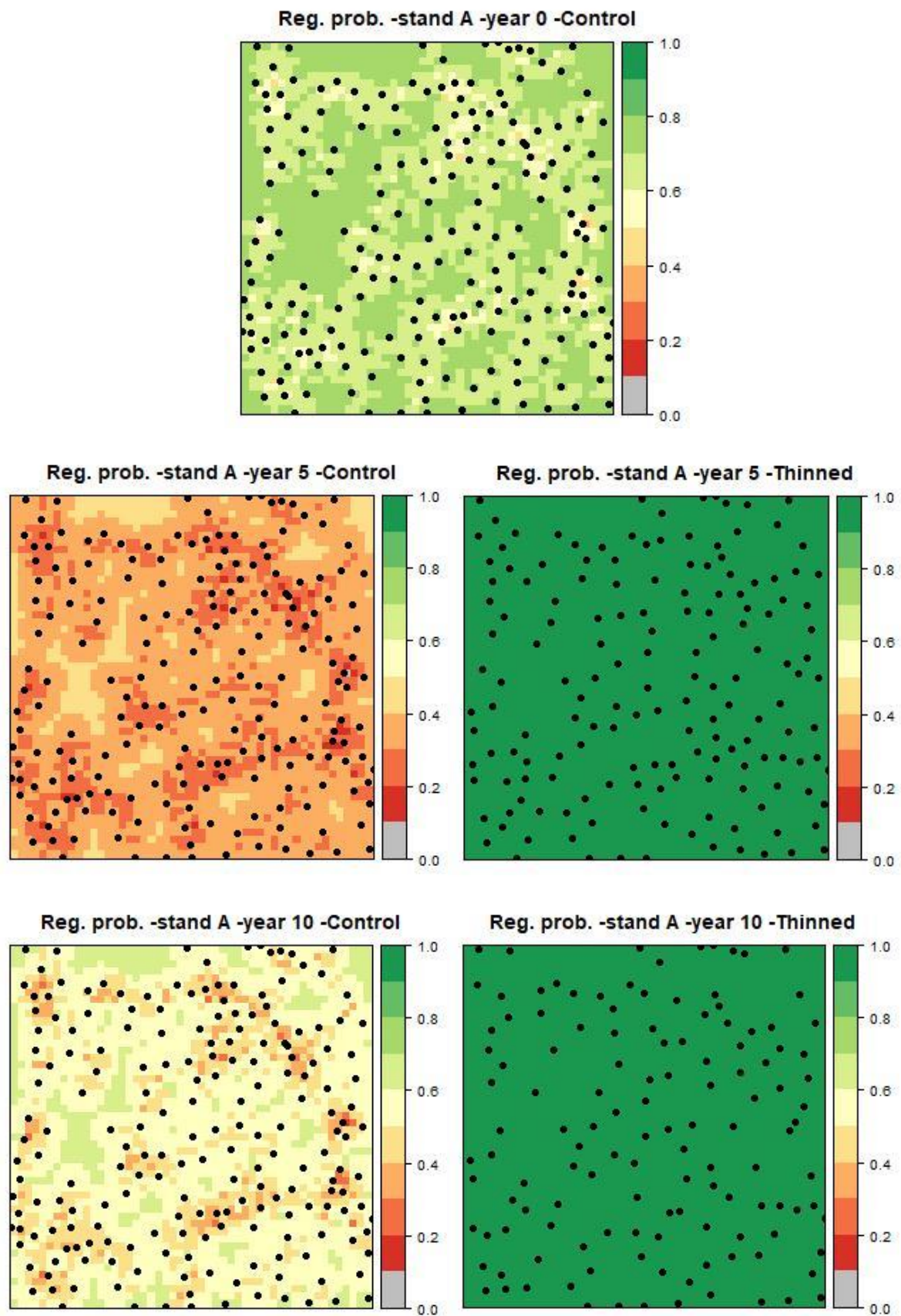
Figure 8.6. Maps of regeneration presence likelihood (Reg. prob.) of stand A under different thinning regimes, from year 0 to 10, spatially-explicit approach. The legend is displayed in the scaled colour bar. The small squares represent the regeneration plots. The black points represent the overstorey trees.

123

Figure 8.7 displays the differences in the local regeneration DBH for both stands and both the different thinning regimes, at year 10, before the trees with DBH above 7 cm were moved to the overstorey class. As previously mentioned, the gap and edge effects were crucial to promote the regeneration growth, and they were the areas were most of the recruitment eventually occurred. However, the local stand density did not influence the regeneration presence as much. Particularly in the thinned regime, stand A, it occurred more evenly in all the area.
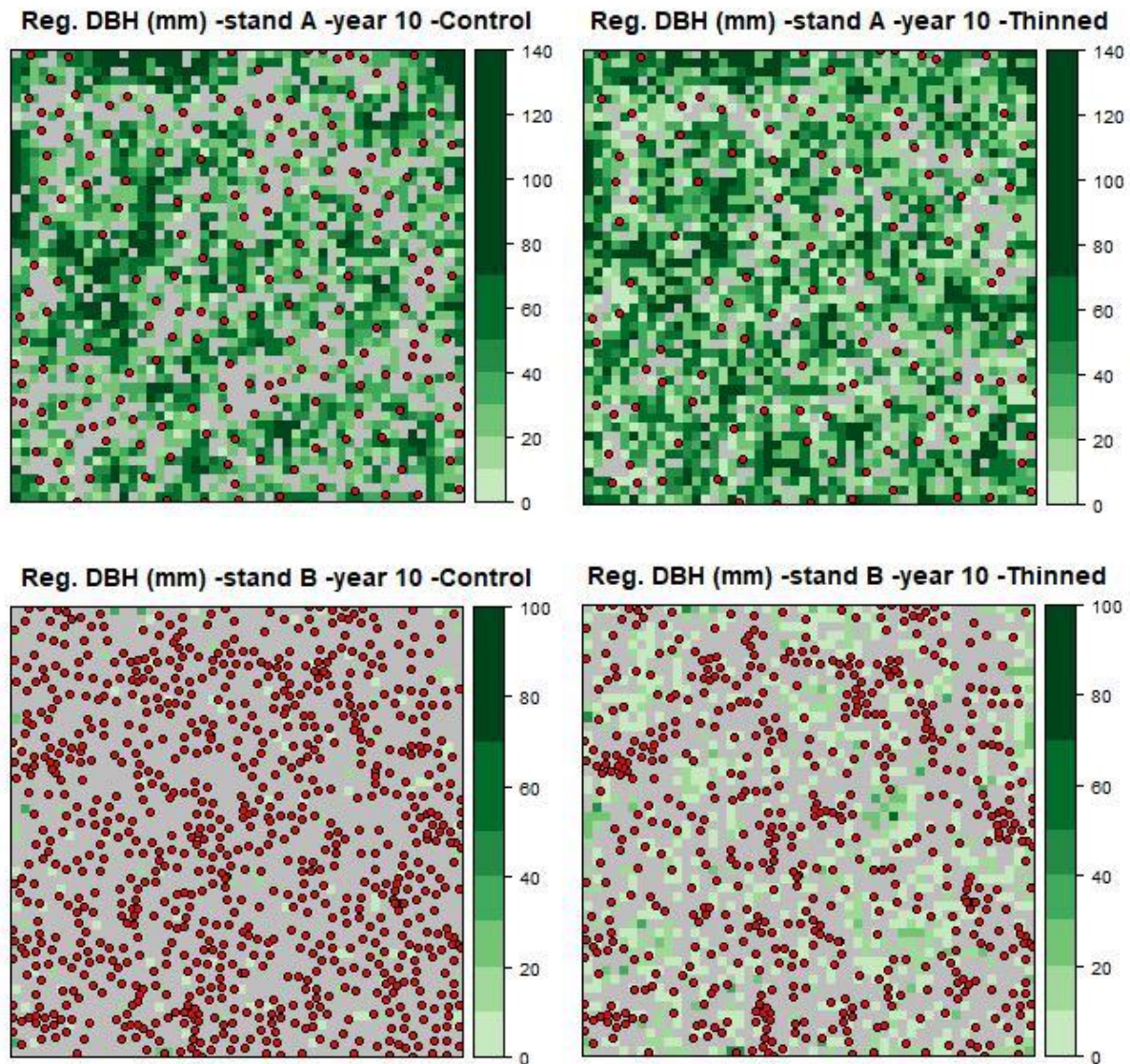
Figure 8.7. Maps of regeneration DBH for different spatially-explicit scenarios. The legend is displayed in the scaled colour bar. The small squares represent the regeneration plots. The black points with red filling represent existing overstorey trees.

8.4 Discussion

There were differences in the overall recruitment process between simulation approaches (it started earlier in the spatially-explicit simulation), between thinning regimes (more trees were recruited in the thinned), and between stands (more trees were recruited for stand A). The regeneration presence and density processes, dependent mainly on the starting stand characteristics and then on the thinning regime, were generally similar between the simulation approaches. The regeneration growth, dependent mainly on the light availability, were affected by the thinning regimes and the spatial simulation approach. For stand A, after 15 years a similar number of trees were recruited in the overstorey in all scenarios except for the control regime, non-spatially-explicit approach, where it was lower mostly due to the lower light availability simulated in that case. For stand B, the recruitment process after 15 years was null or negligible in all scenarios.

The similarities in regeneration likelihood, coverage and density at stand-level between the simulation approaches, until ingrowth was considered, were due to the original structure of the models. The local variations of basal area in the spatially-explicit approach did not much affect the regeneration presence because basal area is the weakest predictor of the regeneration likelihood model (see Chapter 4). Stand density is not even considered in the regeneration density model. Thinning Class, age and moss are the most important factors for regeneration presence, and density simulations use only Thinning Class as a predictor. All these variables were considered homogenous within each stand and the same in both approaches, hence the similar results. The models for regeneration presence and density, considering years after the last thinning as the most important factor, or the only one, and regardless of the intensity of such thinning, led to unrealistic results where the denser stand B had higher seedling densities in the thinned regime, for both simulation approaches. However, that abundant regeneration failed to reach the overstorey class because the environment of stand B was not favourable to regeneration growth, an indication of inconsistency between the models.

One of the problems already identified at the beginning of the study, the lack of a proper model for the starting regeneration height, clearly influenced the simulations, but because of the lack of validation data it was not possible to analyse its long-term effect. Generating additional regeneration at the end of each 5-year period did not much change the situation in the control regime scenarios, due to the low regeneration presence likelihood, but led to stands fully covered by regeneration after 1-2 cycles under thinning. Another problem in generating

additional regeneration, was that it could have had too high a starting height for its young age. As stated in Chapter 4, the regeneration presence and density models were calibrated without a clear temporal horizon, and so were less appropriate to be used in such short five-years cycles. Regeneration mortality due to timber extraction influenced the simulation by reducing the number of the recruited trees in the thinned regime to values like the control. The same Stokes, Kerr & Ireland (2009) study that I used as the basis for the mortality rates, stated that after harvesting damage the natural regeneration density could be still likely enough to restock their study sites.

There were differences between the simulation approaches for the regeneration growth, which was faster in the spatially-explicit due to the higher light availability due to the presence of gaps and edges in the tree maps. Gaps in the canopy due to small disturbances, such as can be considered the small random gaps here created at year 0 or after the thinning events in subsequent years, have an important role in stand dynamics where stand-replacing disturbances are absent, due to the localised increase of light reaching the forest floor (e.g. Schneider & Larson 2017). The positive edge effect for regeneration growth was recognised in MOSES and included in the early growth models for all species (Hasenauer & Kindermann 2006). These local areas of higher light availability could be necessary when modelling mixed-species forests for the development of more light-demanding species, which could maybe not survive at all in the lower and homogenous light levels estimated in the non-spatially-explicit approach. However, even if with a five-year delay, the recruitment process in stand A, thinned regime and non-spatially-explicit approach, was eventually equivalent to both the thinning regimes in the spatially-explicit approach. This is because the very open forest structure considered in the former (at year 10, only around 128 overstorey trees per hectare were present) still provided relatively high-light estimates at stand level even without considering gaps and edges. In the denser stand B, the differences between approaches were more evident: the maximum DBH was higher in the spatially-explicit approach, even if no regenerating trees reached 7 cm DBH in the simulation timeframe. Although the spatially-explicit approach seemed more realistic in considering within-stand variations in the canopy, various issues were identified in the estimation of light availability. First, the light model provided maximum values of only 0.56 even in the absence of any canopy trees at local level. For the Sitka spruce height model used here, at this value the growth was already very close to the maximum possible at full light, but this might not be the case for other species. Second, without tree removal, the local light availability was affected only by the DBH growth of mature trees within the 5.6 m radius,

which could be relatively slow, and gaps never closed. However, especially after thinning, the canopy could revert quickly to a closed status by extending branch growth to close the gaps (Hale *et al.* 2009). Third, the model was developed to be used at stand-level, where it gave reliable results, while the predictions for the 5.6 m plot used in this study were quite discordant with the observations (see Annex IV). Fourth, the response of existing regeneration to overstorey removals can be affected by several factors, such as its shade-tolerance and vigour before the release, and be different between height and DBH growth (the former may be lower) (Ruel *et al.* 2000; Metslaid *et al.* 2007). There could also be a delay of some years before suppressed regeneration can get acclimated to the new light level and exploit the higher light availability (Eerikäinen, Valkonen & Saksa 2014). In this simulation, I assumed that as soon as a gap is created due to a thinning, the height growth increased directly with the increase in light availability.

A major inconsistency was found for the simulated DBH growth of trees around or bigger than the 7-cm threshold, between the MOSES_GB growth module for the overstorey and the regeneration early growth models prepared here. The latter provided much higher results than the former. A possible solution for saplings around or above the 7 cm DBH but still in the regeneration class, would be to use the existing MOSES_GB growth functions, or average the results of the two system like in the forest growth simulator FVS (Crookston & Dixon 2005).

The methods used to estimate the mortality in the simulations led to biologically-consistent values of saplings recruited in the overstorey for each plot (on average only 1-2 for a 4 m^2 plot). However, such values could not be verified. Better light-growth mortality functions for regeneration should be developed, maybe together with additional random mortality tools for all regenerating trees.

9 Conclusions

In this chapter, I summarise the findings of this thesis according to the original research questions, identify some of the limitations of the studies, suggest areas for further development, and highlight the novel contributions made by the study.

9.1 Summary of findings

The overall aim of this thesis was the development of natural regeneration models for Sitka spruce and other companion species, which could be applied to stands managed using continuous cover forestry approaches in the UK. I followed the development of Sitka spruce seedlings from their establishment until their recruitment to the overstorey. There was a special focus on the light-growth responses of regeneration, and on the assessment of the below-canopy light regime. In this section I summarize the main findings of the thesis and how they answer the research questions originally posed.

1. ***What are the best structures for Sitka spruce natural regeneration occurrence and density models?***

I developed models for estimating the presence and density of Sitka spruce natural regeneration under canopy cover. I used as a calibration dataset an existing regeneration survey carried out in traditionally-managed Sitka spruce dominated stands, covering a wide range of forest structures and geographical areas. As independent validation, I used plots newly collected in different Sitka spruce dominated stands, which were, however, managed for transformation to continuous cover forestry. The likelihood of regeneration presence was estimated using a Generalized Linear Mixed Model with Binomial function and Logit link. The selected variables were a combination of stand characteristics (age of the plantation and local basal area), management history (years since the last thinning) and site characteristics (percentage of plot area covered by moss). If regeneration was present, the density of seedling was estimated by generating random numbers from a Weibull distribution function. Such functions were fitted to the observed data, grouped into different classes according to the years since the last thinning. The model of regeneration presence correctly simulated most of the plots after a cross-validation process with the calibration dataset. However, it had lower accuracy in the independent validation. The model for seedling density did not have a good performance in both the cross-validation and independent validation.

2. Can the early growth of Sitka spruce, western hemlock, and Douglas fir be modelled as a function of the light environment under canopy cover?

I modelled, as a function of light availability, the early growth of Sitka spruce regeneration in continuous cover forestry stands, and of possible companion species, namely western hemlock and Douglas fir. I developed light-growth models, for the height of all species, and for the diameter of Sitka spruce and western hemlock. I tested different model structures based on three non-linear asymptotic functions (namely the Michaelis-Menten, the 3-points Logistic and the Asymptotic-with-offset). I included tree size and intra-regeneration competition, which affected some or all the non-linear parameters of the original functions. I tested a total of 60 different model structures for each species and growth variable considered.

The results showed that for each species, a different non-linear function best simulated the growth (namely the 3-points Logistic for Sitka spruce, the Michaelis-Menten for western hemlock, and the Asymptotic-with-offset for Douglas fir). For Sitka spruce and western hemlock, there were differences in the model structures for the height and diameter growth. Tree size affected the maximum growth in all models, and in some cases also the growth rate (i.e. the speed at which the maximum growth was reached). The intra-regeneration competition seemed to have a stronger effect in reducing the diameter than the height growth. Douglas fir compared to Sitka spruce had a slightly slower height growth at low-light, and a markedly higher growth at high-light. Western hemlock had the highest height growth at all light levels. Sitka spruce compared to western hemlock had slower diameter growth at low-light, and higher growth at high-light.

3. Can the light-growth responses, regarding growth and canopy architecture, for Sitka spruce, western hemlock and Douglas fir be used to define a shade tolerance ranking?

I carried out an analysis of the crown plasticity of these species. I modelled the apical dominance and live crown ratios as functions of light availability, tree size and intra-regeneration competition. For all species, only light availability was statistically significant and negatively correlated with those ratios. In the case of the apical dominance ratio, there were no species-specific differences between Sitka spruce and Douglas fir (western hemlock was not analysed due to differences in its crown architecture). For the live crown ratio, I observed that at all light levels, western hemlock maintained the longest live crown, followed by Sitka spruce and then Douglas fir. I fitted a model of height growth for Sitka spruce as a function of the

apical dominance ratio. From the results, I suggested an apical dominance ratio of 1.5 as a quick field indicator for defining Sitka spruce seedlings with an adequate growth potential. Overall, considering both the comparisons in the light-growth and crown plasticity responses, I defined an increasing shade tolerance ranking as Douglas fir $\leq$ Sitka spruce $<$ western hemlock. However, using only one parameter to define the ranking could have been misleading.

4. Can the light environment under canopy cover be adequately described using smartphone technology?

Given the importance of the forest light environment analysis in this research, I explored a possible technological improvement for its assessment. I carried out hemispherical photography with a smartphone camera equipped with a fish-eye lens and demonstrated that it can be an adequate alternative to hemispherical photography with traditional cameras. Smartphone equipment is cheaper, easier to carry, widely available, and with internet connectivity. The data collection can be carried out in a shorter time. I showed methods for processing single smartphone images, and for merging two images with different orientations to obtain an image closer to a full hemispherical picture. The various parameters calculated from smartphone camera images (related to canopy openness and light availability) were always on average significantly higher than those from traditional cameras images, although with relatively little absolute differences and scatter. I fitted Generalized Linear Mixed Models to remove such differences and transform the smartphone outputs to values closer to those obtained by traditional camera ones. I proved that values estimated from smartphone cameras could be used as they are in ecological studies, or after being transformed with the models that I provided. The study has been published as:

Bianchi S., Cahalan C., Hale S., and Gibbons J.M. (2017). Rapid assessment of forest canopy and light regime using smartphone hemispherical photography. *Ecology and Evolution*. DOI: 10.1002/ece3.3567.

The study was developed for a possible crowd-sourced data collection, where forestry practitioners or citizen scientists could have collected regeneration growth information with quick smartphone hemispherical photography images. Unfortunately, the project was not successful in recruiting enough participants.

5. ***Can the models for regeneration occurrence and early growth prepared in this thesis be integrated into MOSES_GB?***

I integrated the Sitka spruce regeneration presence, density, and early growth models into MOSES_GB, an existing forest growth simulator in development by the Forestry Commission. For this study, I needed to model the growth of regeneration until it reached a size threshold of 7 cm DBH when it is technically classified as overstorey.

First, I developed new methods for simulating the DBH development, namely a model of total DBH as a function of total height and a model of DBH growth as a function of height growth, and compared them with the light-DBH growth model already developed. I selected the model of DBH growth as a function of the height growth for the use in the following simulations. Next, I simulated the development of a regeneration layer under an overstorey layer over 15 years, using the models so far prepared to simulate the regeneration layer, and MOSES_GB to simulate the overstorey layer. I simulated two different virtual stands and followed the regeneration establishment and growth until it was recruited into the overstorey, comparing different spatial modelling approaches and two thinning regimes. In this way, I tested the feasibility of integrating the models prepared in this thesis into MOSES_GB and the best methods to do so. Thus, the results of this chapter provided some insights to the overall aim of this thesis.

The spatially-explicit approach, which considers the local variability in the light-availability, seemed to be more accurate for the growth modelling. However, there is still room for improvement in the simulation of light-availability below the canopy, and some issues to address in this step were identified. The regeneration presence and density models, on the contrary, were less affected by the differences in the spatial modelling approaches. Other issues and potential problems in the simulations were identified, that will be highlighted in the following section.

9.2 Limitations

A critical evaluation of the study is necessary to identify limitations that affected the results, and so the areas where further work may be most needed.

For the regeneration presence and density models, the most important limitation was the lack of information on the size or age of the seedlings surveyed. This made it impossible to define a clear temporal horizon for the regeneration establishment. The stand characteristics at the time of the survey could have been different from those when the regeneration establishment

occurred, and the regeneration presence could have been affected by mortality processes. The same lack of data made it impossible to prepare a model for the initial height, which ranged from 20 cm to 130 cm. Those problems, together with the poor performance of the density model, led to some problematic issues during the integration of the models with MOSES_GB. Moreover, the models did not address the local seed availability, and thus will likely not be appropriate for uneven-aged, mixed-species stands.

For the light-growth models, the comparison between species was not complete because of the lack of diameter growth data for Douglas fir. There was also a lack of trees sampled at high-light levels, especially for western hemlock and to some extent for Douglas fir, and this may have influenced the model fitting through a wrong identification of the asymptotic maximum growth. The analysis at low-light may have been affected by a non-optimal sampling, and by a lower accuracy of hemispherical photography at those levels. However, I covered the light-range most commonly present in continuous cover forestry stands.

Intra-regeneration competition was significant in improving the fit in many cases, but its measurement did not consider some variables that could have been useful to obtain more precise results, such as the distance, the height and the species of the competitors.

Regeneration mortality studies were not carried out due to a lack of time and resources. This most crucially affected the overall simulations during the integration of the models with MOSES_GB. However, even if not verified against existing data, the resulting density outputs of such simulations seemed biologically valid.

Climatic variables were not considered in any model. Even if hybrid models with climatic inputs can be useful in climate change scenarios, collecting micro-climatic information within the stands considered was not possible due to lack of time and resources. As demonstrated by Sellars (2005), the climate below a canopy can vary from open conditions according to the tree density.

9.3 Future developments

Given these limitations, I suggest the following areas of future studies to complement and improve on the results of this thesis.

- Regeneration presence and density studies for Sitka spruce and companion species, in mixed-species stands and in advanced stages of transformation to CCF. Such studies can follow the data collection and analysis framework used here, with the following improvements: 1) detailed assessment of size and/or age of seedlings; 2) better analysis

of the interaction between intensity of thinning events and regeneration; 3) improved analysis of the effect of local seed sources (e.g. mother trees).

- Establishment of permanent sample plots to study regeneration dynamics, to complement or substitute for the above studies.

- Diameter growth studies for Douglas fir regeneration, necessary for its future integration into MOSES_GB, and to complement the comparisons with the other species considered here.

- Definition of a simple but effective indicator of intra-regeneration competition that can be used during regeneration growth surveys, and be easily integrated into a forest growth simulator such as MOSES_GB.

- Growth-mortality studies for regenerating trees of Sitka spruce, western hemlock and Douglas fir. Since I present light-growth functions in this thesis, only the analysis of growth and frequency of deceased seedling are required to develop light-mortality functions.

- More studies of damage and mortality on existing regeneration during thinning and timber extraction activities.

- Development of a spatially-explicit model of light availability below canopy cover, starting in pure Sitka spruce stands, and then moving on to mixed-species situations.

- Design of a crowd-sourcing data collection campaign for regeneration growth studies, with better engagement of the potential citizen-scientists. To make the data collection easier, the preparation of a better smartphone application for taking hemispherical images could be explored. For example, the compass and level bubble could be displayed live on the screen when taking a picture, and, if the merging processing method is desired, also a 90° angle feature for rotation.

- Measurement of micro-climatic conditions under canopy cover with meteorological stations, and test which are the ones most affecting the regeneration processes. Then, more focused studies can be carried out on how to model those variables under canopy cover from general meteorological data collected in open conditions.

9.4 Novel contributions

The most important novel contributions of this thesis, are:

- The development of Sitka spruce regeneration presence and density models, which can be used to simulate the regeneration establishment in Sitka spruce dominated stands in the UK, under a wide range of forest conditions.

- The development of light-growth functions for Sitka spruce, western hemlock and Douglas fir, which can be used as supporting tool for practical applications in stands under continuous cover forestry.

- Demonstrating that different non-linear functions, customized in their parameters to include additional predictors, may best describe species-specific light-growth responses.

- The use of smartphone cameras as an adequate alternative to traditional cameras and methods for hemispherical photography studies, such as the rapid assessment of forest canopy and light regime.

- The integration of regeneration models in MOSES_GB for continuous cover forestry scenarios in the UK, with suggestions on the best methods to use and the issues that still need to be resolved.

10 List of references

Anderson, M.C. (1964a). Light Relations of Terrestrial Plan Communities and Their Measurement. *Biological Reviews*, **39**, 425–486.

Anderson, M.C. (1966). Stand Structure and Light Penetration. II. A Theoretical Analysis. *Journal of Applied Ecology*, **3**, 41–54.

Anderson, M.C. (1964b). Studies of the Woodland Light Climate: I . The Photographic Computation of Light Conditions. *Journal of Ecology*, **52**, 27–41.

Bates, D., Maechler, M., Bolker, B. & Walker, S. (2014). lme4: Linear mixed-effects models using Eigen and S4.

Battaglia, M. & Sands, P.J. (1998). Process-based forest productivity models and their application in forest management. *Forest Ecology and Management*, **102**, 13–32.

Beaudet, M., Harvey, B.D., Messier, C., Coates, K.D., Poulin, J., Kneeshaw, D.D., Brais, S. & Bergeron, Y. (2011). Managing understory light conditions in boreal mixedwoods through variation in the intensity and spatial pattern of harvest: A modelling approach. *Forest Ecology and Management*, **261**, 84–94.

Beckschäfer, P., Seidel, D., Kleinn, C. & Xu, J. (2013). On the exposure of hemispherical photographs in forests. *iForest*, **6**, 228–237.

Bennett, N.D., Croke, B.F.W., Guariso, G., Guillaume, J.H. a, Hamilton, S.H., Jakeman, A.J., Marsili-Libelli, S., Newham, L.T.H., Norton, J.P., Perrin, C., Pierce, S. a., Robson, B., Seppelt, R., Voinov, A. a., Fath, B.D. & Andreassian, V. (2013). Characterising performance of environmental models. *Environmental Modelling & Software*, **40**, 1–20.

Bertin, S. (2009). Physiological ecology of understorey trees in low impact silvicultural systems. University of Edinburgh.

Bertin, S., Palmroth, S., Kim, H.S., Perks, M.P., Mencuccini, M. & Oren, R. (2011). Modelling understorey light for seedling regeneration in continuous cover forestry canopies. *Forestry*, **84**, 397–409.

Bianchi, S., Cahalan, C., Hale, S. & Gibbons, J.M. (2017). Rapid assessment of forest canopy and light regime using smartphone hemispherical photography. *Ecology and Evolution*, **7**,

10556–10566.

Binkley, D., Campoe, O.C., Gspaltl, M. & Forrester, D.I. (2013). Light absorption and use efficiency in forests: Why patterns differ for trees and stands. *Forest Ecology and Management*, **288**, 5–13.

Bivand, R., Keitt, T. & Rowlingson, B. (2017). rgdal: Bindings for the 'Geospatial' Data Abstraction Library.

Bivand, R. & Rundel, C. (2017). rgeos: Interface to Geometry Engine - Open Source ('GEOS').

Black, T. (2013). Age dependence in the light-growth reaction of Sitka spruce seedlings (*Picea sitchensis* (Bong.) Carr.). Newton Rigg College.

Boisvenue, C., Temesgen, H. & Marshall, P. (2004). Selecting a small tree height growth model for mixed-species stands in the southern interior of British Columbia, Canada. *Forest Ecology and Management*, **202**, 301–312.

Botkin, D.B., Janak, J.F. & Wallis, J.R. (1972). Some ecological consequences of a computer model of forest growth. *The Journal of Ecology*, **60**, 849–872.

Brix, H. (1972). Growth response of Sitka spruce and White spruce seedlings to temperature and light intensity. Pacific Forest Research Centre - Canadian Forestry Service, Victoria, British Columbia.

Burton, P. (2016). Using natural disturbance regimes to guide the management of northwestern coastal forests. *Ecological Forest Management Handbook* (ed G.R. Larocque), pp. 17–21. CRC Press, Boca Raton, Florida.

Butler, B.R. (2016). Growth, mortality and canopy cover in naturally regenerated Sitka spruce (*Picea sitchensis*) seedlings in UK forest stands. Bangor University.

Cameron, A.D. (2015). Building Resilience into Sitka Spruce (*Picea sitchensis* (Bong.) Carr.) Forests in Scotland in Response to the Threat of Climate Change. *Forests*, **6**, 398–415.

Carter, R.E. & Klinka, K. (1992). Variation in shade tolerance of Douglas fir, western hemlock, and western red cedar in coastal British Columbia. *Forest Ecology and Management*, **55**, 87–105.

Čater, M., Schmid, I. & Kazda, M. (2013). Instantaneous and potential radiation effect on underplanted European beech below Norway spruce canopy. *European Journal of Forest Research*, **132**, 23–32.

Cawley, G.C. & Talbot, N.L.C. (2004). Fast exact leave-one-out cross-validation of sparse least-squares support vector machines. *Neural Networks*, **17**, 1467–1475.

Chianucci, F. & Cutini, A. (2012). Digital hemispherical photography for estimating forest canopy properties: Current controversies and opportunities. *iForest*, **5**, 290–295.

Chianucci, F. & Cutini, A. (2013). Estimation of canopy properties in deciduous forests with digital hemispherical and cover photography. *Agricultural and Forest Meteorology*, **168**, 130–139.

Chrimes, D. & Nilson, K. (2005). Overstorey density influence on the height of *Picea abies* regeneration in northern Sweden. *Forestry*, **78**, 433–442.

Clarke, G.C. (1992). The Natural Regeneration of Spruce. *Scottish Forestry*, **46**, 107–129.

Claveau, Y., Messier, C., Comeau, P.G. & Coates, K.D. (2002). Growth and crown morphological responses of boreal conifer seedlings and saplings with contrasting shade tolerance to a gradient of light and height. *Canadian Journal of Forest Research*, **32**, 458–468.

Coates, K.D., Canham, C.D., Beaudet, M., Sachs, D.L. & Messier, C. (2003). Use of a spatially explicit individual-tree model (SORTIE/BC) to explore the implications of patchiness in structurally complex forests. *Forest Ecology and Management*, **186**, 297–310.

Collet, C. & Chenost, C. (2006). Using competition and light estimates to predict diameter and height growth of naturally regenerated beech seedlings growing under changing canopy conditions. *Forestry*, **79**, 489–502.

Comeau, P.G., Kerr, G. & Hale, S.E. (2010). Application of North American stand density indices as tools to aid the management of Sitka spruce and Douglas-fir stands in Great Britain being transformed to continuous cover forestry. *Scottish Forestry Trust Fellowship 2008/09, Final Report*, 1–19.

van Couwenberghe, R., Gégout, J.C., Lacombe, E. & Collet, C. (2013). Light and competition gradients fail to explain the coexistence of shade-tolerant *Fagus sylvatica* and shade-intermediate *Quercus petraea* seedlings. *Annals of Botany*, **112**, 1421–1430.

Crookston, N.L. & Dixon, G.E. (2005). The forest vegetation simulator: A review of its structure, content, and applications. *Computers and Electronics in Agriculture*, **49**, 60–80.

Curtis, R.O. (1972). Yield tables Past and Present. *Journal of Forestry*, **70**, 28–32.

Dale, V.H., Doyle, T.W. & Shugart, H.H. (1985). A comparison of tree growth models. *Ecological Modelling*, **29**, 145–169.

Davies, O., Haufe, J. & Pommerening, A. (2008). Silvicultural principles of continuous cover forestry: a guide to best practice. Tyfiant Coed Project.

Deal, R.L. & Farr, W.A. (1994). Composition and development of conifer regeneration in thinned and unthinned natural stands of western hemlock and Sitka spruce in southeast Alaska. *Canadian Journal of Forest Research*, **24**, 976–984.

Deichmann, J.L., Hernandez-Serna, A., Delgado C., J.A., Campos-Cerqueira, M. & Aide, T.M. (2017). Soundscape analysis and acoustic monitoring document impacts of natural gas exploration on biodiversity in a tropical forest. *Ecological Indicators*, **74**, 39–48.

Delagrange, S., Messier, C., Lechowicz, M.J. & Dizengremel, P. (2004). Physiological, morphological and allocational plasticity in understory deciduous trees: importance of plant size and light availability. *Tree physiology*, **24**, 775–784.

Diaz, G.M. & Lencinas, J.D. (2015). Enhanced Gap Fraction Extraction From Hemispherical Photography. *IEEE Geoscience and Remote Sensing Letters*, **12**, 1785–1789.

Dixon, G. (2015). Essential FVS : A User's Guide to the Forest Vegetation Simulator. USDA, Forest Management Service Center, Fort Collins, CO, USA.

Duchesneau, R., Lesage, I., Messier, C. & Morin, H. (2001). Effects of light and intraspecific competition on growth and crown morphology of two size classes of understory balsam fir saplings. *Forest Ecology and Management*, **140**, 215–225.

Edwards, P.N. & Christie, J.M. (1981). Yield Models for Forest Management. *Forestry Commission Booklet*, **48**.

Eerikäinen, K., Miina, J. & Valkonen, S. (2007). Models for the regeneration establishment and the development of established seedlings in uneven-aged, Norway spruce dominated forest stands of southern Finland. *Forest Ecology and Management*, **242**, 444–461.

Eerikäinen, K., Valkonen, S. & Saksa, T. (2014). Ingrowth, survival and height growth of small trees in uneven-aged *Picea abies* stands in southern Finland. *Forest Ecosystems*, **1**, 5.

Ek, A.R., Robinson, A.P., Radtke, P.J. & Walters, D.K. (1997). Development and testing of regeneration imputation models for forests in Minnesota. *Forest Ecology and*

Management, **94**, 129–140.

Evans, G.C. & Coombe, D.E. (1959). Hemisperical and Woodland Canopy Photography and the Light Climate. *Journal of Ecology*, **47**, 103–113.

Fairbairn, W.A. & Neustein, S.A. (1970). Study of response of certain coniferous species to light intensity. *Forestry*, **43**, 57–71.

Fekedulegn, D., Siurtain, M. Mac & Colbert, J. (1999). Parameter estimation of nonlinear growth models in forestry. *Silva Fennica*, **33**, 327–336.

Ferguson, I.S. (1996). Sustainable Forest Management. *Sustainable Forest Management - Growth Models for Europe* (ed H. Hasenauer), p. 161. Springer Berlin Heidelberg, Berlin, Heidelberg.

Ferguson, D.E. & Carlson, C.E. (1991). Natural regeneration of interior Douglas-fir in the northern Rocky Mountains. *Interior Douglas-fir: the species and its management*, p. 8.

Ferguson, D.E. & Carlson, C.E. (1993). Predicting regeneration establishment with the Prognosis Model. *Research Paper INT-467*. USDA, Intermountain Research Station.

Ferguson, D.E. & Crookston, N.L. (1991). User's Guide to Version 2 of the Regeneration Establishment Model: Part of the Prognosis Model. *General Technical Report INT-279*. USDA, Intermountain Research Station.

Ferguson, D.E., Stage, A.R. & Boyd, R.J. (1986). Predicting regeneration in the grand fir-cedar-hemlock ecosystem of the northern Rocky Mountains. *Forest Science, Monograph*, **26**.

Finzi, A.C. & Canham, C.D. (2000). Sapling growth in response to light and nitrogen availability in a southern New England forest. *Forest Ecology and Management*, **131**, 153–165.

Forest Research. (2010). Modelling mixed-age and mixed species stands. URL http://www.forestry.gov.uk/fr/INFD-8BXETZ [accessed 1 August 2017]

Forestry Commission. (2011a). National Forest Inventory 2011 woodland map. Edinburgh, Scotland, UK.

Forestry Commission. (1928). Report on census of woodlands and census of production of home grown timber. London, UK.

Forestry Commission. (2011b). Standing timber volume for coniferous trees in Britain.

Edinburgh, Scotland, UK.

Forestry Commission. (2017). The UK Forestry Standard. Edinburgh, Scotland, UK.

Fournier, R.A., Landry, R., August, N.M., Fedosejevs, G. & Gauthier, R.P. (1996). Modelling light obstruction in three conifer forests using hemispherical photography and fine tree architecture. *Agricultural and Forest Meteorology*, **82**, 47–72.

Führer, E. (2000). Forest functions, ecosystem stability and management. *Forest Ecology and Management*, **132**, 29–38.

von Gadow, K. & Hui, G. (1999). Modelling Forest Development. Springer Netherlands, Dordrecht.

von Gadow, K., Nagel, J. & Saborowski, J. (2002). Continuous Cover Forestry. Kluwer Academic Publishers.

Gamfeldt, L., Snäll, T., Bagchi, R., Jonsson, M., Gustafsson, L., Kjellander, P., Ruiz-Jaen, M.C., Fröberg, M., Stendahl, J., Philipson, C.D., Mikusiński, G., Andersson, E., Westerlund, B., Andrén, H., Moberg, F., Moen, J. & Bengtsson, J. (2013). Higher levels of multiple ecosystem services are found in forests with more tree species. *Nature Communications*, **4**, 1340.

Givnish, T.J. (1988). Adaptation to Sun and Shade: A Whole-Plant Perspective. *Aust. J. Plant Physiol.*, **15**, 63–92.

Glendinning, A. (2014). Compare and contrast natural regeneration of Sitka spruce (*Picea sitchensis* (Bong.) Carr) managed under different silviculture systems and assess balance between overstorey and understorey carbon. Bangor University.

Gonsamo, A., D'Odorico, P. & Pellikka, P. (2013). Measuring fractional forest canopy element cover and openness - definitions and methodologies revisited. *Oikos*, **122**, 1283–1291.

Gonsamo, A., Walter, J.M.N. & Pellikka, P. (2011). CIMES: A package of programs for determining canopy geometry and solar radiation regimes through hemispherical photographs. *Computers and Electronics in Agriculture*, **79**, 207–215.

Gonsamo, A., Walter, J.-M.N. & Pellikka, P. (2010). Sampling gap fraction and size for estimating leaf area and clumping indices from hemispherical photographs. *Canadian Journal of Forest Research*, **40**, 1588–1603.

Grassi, G. & Giannini, R. (2005). Influence of light and competition on crown and shoot

morphological parameters of Norway spruce and silver fir saplings. *Annals of Forest Science*, **62**, 269–274.

Greene, D.F., Zasada, J.C., Sirois, L., Kneeshaw, D., Morin, H., Charron, I. & Simard, M.J. (1999). A review of the regeneration dynamics of North American boreal forest tree species. *Canadian Journal of Botany - Revue Canadienne de Botanique*, **29**, 824–839.

Grossnickle, S.C. & Arnott, J.T. (1992). Gas exchange response of western hemlock seedlings from various dormancy-induction treatments to reforestation site environmental conditions. *Forest Ecology and Management*, **49**, 177–193.

Hale, S.E. (2003). The effect of thinning intensity on the below-canopy light environment in a Sitka spruce plantation. *Forest Ecology and Management*, **179**, 341–349.

Hale, S.E., Edwards, C., Mason, W.L., Price, M. & Peace, A. (2009). Relationships between canopy transmittance and stand parameters in Sitka spruce and Scots pine stands in Britain. *Forestry*, **82**, 503–513.

Hale, S.E., Jenkins, T. & Arcangeli, C. (2012). MosesGB User Guide - prototype version. 71.

Hale, S.E., Levy, P. & Gardiner, B. (2004). Trade-offs between seedling growth, thinning and stand stability in Sitka spruce stands: a modelling analysis. *Forest Ecology and Management*, **187**, 105–115.

Harmon, M.E. & Franklin, J.F. (1989). Tree Seedlings on Logs in Picae-Tsuga Forests of Oregon and Washington. *Ecology*, **70**, 48–59.

Hasenauer, H. (2006). Concepts within tree growth modelling. *Sustainable Forest Management - Growth Models for Europe* (ed H. Hasenauer), p. 400. Spinger Berlin Heidelberg.

Hasenauer, H. & Kindermann, G. (2002). Methods for assessing regeneration establishment and height growth in uneven-aged mixed species stands. *Forestry*, **75**, 385–394.

Hasenauer, H. & Kindermann, G. (2006). Modelling Regeneration in Even and Uneven-Aged Mixed Species Forests. *Sustainable Forest Management - Growth Models for Europe* (ed H. Hasenauer), pp. 167–194. Spinger Berlin Heidelberg.

Hasenauer, H., Kindermann, G. & Steinmetz, P. (2006). The tree growth model MOSES 3.0. *Sustainable Forest Management - Growth Models for Europe* (ed H. Hasenauer), p. 400. Springer Berlin Heidelberg.

Hassani, B.T., LeMay, V., Marshall, P., Temesgen, H. & Zumrawi, A.-A. (2004). Regeneration imputation models for complex stands of southeastern British Columbia. *The Forestry Chronicle*, **80**, 271–278.

Herd, A. (2003). Morphological and physiological responses of Sitka spruce seedlings to varying light regimes. University of Edinburgh.

Hijmans, R.J. (2016). raster: Geographic Data Analysis and Modeling.

Hill, R. (1924). A lens for whole sky photographs. *Quarterly Journal of the Royal Meteorological Society*, **50**, 227–235.

Huang, S., Yang, Y. & Wang, Y. (2003). A Critical Look at Procedures for Validating Growth and Yield Models. *Modelling Forest Systems* (eds A. Amaro, D. Reed & P. Soares). CABI Publishing, Wallingford, Oxon, UK.

Hugin. URL http://hugin.sourceforge.net/ [accessed 18 January 2017]

Hyndman, R.J. & Koehler, A.B. (2006). Another look at measures of forecast accuracy. *International Journal of Forecasting*, **22**, 679–688.

James, N.D.G. (1981). A History of English Forestry. Basil Blackwell Publisher, Oxford, England.

Kellomäki, S., Väisänen, H. & Hänninen, H. (1992). A simulation model for the succession of the boreal forest ecosystem. *Silva fennica*, **26**, 1–18.

Kerr, G. & Mackintosh, H. (2012). Long-Term Survival of Saplings during the Transformation to Continuous Cover. *Forests*, **3**, 787–798.

Kerr, G., Stokes, V., Peace, A. & Wylder, B. (2011). Prediction of conifer natural regeneration in a ' data-poor ' environment. *Scottish Forestry*, **65**, 28–36.

Kerr, G., Stokes, V., Peace, A., Wylder, B., Pearce, A. & Wylder, B. (2012). Natural Regeneration of Conifers - helping forest managers to predict success. *Quarterly Journal of Forestry*, **106**, 23–30.

King, D.A. (1990). The Adaptive Significance of Tree Height. *The American Naturalist*, **135**, 809–828.

Kobe, R.K. & Coates, K.D. (1997). Models of sapling mortality as a function of growth to characterize interspecific variation in shade tolerance of eight tree species of northwestern British Columbia. *Canadian Journal of Forest Research*, **27**, 227–236.

Kobe, R.K., Pacala, S.W., Silander Jr., J.A. & Canham, C.D. (1995). Juvenile tree survivorship as a component of shade tolerance. *Ecological Applications*, **5**, 517–532.

Koch, N. & Skovsgaard, J.P. (1999). Sustainable management of planted forests: some comparisons between Central Europe and the United States. *New Forests*, **17**, 11–22.

Korhonen, L., Korhonen, K., Rautiainen, M. & Stenberg, P. (2006). Estimation of forest canopy cover: a comparison of field measurement techniques. *Silva Fennica*, **40**, 577–588.

Kunstler, G., Curt, T., Bouchaud, M. & Lepart, J. (2005). Growth, mortality, and morphological response of European beech and downy oak along a light gradient in sub-Mediterranean forest. *Canadian Journal of Forest Research*, **35**, 1657–1668.

LePage, P.T., Canham, C.D., Coates, K.D. & Bartemucci, P. (2000). Seed abundance versus substrate limitation of seedling recruitment in northern temperate forests of British Columbia. *Canadian Journal of Forest Research*, **30**, 415–427.

Leverenz, J.. & Jarvis, P.G. (1980). Photosynthesis in Sitka Spruce (*Picea Sitchensis* (Bong.) Carr.): X. Acclimation to Quantum Flux Density Within and Between Trees. *Journal of Applied Ecology*, **17**, 697–708.

Lieffers, V.J., Messier, C., Stadt, K.J., Gendron, F. & Comeau, P.G. (1999). Predicting and managing light in the understory of boreal forests. *Canadian Journal of Forest Research*, **29**, 796–811.

Ligot, G. & Balandier, P. (2014). Forest radiative transfer models: which approach for which application? *Canadian Journal of Forest Research*, **403**, 391–403.

Ligot, G., Balandier, P., Fayolle, A., Lejeune, P. & Claessens, H. (2013). Height competition between *Quercus petraea* and *Fagus sylvatica* natural regeneration in mixed and uneven-aged stands. *Forest Ecology and Management*, **304**, 391–398.

Lusk, C.H. & Jorgensen, M.A. (2013). The whole-plant compensation point as a measure of juvenile tree light requirements. *Functional Ecology*, **27**, 1286–1294.

Macfarlane, C., Grigg, A. & Evangelista, C. (2007). Estimating forest leaf area using cover and fullframe fisheye photography: Thinking inside the circle. *Agricultural and Forest Meteorology*, **146**, 1–12.

Machado, J.-L. & Reich, P.B. (1999). Evaluation of several measures of canopy openness as

predictors of photosynthetic photon flux density in deeply shaded conifer-dominated forest understory. *Canadian Journal of Forest Research*, **29**, 1438–1444.

Macpherson, M.F., Kleczkowski, A., Healey, J.R., Quine, C.P. & Hanley, N. (2017). The effects of invasive pests and pathogens on strategies for forest diversification. *Ecological Modelling*, **350**, 87–99.

Malcolm, D.C., Mason, W.L. & Clarke, G.C. (2001). The transformation of conifer forests in Britain — regeneration, gap size and silvicultural systems. *Forest Ecology and Management*, **151**, 7–23.

Mason, W.L. (2015). Implementing Continuous Cover Forestry in Planted Forests: Experience with Sitka Spruce (*Picea Sitchensis*) in the British Isles. *Forests*, **6**, 879–902.

Mason, B., Edwards, C. & Hale, S.E. (2011). Continuous Cover Forestry in larch plantations: a case study in central Scotland. *Scottish Forestry*, **65**, 14–22.

Mason, W.L., Edwards, C. & Hale, S.E. (2004). Survival and Early Seedling Growth of Conifers with Different Shade Tolerance in a Sitka Spruce Spacing Trial and Relationship to Understorey Light Climate. *Silva fennica*, **38**, 357–370.

Mason, B. & Kerr, G. (2004). Transforming even-aged conifer stands to continuous cover management. *Forestry Commission Information Note*, **40**, 1–8.

Mason, B., Kerr, G. & Simpson, J. (1999). What is continuous cover forestry? *Forestry Commission Information Note*, **29**.

Maw, P.T. (1912). Complete Yield Tables for British Woodlands and the Finance of British Forestry.

McDonald, H. & McDonald, G. (2016). HabitApp. URL http://www.scrufster.com/habitapp/ [accessed 18 January 2017]

McNeill, J.D. & Thompson, D.A. (1982). Natural regeneration of Sitka spruce in the forest of Ae. *Scottish Forestry*, 269–282.

Met Office. (2006). Met Office Land Surface Stations Data (1900-2000). NCAS British Atmospheric Data Centre. URL http://catalogue.ceda.ac.uk/uuid/ea2d5d8bce505ad4b10e06b45191883b [accessed 14 October 2016]

Metslaid, M., Jõgiste, K., Nikinmaa, E., Moser, W.K. & Porcar-Castell, A. (2007). Tree

variables related to growth response and acclimation of advance regeneration of Norway spruce and other coniferous species after release. *Forest Ecology and Management*, **250**, 56–63.

Mielikäinen, K. & Hynynen, J. (2003). Silvicultural management in maintaining biodiversity and resistance of forests in Europe-boreal zone: Case Finland. *Journal of Environmental Management*, **67**, 47–54.

Miina, J., Eerikäinen, K. & Hasenauer, H. (2006). Modeling Forest Regeneration. *Sustainable Forest Management - Growth Models for Europe* (ed H. Hasenauer), pp. 93–109. Springer Berlin Heidelberg, Berlin/Heidelberg.

Miina, J. & Saksa, T. (2006). Predicting regeneration establishment in Norway spruce plantations using a multivariate multilevel model. *New Forests*, **32**, 265–283.

Minore, D. (1979). *Comparative Autecological Characteristics of Northwestern Tree Species - A Literature review*. USDA Forest Service, Pacific Northwest Forest and Range Experiment Station, Portland, Oregon.

Monserud, R. a. (2003). Evaluating forest models in a sustainable forest management context. *Forest Biometry, Modelling and Information*, **1**, 35–47.

Monserud, R. & Ek, A. (1977). Prediction of understory tree height growth in northern hardwood stands. *Forest Science*, **23**, 391–400.

Moore, J.R., Lyon, A.J., Searles, G.J. & Vihermaa, L.E. (2009). The effects of site and stand factors on the tree and wood quality of Sitka spruce growing in the United Kingdom. *Silva Fennica*, **43**, 383–396.

Motta, R. (2000). Case study: 'Close-to-nature' silviculture in the Italian Alps: the forest of Paneveggio. *Forests in Sustainable Mountain Development: A State of Knowledge Report for 2000* (eds M.F. Price & N. Butt). IUFRO Research Series, Vol. 5, Wallingford, Oxon, UK.

Munro, D.D. (1974). Forest growth models—a prognosis. *Research Note 30.* Royal College of Forestry, Stockholm.

Newnham, R.M. (1964). The development of a stand model for Douglas fir. University of British Columbia, Vancouver.

Ní Dhubháin, Á. (2003). Continuous Cover Forestry. *COFORD Connects*.

Nixon, C.J. & Worrell, R. (1999). The Potential for the Natural Regeneration of Conifers in Britain. *Forestry Commission Bullettin*, **120**.

Nobis, M. & Hunziker, U. (2005). Automatic thresholding for hemispherical canopy-photographs based on edge detection. *Agricultural and Forest Meteorology*, **128**, 243–250.

O'Connell, B.M. & Kelty, M.J. (1994). Crown architecture of understory and open-growth white pine (*Pinus strobus* L.) saplings. *Tree Physiology*, **14**, 89–102.

O'Hara, K.L. (2001). The silviculture of transformation — a commentary. *Forest Ecology and Management*, **151**, 81–86.

Oliver, D.C. & Larson, B.C. (1996). Forest stand dynamics. Wiley, NewYork.

Open Data Kit. URL https://opendatakit.org/

von Ow, F., Joyce, P. & Keane, M. (1996). Factors affecting the establishment of natural regeneration of Sitka spruce. *Irish Forestry*, **53**, 2–18.

Pacala, S.W., Canham, C.D., Saponara, J., Silander Jr., J.A., Kobe, R.K. & Ribbens, E. (1996). Forest models defined by field measurements: estimation, error analysis and dynamics. *Ecological Monographs*, **66**, 1–43.

Pacala, S.W., Canham, C.D., Silander Jr., J.A. & Kobe, R.K. (1994). Sapling growth as a function of resources in a north temperate forest. *Canadian Journal of Forest Research*, **24**, 2172–2183.

Paci, M. (2004). Problemi attuali della selvicoltura naturalistica. *Forest@ - Rivista di Selvicoltura ed Ecologia Forestale*, **1**, 59–69.

Page, L.M. & Cameron, A.D. (2006). Regeneration dynamics of Sitka spruce in artificially created forest gaps. *Forest Ecology and Management*, **221**, 260–266.

Page, L.M., Cameron, A.D. & Clarke, G.C. (2001). Influence of overstorey basal area on density and growth of advance regeneration of Sitka spruce in variably thinned stands. *Forest Ecology and Management*, **151**, 25–35.

Paine, C.E.T., Marthews, T.R., Vogt, D.R., Purves, D., Rees, M., Hector, A. & Turnbull, L.A. (2012). How to fit nonlinear plant growth models and calculate growth rates: An update for ecologists. *Methods in Ecology and Evolution*, **3**, 245–256.

Pardé, J. (1991). La méthode du Contrôle, d'hier à aujourd'hui. *Revue Forestière Française*,

43, 185–202.

Pausas, J.G., Ribeiro, E. & Dias, S.G. (2006). Regeneration of a marginal *Quercus suber* forest in the eastern Iberian Peninsula. *Journal of Vegetation Science*, **17**, 729–738.

Peng, C. (2000). Growth and yield models for uneven-aged stands: past, present and future. *Forest Ecology and Management*, **132**, 259–279.

Peterson, E.B., Peterson, N.M., Weetman, G.F. & Martin, P.J. (1997). Ecology and Management of Sitka spruce, emphasizing its natural range in British Columbia (U. Press, Ed.). Vancouver.

Pignatti, G. (2012). Bärenthoren's Dauerwald and its actuality. *Forest@ - Rivista di Selvicoltura ed Ecologia Forestale*, **9**, 260–272.

Pinheiro, J., Bates, D., DebRoy, S., Sarkar, D. & Team, R.C. (2016). nlme: Linear and Nonlinear Mixed Effects Models.

Pommerening, A. & Murphy, S.T. (2004). A review of the history, definitions and methods of continuous cover forestry with special attention to afforestation and restocking. *Forestry*, **77**, 27–44.

Porté, A. & Bartelink, H.H. (2002). Modelling mixed forest growth: a review of models for forest management. *Ecological Modelling*, **150**, 141–188.

Pretzsch, H. (2009). Forest Dynamics, Growth and Yield. Springer Berlin Heidelberg.

Pretzsch, H., Biber, P., Durksy, J., von Gadow, K., Hasenauer, H., Kandler, G., Kenk, G., Kublin, E., Nagel, J., Pukkala, T., Skovsgaard, J.P., Sodtke, R. & Sterba, H. (2006). Standardizing and Categorizing Tree Growth Models. *Sustainable Forest Management - Growth Models for Europe* (ed H. Hasenauer), p. 400. Springer Berlin Heidelberg.

Pretzsch, H., Grote, R., Reineking, B., Rötzer, T. & Seifert, S. (2008). Models for forest ecosystem management: A European perspective. *Annals of Botany*, **101**, 1065–1087.

Price, D.., Zimmermann, N.E., Van der Meer, P.J., Lexer, M.J., Leadley, P., Jorritsma, I.T.M., Schaber, J., Clark, D.F., Lasch, P., McNulty, S., Wu, J. & Smith, B. (2001). Regeneration in Gap Models: Priority Issues for Studying Forest Responses to Climate Change. *Climatic Change*, **51**, 475–508.

Promis, A., Gärtner, S., Butler-Manning, D., Durán-Rangel, C., Reif, A., Cruz, G. & Hernández, L. (2011). Comparison of four different programs for the analysis of

hemispherical photographs using parameters of canopy structure and solar radiation transmittance. *Waldokologie Online*, **11**, 19–33.

Pukkala, T., Lähde, E., Laiho, O., Salo, K. & Hotanen, J.-P. (2011). A multifunctional comparison of even-aged and uneven-aged forest management in a boreal region. *Canadian Journal of Forest Research*, **41**, 851–862.

Pyatt, G., Ray, D. & Fletcher, J. (2001). An Ecological Site Classification for Forestry in Great Britain. *Bullettin*, **124**, 96.

R Core Team. (2017). R: A language and environment for statistical computing.

Ribbens, E., Siilander, J.A.J. & Pacala, S.W. (1994). Seedling recruitment in forests: calibrating models to predict patterns of tree seedling dispersion. *Ecology*, **75**, 1794–1806.

Rich, P.M. (1990). Characterizing plant canopies with hemispherical photographs. *Remote Sensing Reviews*, **5**, 13–29.

Ridler, T.W. & Calvard, S. (1978). Picture Thresholding Using an Iterative Slection Method. *IEEE Transactions on Systems, Man and Cybernetics*, **8**, 630–632.

Robin, X., Turck, N., Hainard, A., Tiberti, N., Lisacek, F., Sanchez, J.-C. & Müller, M. (2011). pROC: an open-source package for R and S+ to analyze and compare ROC curves. *BMC Bioinformatics*, **12**, 77.

Robinson, A.P. & Ek, A.R. (2000). The consequences of hierarchy for modeling in forest ecosystems. *Canadian Journal of Forest Research*, **30**, 1837–1846.

Ruel, J.C., Messier, C., Doucet, R., Claveau, Y. & Comeau, P. (2000). Morphological indicators of growth response of coniferous advance regeneration to overstorey removal in the boreal forest. *Forestry Chronicle*, **76**, 633–642.

Salas, C., Gregoire, T.G., Craven, D.J. & Gilabert, H. (2016). Modelación del crecimiento de bosques: estado del arte. *Bosque*, **37**, 03–12.

Schindelin, J., Arganda-Carreras, I., Frise, E., Kaynig, V., Longair, M., Pietzsch, T., Preibisch, S., Rueden, C., Saalfeld, S., Schmid, B., Tinevez, J.-Y., White, D.J., Hartenstein, V., Eliceiri, K., Tomancak, P. & Cardona, A. (2012). Fiji: an open-source platform for biological-image analysis. *Nature Methods*, **9**, 676–682.

Schneider, E.E. & Larson, A.J. (2017). Spatial aspects of structural complexity in Sitka spruce – western hemlock forests , including evaluation of a new canopy gap delineation method.

Canadian Journal of Forest Research, **1044**, 1033–1044.

Schneider, D., Schwalbe, E. & Maas, H.G. (2009). Validation of geometric models for fisheye lenses. *ISPRS Journal of Photogrammetry and Remote Sensing*, **64**, 259–266.

Schütz, J.P. (2006). Modelling the demographic sustainability of pure beech plenter forests in Eastern Germany. *Annals of Forest Science*, **63**, 93–100.

Schütz, J.P. (2002). Silvicultural tools to develop irregular and diverse forest structures. *Forestry*, **75**, 329–337.

Schütz, J.P., Pukkala, T., Donoso, P.J. & von Gadow, K. (2011). Historical Emergence and Current Application of CCF. *Continuous Cover Forestry* (eds T. Pukkala & K. von Gadow), pp. 1–28. Springer Science & Business Media.

Schweiger, J. & Sterba, H. (1997). A model describing natural regeneration recruitment of Norway spruce (*Picea abies* (L.) Karst.) in Austria. *Forest Ecology and Management*, **97**, 107–118.

Sellars, H. (2005). Undercanopy microclimatology of Sitka spruce plantation forests: implications for natural regeneration. University of Liverpool.

Spiecker, H. (2003). Silvicultural management in maintaining biodiversity and resistance of forests in Europe—temperate zone. *Journal of Environmental Management*, **67**, 55–65.

Stokes, V., Kerr, G. & Ireland, D. (2009). Seedling height and the impact of harvesting operations on advance regeneration of conifer species in upland Britain. *Forestry*, **82**, 185–198.

Susmel, L. (1980). Normalizzazione delle foreste alpine. Basi ecosistemiche, equilibrio, modelli colturali, produttività. Liviana Edn. Padova.

Symonds, M.R.E. & Moussalli, A. (2011). A brief guide to model selection, multimodel inference and model averaging in behavioural ecology using Akaike's information criterion. *Behavioral Ecology and Sociobiology*, **65**, 13–21.

Taylor, A.H. (1990). Disturbance and persistence of sitka spruce (*Picea sitchensis* (Bong) Carr.) in coastal forests of the pacific Northwest, North America. *Journal of Biogeography*, **17**, 47–58.

Tchebakova, N.M. & Parfenova, E.I. (2003). Stand growth and productivity of mountain forests in Southern Siberia in a changing climate. *Modelling Forest Systems* (eds A.

Amaro, D. Reed & P. Soares). CABI Publishing, Wallingford, Oxon, UK.

von Teuffel, K., Hein, S., Kotar, M., Preuhsler, E.P., Puumalainen, J. & Weinfurter, P. (2006). End User Needs and Requirements. *Sustainable Forest Management - Growth Models for Europe* (ed H. Hasenauer), pp. 19–38. Springer Berlin Heidelberg, Berlin, Heidelberg.

Tichý, L. (2015). Field test of canopy cover estimation by hemispherical photographs taken with a smartphone. *Journal of Vegetation Science*, **27**, 427–435.

UKWAS. (2012). Third Edition (version 3.1). www.ukwas.org.uk.

Vanclay, J.K. (1994). Modelling forest growth and yield: applications to mixed tropical forests. CAB International, Wallingford, UK.

Venables, W.N. & Ripley, B.D. (2002). Modern Applied Statistics with S. Fourth Edition.

Wagner, S., Madsen, P. & Ammer, C. (2009). Evaluation of different approaches for modelling individual tree seedling height growth. *Trees*, **23**, 701–715.

Williams, H., Messier, C. & Kneeshaw, D.D. (1999). Effects of light availability and sapling size on the growth and crown morphology of understory Douglas-fir and lodgepole pine. *Canadian Journal of Forest Research*, **29**, 222–231.

Wright, E.F., Coates, K.D., Canham, C.D. & Bartemucci, P. (1998). Species variability in growth response to light across climatic regions in northwestern British Columbia. *Canadian Journal of Forest Research*, **28**, 871–886.

Wyckoff, P.H. & Clark, J.S. (2000). Predicting tree mortality from diameter growth: a comparison of maximum likelihood and Bayesian approaches. *Canadian Journal of Forest Research*, **30**, 156–167.

Yamashita, T., Yamashita, K. & Kamimura, R. (2007). A Stepwise AIC Method for Variable Selection in Linear Regression. *Communications in Statistics - Theory and Methods*, **36**.

ANNEX I: Supplementary information for Chapter 5

I show here the full list of Akaike Information Criteria (AIC) values for each model tested (Table 10.1) the distribution of the standardized residuals according to the forest areas used as random effects (Figure 10.1); and the 95% prediction intervals for each model (Figure 10.2). The standardized residuals were generally homogenously distributed across all forest areas, except for two forests for the WH/Height models, that anyway comprised few observations each. The prediction intervals for each model were calculated for each model by i) resampling 1,000 times the coefficients according to a multivariate distribution using the same variance-covariance of the calibrated model; ii) calculating the predictions using all the new combinations of coefficients; iii) identify the 97.5% and 2.5% quantiles of those predicted values as upper and lower boundaries.

Table 10.1. Akaike Information Criteria (AIC) for all light-growth models. SS, Sitka spruce; DF, Douglas fir; WH, western hemlock; DRC, diameter above root collar; DBH, diameter at breast height. Under Size and Competition, indication of main parameters influenced by respectively tree size and intra-regeneration competition. AIC values: bold, all the models considered in the group of best candidates (difference in AIC less than 2 points from the model with lowest AIC, models with no biological validity discarded); bold and italicized, the best model selected for each combination growth/species empty, a model could not be successfully calibrated.

Equation	Size	Competition	SS/ Height	SS/ DRC	SS/ DBH	WH/ Height	WH/ DRC	DF/ Height
Logistic	None	None	1509	-	276	-	-	830
Logistic	None	A	1512	-	273	-	-	831
Logistic	None	K	-	-	-	-	-	-
Logistic	A	None	1357	315	253	-	173	794
Logistic	A	A	1345	*283*	**249**	-	**171**	795
Logistic	A	K	1345	**284**	*248*	-	**171**	796
Logistic	K	None	1406	333	263	-	-	813
Logistic	K	A	1398	304	257	-	-	808
Logistic	K	K	1386	305	257	-	-	809
Logistic	S	None	1401	-	260	-	-	821
Logistic	S	A	1393	339	262	-	-	-
Logistic	S	K	1392	339	-	-	-	-
Logistic	A-K	None	1354	315	254	-	-	795
Logistic	A-K	A	1345	**284**	**250**	-	173	796
Logistic	A-K	K	*1340*	286	-	**517**	**170**	806
Logistic	A-S	None	1357	347	256	-	176	794
Logistic	A-S	A	-	**285**	**249**	-	173	795
Logistic	A-S	K	1347	-	-	-	-	796
Logistic	K-S	None	1359	315	255	-	-	798
[Table continues across page]								

Model								
Logistic	K-S	A	-	292	253	-	172	-
Logistic	K-S	K	-	295	251	-	173	-
Logistic	A-K-S	None	1349	313	258	-	-	795
Logistic	A-K-S	A	1344	286	252	-	**169**	796
Logistic	A-K-S	K	**1339**	289	258	-	174	797
Michaelis-Menten	None	None	1516	-	383	541	233	-
Michaelis-Menten	None	A	1518	-	-	-	-	-
Michaelis-Menten	None	K	1517	628	377	-	225	-
Michaelis-Menten	A	None	1370	-	261	521	178	-
Michaelis-Menten	A	A	1359	-	254	607	*171*	-
Michaelis-Menten	A	K	1358	-	253	-	172	-
Michaelis-Menten	K	None	1365	617	256	*519*	177	1014
Michaelis-Menten	K	A	1359	629	253	**518**	-	1011
Michaelis-Menten	K	K	1356	652	252	-	173	-
Michaelis-Menten	A-K	None	1366	-	-	-	179	-
Michaelis-Menten	A-K	A	-	-	-	-	-	-
Michaelis-Menten	A-K	K	-	-	-	-	-	-
Asymptotic-with-offset	None	None	-	-	-	-	-	-
Asymptotic-with-offset	None	A	-	-	-	-	-	-
Asymptotic-with-offset	None	K	-	-	-	-	-	-
Asymptotic-with-offset	A	None	1365	-	-	-	-	***790***
Asymptotic-with-offset	A	A	1353	313	-	-	-	801
Asymptotic-with-offset	A	K	1353	-	-	-	-	-
Asymptotic-with-offset	K	None	1377	-	-	-	-	793
Asymptotic-with-offset	K	A	1371	-	-	524	-	795
Asymptotic-with-offset	K	K	-	335	-	-	-	-
Asymptotic-with-offset	C	None	-	-	-	-	-	-
Asymptotic-with-offset	C	A	-	-	-	-	-	-
Asymptotic-with-offset	C	K	-	-	-	-	-	-
Asymptotic-with-offset	A-K	None	1353	-	-	-	-	-
Asymptotic-with-offset	A-K	A	-	-	-	-	-	801
Asymptotic-with-offset	A-K	K	1347	-	-	-	-	-
Asymptotic-with-offset	A-C	None	1365	-	-	-	-	800
Asymptotic-with-offset	A-C	A	1355	-	-	-	-	802
Asymptotic-with-offset	A-C	K	1353	-	-	-	-	-
Asymptotic-with-offset	K-C	None	1368	369	-	-	-	-
Asymptotic-with-offset	K-C	A	-	-	-	-	-	-
Asymptotic-with-offset	K-C	K	-	-	-	-	-	-
Asymptotic-with-offset	A-K-C	None	1354	-	-	-	-	-
Asymptotic-with-offset	A-K-C	A	-	-	-	-	-	-
Asymptotic-with-offset	A-K-C	K	-	-	-	-	-	-
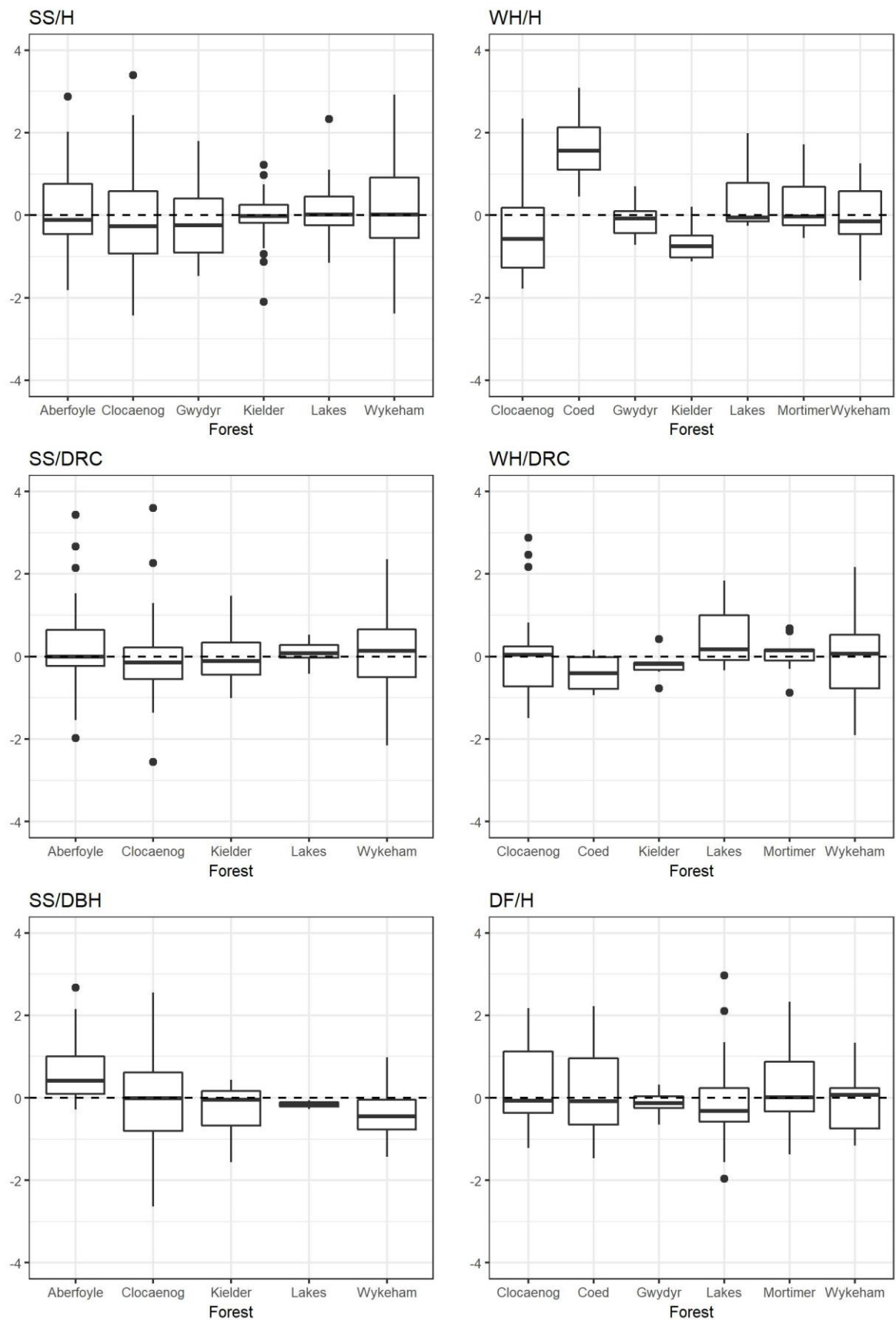
Figure 10.1. Boxplots of standardized residuals for the selected best models for each forest area used as random effect. SS is Sitka spruce, WH is western hemlock, DF is Douglas fir, H is height, DRC is diameter above root collar, DBH is diameter at breast height. Coed is Coed-Y-Brenin as named in Table 1
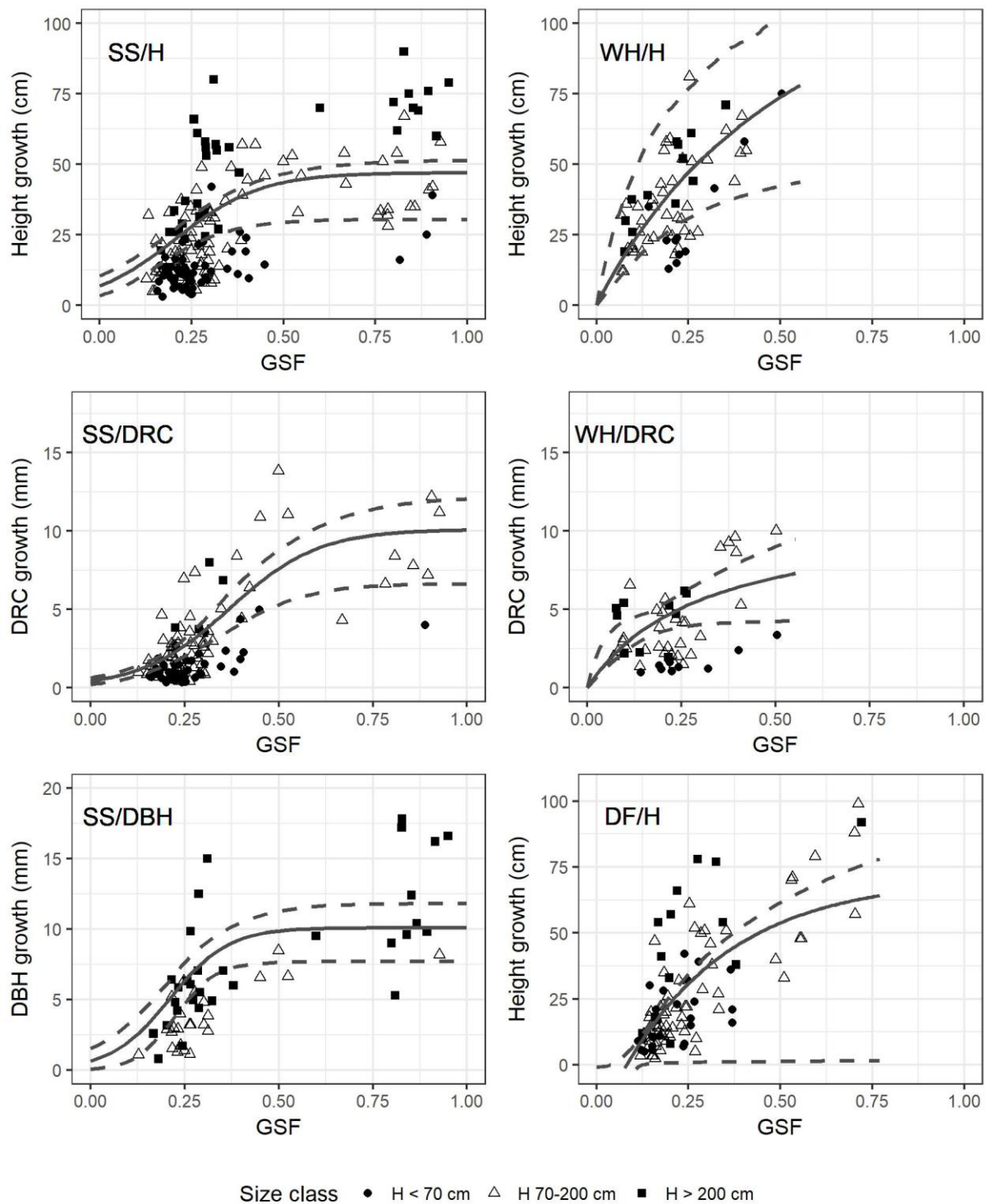
153

Figure 10.2. Simulated growth patterns (continuous line) of each growth model as a function of light (GSF, Global Site Factor), for a tree of average height or diameter, and in absence of competition, plotted with the observations (points). SS is Sitka spruce; DF, Douglas fir; WH, western hemlock; H, Height; DRC, Diameter above Root Collar; DBH, Diameter at Breast Height. The dashed lines are the upper and lower boundaries defining a 95% prediction Interval

ANNEX II: Supplementary Information for Chapter 6

This section has been included as Supporting Information for the online version of the paper presented in Chapter 6.

Examples of smartphone hemispherical pictures

Figure 10.3 shows a circular hemispherical picture and the two smartphone hemispherical pictures in the same plot, providing guides to compare the respective coverages. Note that the Nikon Coolpix hemispherical photography famously excludes a small portion on the bottom of the pictures, while the smartphone hemispherical photography employed here sometimes had a diagonal field-of-view slightly smaller than the frame of the picture (see the black corners). In both cases, those areas were considered by the software as blocking elements.
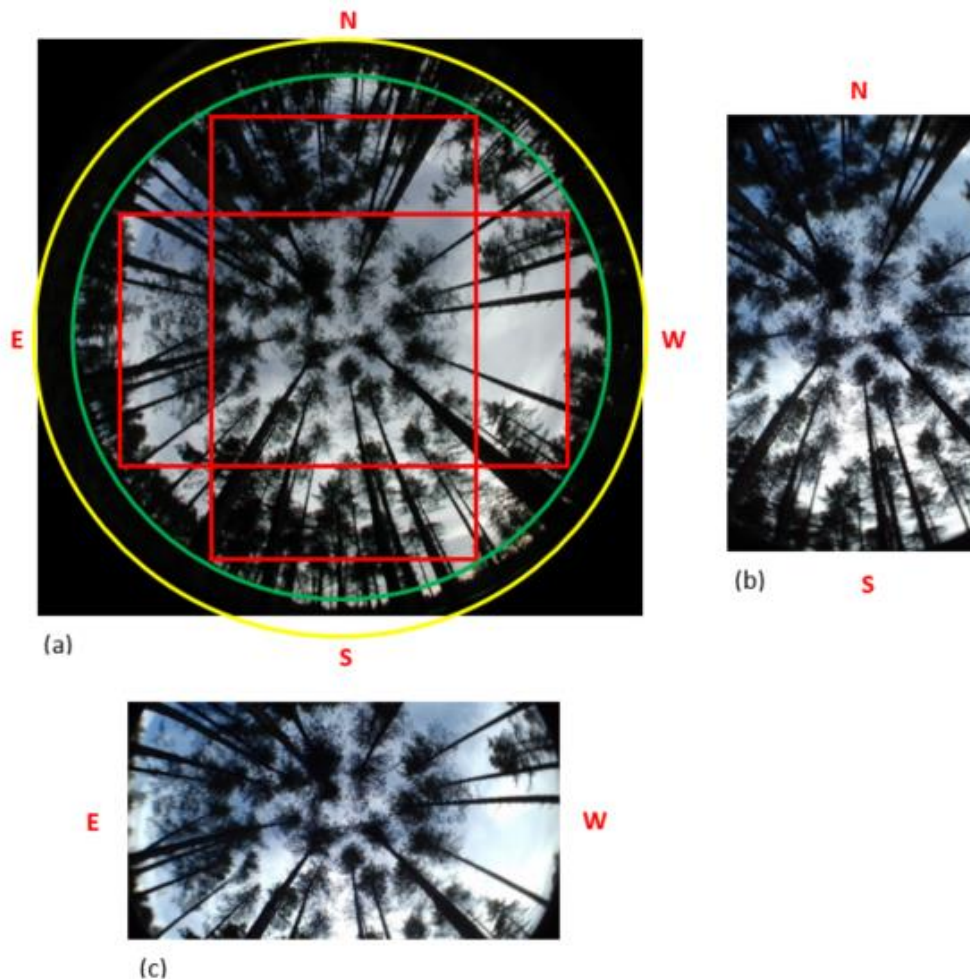
Figure 10.3. Examples of the circular picture (a) and of the two smartphone pictures (b and c) for the same plot. The yellow circle represents the 183° FOV of the Nikon Coolpix. The green circle is the 150° FOV of the smartphone. The red rectangles show the approximate areas on the Nikon picture covered by each Smartphone picture. Note that in hemispherical pictures the East and West directions are reversed

Figure 10.4 shows the results of the merging process for the smartphone images in two plots. In the left picture, we took the two smartphone pictures with the correct alignment in the field, with angle of 90° from each other. In the right picture, we took the images with a slightly wrong alignment but the Hugin software automatically corrected the error. Note that the area with missing information within the yellow circle was considered as obstructed view.

(a)   (b)
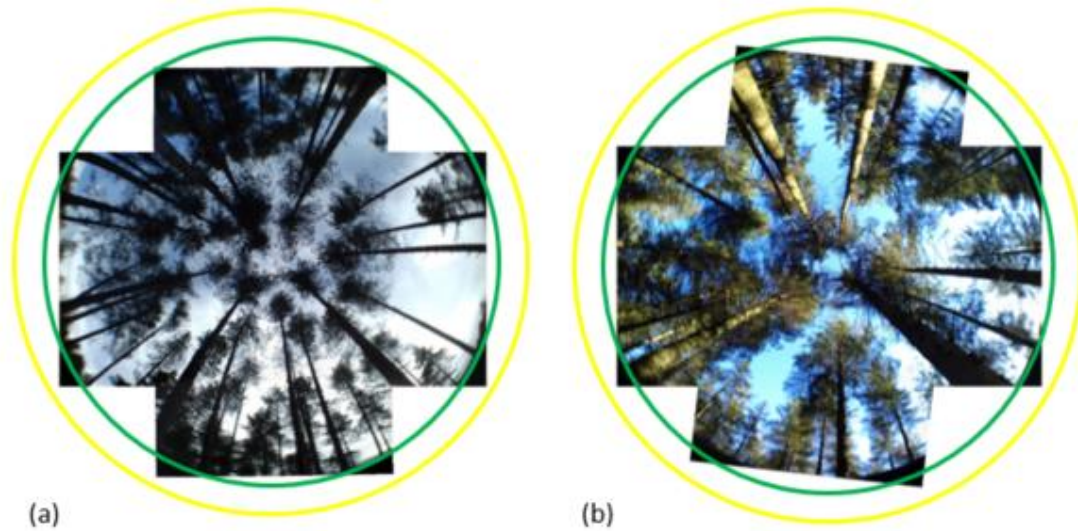
Figure 10.4. Examples of the results of the merging process with Hugin for two plots. The green circles represent the approximate 150° FOV, while the yellow the 180° FOV. The left images were taken with a correct 90° angle from each other in the field, the right with a slight deviation. White pixels outside the merged images and within the yellow circles correspond to the area considered as blocking elements for the parameters estimations.

Additional statistical results

Comparison of classification methods

The comparisons between outputs estimated from the same camera (respectively Total Gap from smartphone and Canopy Openness from circular images) but with different thresholding methods are shown in Figure 10.5.
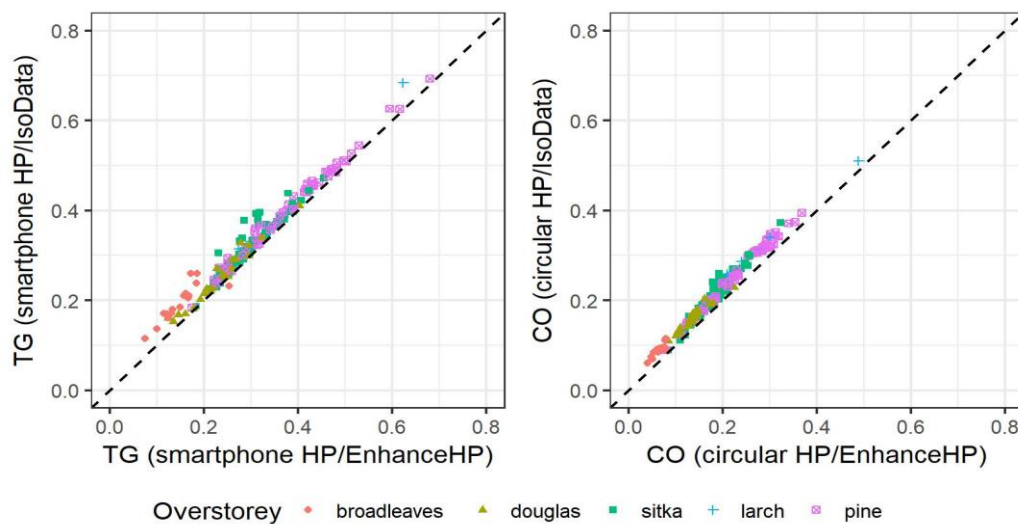
Figure 10.5. Scatterplots of Total Gap (TG, left) and Canopy Openness (CO, right) from same camera pictures but with different classification methods, showing the line of identity (dashed black line).

Comparison of smartphone picture with different orientation

The comparisons between Total Gap estimated from smartphone pictures taken with different orientation, using the same classification methods, are shown in Figure S5.
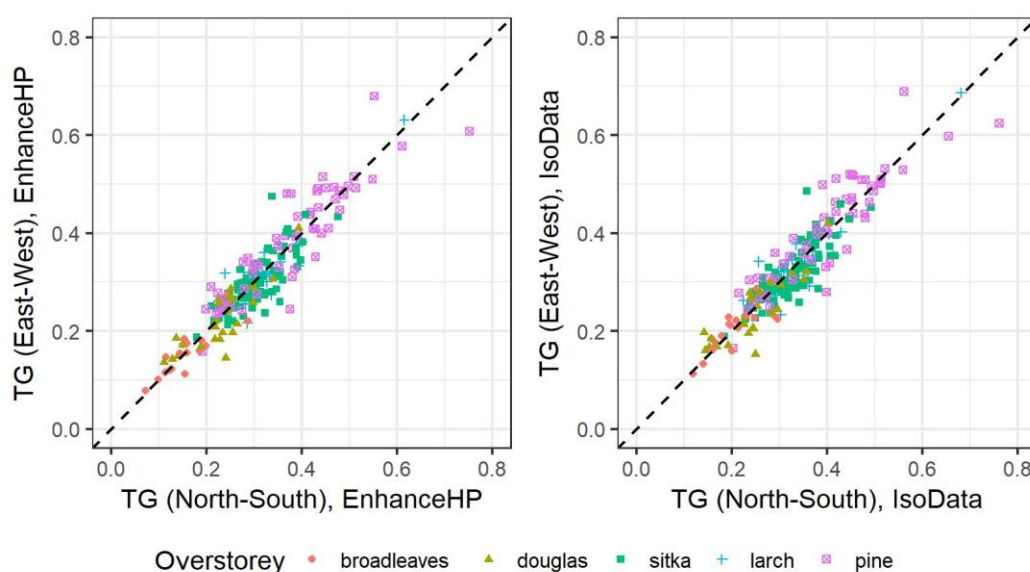
Figure 10.6. Scatterplots of Total Gap (TG) from East-West (E/W) and North-South (N/S) oriented Smartphone pictures with the same classification method (left, EnhanceHP; right, IsoData), showing the line of identity (dashed black line).

Comparison of different FOVs for circular HP

The comparisons of parameters estimated from circular HP images with FOV 150° and 180° are shown in Figure 10.7.
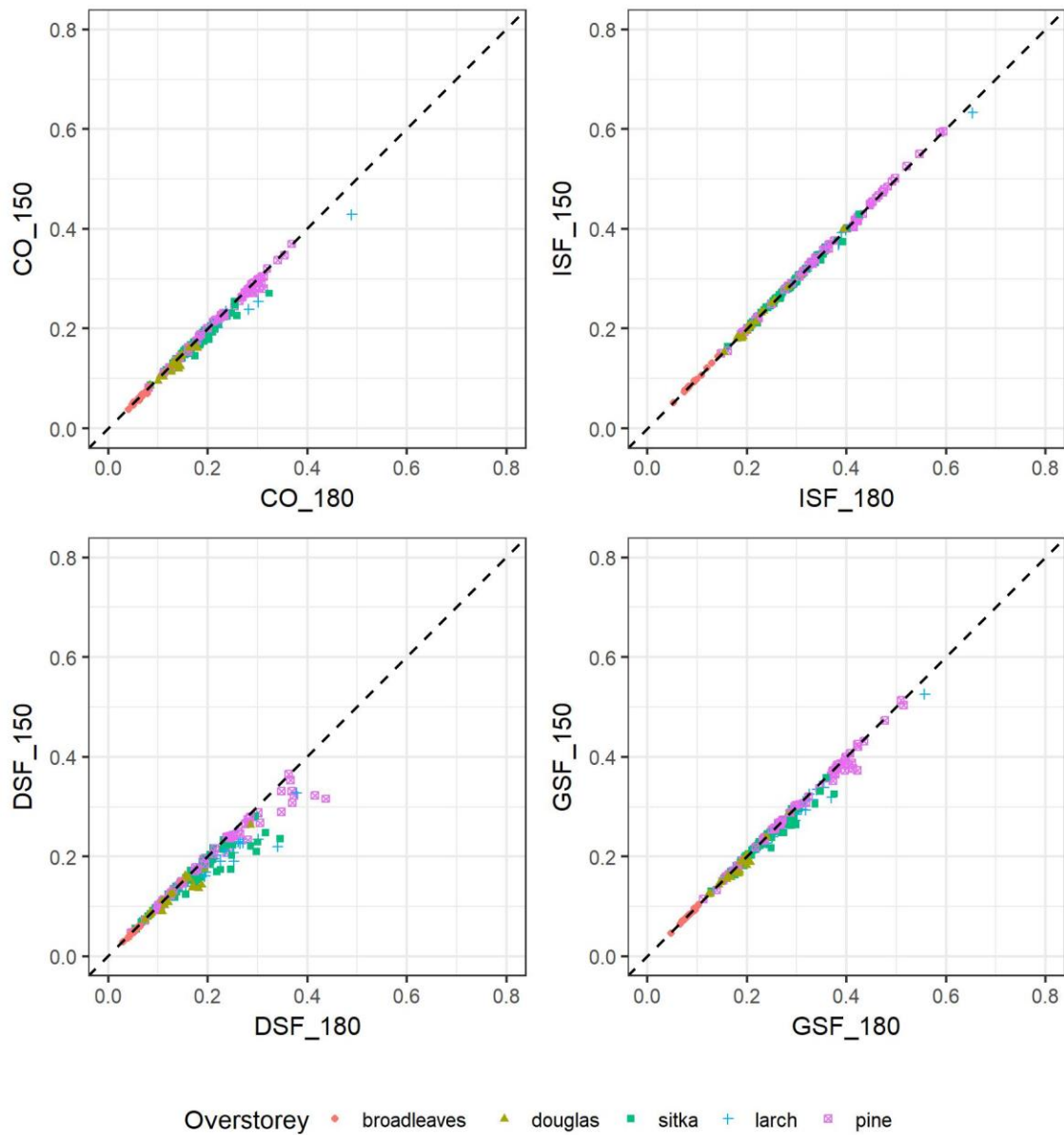
Figure 10.7. Scatterplots of Canopy Openness and Site Factors (ISF, Indirect; DSF, Direct; GSF, Global) estimated from circular HP images with a Field of View of 150° (y-axis) and 180° (x-axis), showing the line of identity (dashed black line).

Comparison of non-merged smartphone HP with circular HP, IsoData method

The comparison of Canopy Openness from circular pictures and Total Gap from smartphone values (averaged between the two pictures), using the IsoData method, is shown in Figure 10.8. CO from circular pictures was significantly higher (p < 0.001) than TG values from the smartphone pictures (mean of differences 0.115, st.dev. 0.04).
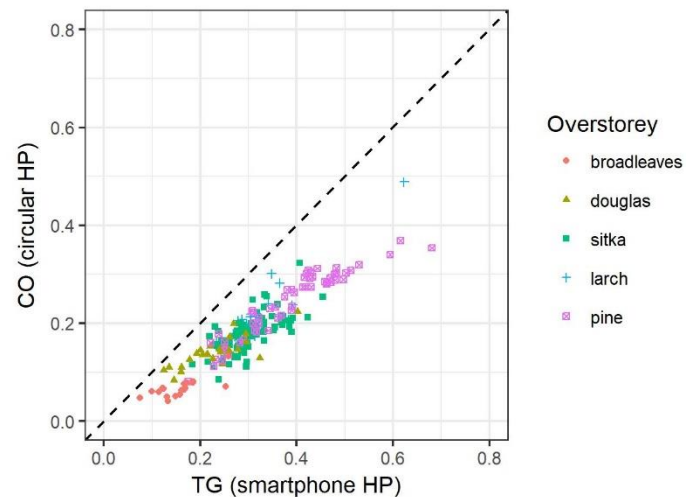
Figure 10.8. Scatterplot of Canopy Openness (CO) from circular images and Total Gap (TG) from smartphone images, using IsoData method, showing the line of identity (dashed black line).

Comparison of stitched Smartphone HP with circular HP, IsoData method

The comparisons between the outputs estimated from the circular and the merged smartphone images, using the IsoData method, are shown in Figure 10.9. There were some plots where the IsoData thresholding applied to the merged smartphone pictures seems to have completely failed, resulting in differences between circular and smartphone values of around 0.3 and more. Even not considering these exceptions, the distribution of circular and smartphone values was generally worse for all parameters than when using EnhanceHP.
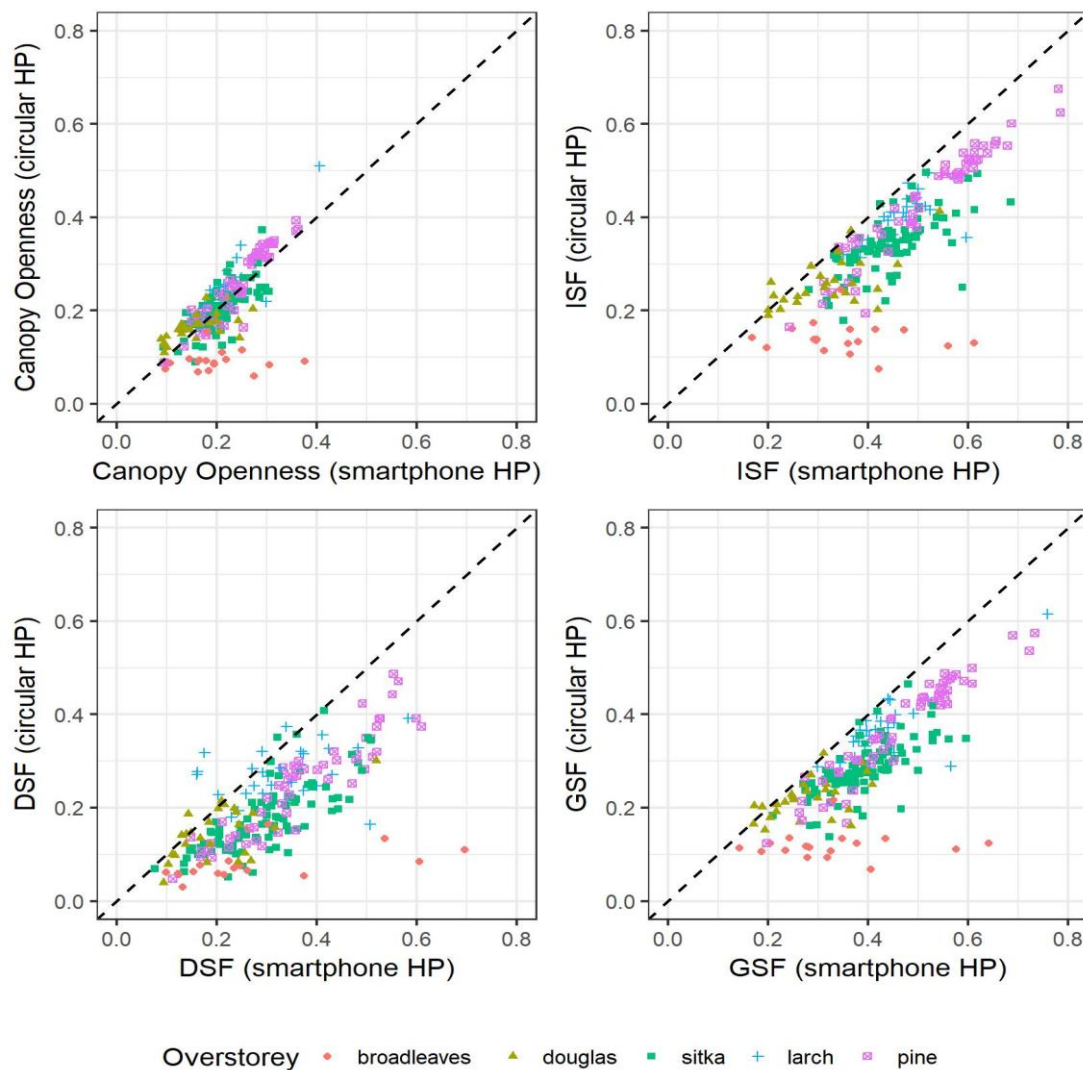
Figure 10.9. Scatterplots of Canopy Openness and Site Factors (ISF, Indirect; DSF, Direct; GSF, Global) from Smartphone merged images versus the same values from the circular Images, using IsoData method. The dashed black line is the line of identity.

ANNEX III: Crowd-sourced data collection project

I investigated the use of smartphone hemispherical photography also for the opportunity to recruit citizen scientists in a crowd-sourced data collection for regeneration growth. The rationale was the possibility to collect in such way a larger dataset than I could have done on my own, and with more geographical areas covered.

Using 'Open Data Kit', a free and open-source application for mobile data collection, I prepared a simple data entry form that everyone could have downloaded on his/her smartphone or table (**Error! Reference source not found.**). Following such form, a user could have taken hemispherical images above seedlings, record the GPS coordinates, and insert few simple information about the trees (species, total height, leader length). All the data would have been uploaded to a server from which I could have easily retrieved them.

I set up a website at www.simonebianchi.eu/crowdsourcing with the information about the project, prepared informative leaflets (attached later), and contacted organizations of forestry practitioners and students. Some people replied and asked to participate in the project. I sent them a fish-eye lens together with more detailed instructions. Unfortunately, these persons were few and they did not follow up with the data collection in the field, so I had to quit the project.

Figure 10.10. Screenshots of mobile data entry prepared with Open Data Kit.

# CROWD-SOURCING DATA COLLECTION OF FOREST REGENERATION GROWTH

Do you want to join a forestry research project?

WHY? Natural regeneration is becoming increasingly important in UK forests managed using a Continuous Cover Approach. I am trying to build a model of regeneration growth as a function of the light regime under a forest canopy. I need data from all over the UK, and you can help me to expand the research range using your smartphone. Become a citizen scientist and participate in a crowd-sourced research!

WHERE? Anywhere in the UK where you find a Sitka spruce (*Picea sitchensis*) or Douglas fir (*Pseudotsuga menziesii*) seedling growing under canopy cover.

HOW? It is very simple:

1) Shoot a picture above the seedling with a fish-eye equipped smartphone!
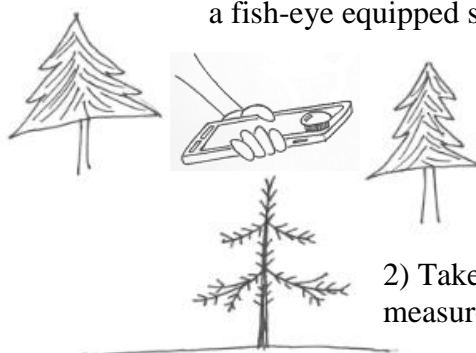
2) Take a few and very simple measurements of the plant!
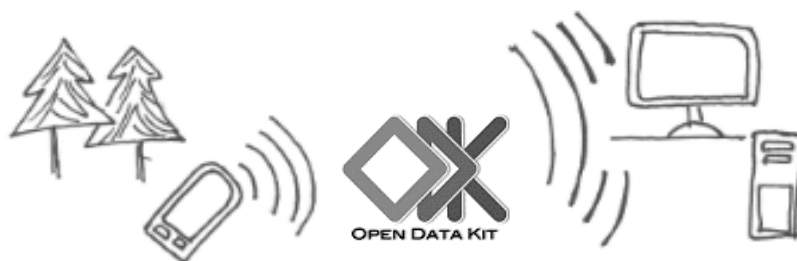
3) Upload your data to a webserver thanks to the free app Open Data Kit!

WHEN? Right now! The project has been launched, and the webserver is ready. Please contact me to receive a **free fish-eye lens** for your device and **more detailed** (but still simple) **instructions** on how to collect and upload the data.
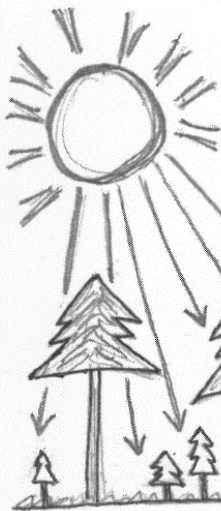
WHAT'S NEXT? The model will be useful to everyone interested in Continuous Cover Forestry. The dataset will be openly released for everyone to make further use of it.
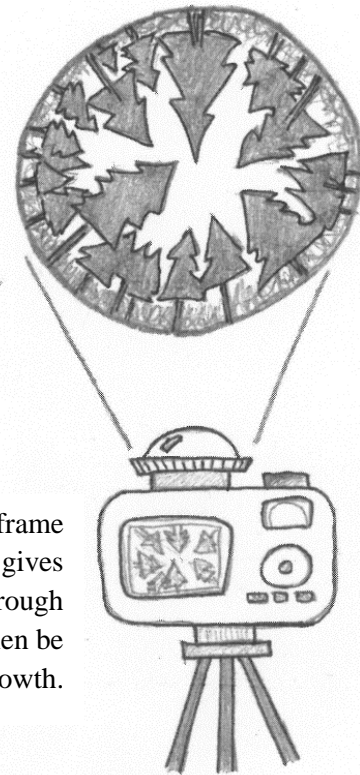
Contact me to join the project!
Email afp462@bangor.ac.uk
website www.simonebianchi.eu/crowdsourcing

More background about the project:

Light is the main factor affecting regeneration growing under canopy cover. The growth rate can be linked to the light availability.

Hemispherical photography, using full-frame cameras equipped with fish-eye lenses, gives reliable estimates of the light transmitted through the canopy. Such measurements can then be linked to the regeneration growth.

What if smartphone cameras, equipped with small and cheap fish eye lenses, can give comparable results?
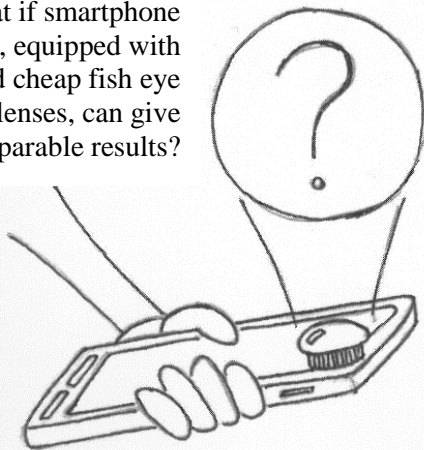
Every person who owns one could take measurements, share them through the internet and help to create the largest forest regeneration growth database in the UK!
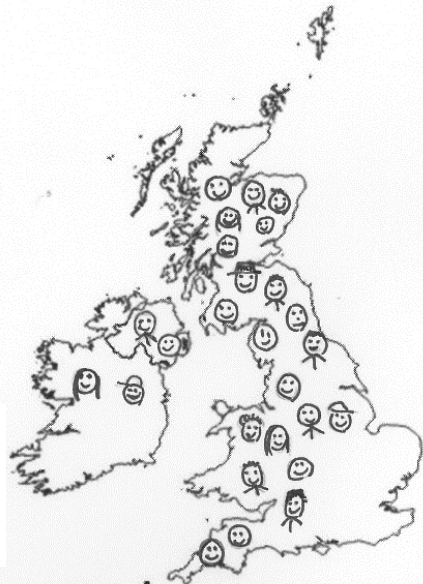
This work will contribute to MOSES_GB, the new individual-tree forest model being developed by Forestry Research, the research agency of Forestry Commission.

More info on: http://www.forestry.gov.uk/fr/INFD-8BXETZ

ANNEX IV: Supplementary Information for Chapter 7

Methodology

I used the 78 plots from the 8 stands of the independent validation datasets presented in Chapter 4 to test the light availability model from Hale *et al.* (2009). I estimated GSF values applying Model 8.1 to the local stand characteristics (basal area BA, stems per ha SPH) measured in each plot (radius 5.6 m), and then averaged them at stand level. In the same plots, using a Nikon Coolpix and the methodology described in Chapter 6 for traditional circular pictures, I calculated GSF values from hemispherical photography), and then averaged them at stand level. I compared both the plot-level and stand-level GSF values from Model 8.1 and hemispherical photography using scatterplots.

Results

Figure 10.11 shows the comparison of GSF values at plot-level (graph a) and at stand-level (graph b). At plot-level, the observed values from HP and the estimated values from Model 8.1 had scarcely a correspondence. Only when averaged at stand-level the values were consistent with each other (six stands out eight had a difference ±10% between observed and estimated values). The two stands with the highest predictions errors, named K_1149 and K_3248, were affected to different degrees by many windblown events. K_1149 was also surrounded by large open areas, thus maybe increasing the observed GSF area through a "edge" effect.
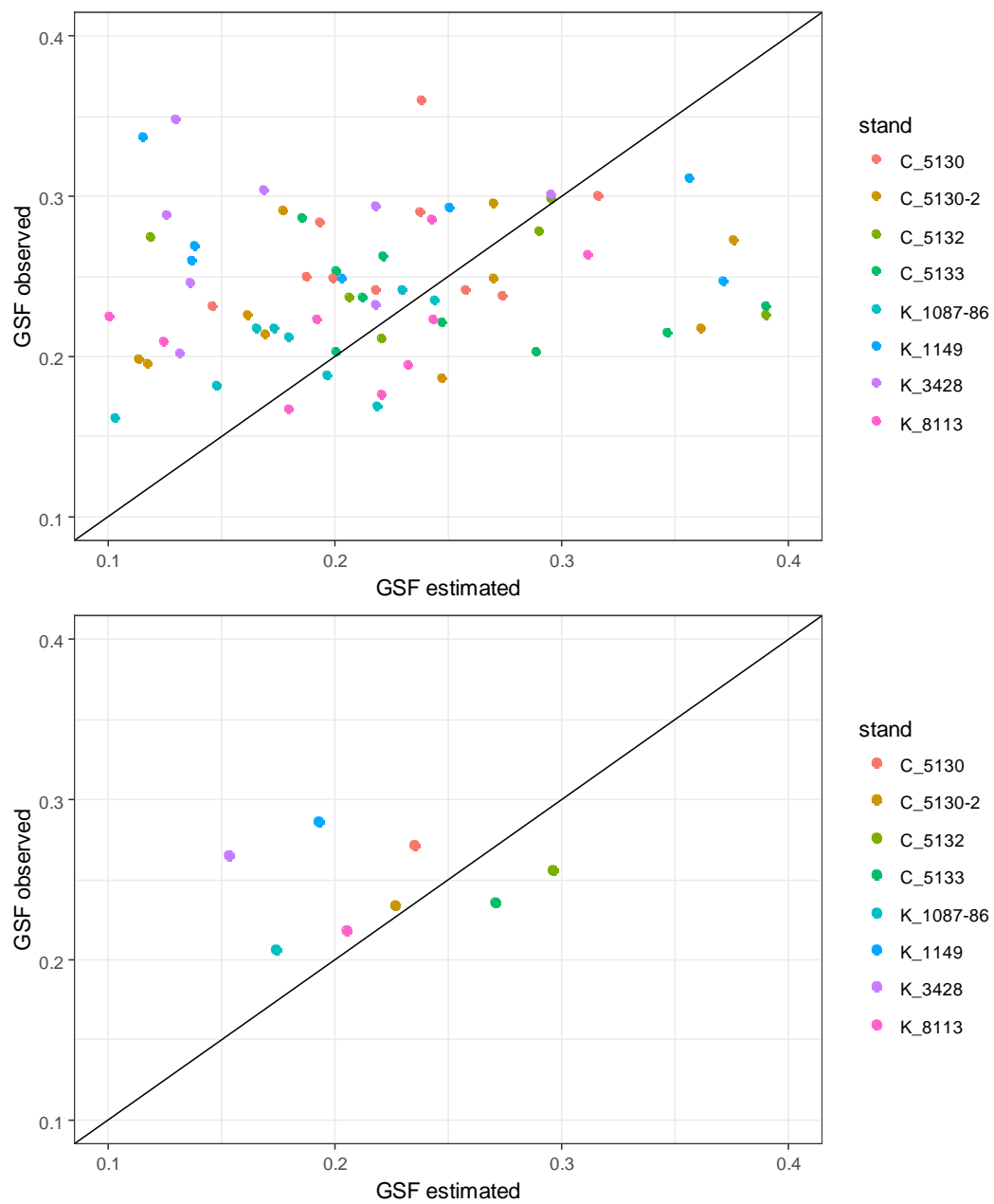
Figure 10.11. Comparison of GSF values, observed with hemispherical photograph (y-axis) and estimated from Model 8.6 (x-axis), at plot-level (graph a) and stand-level (graph b)